IMPROVING SEASONAL RAINFALL PREDICTION OVER WEST AFRICA USING DYNAMIC CLIMATE MODELS

BY

KUMI, NAOMI

B.Ed, MSc (MET/15/5747)

A thesis in the Department of Meteorology and Climate Science, School of Earth and Mineral Sciences, in partnership with the West African Science Service Centre on Climate Change and Adapted Land Use (WASCAL) submitted to the School of Postgraduate Studies in partial fulfilment of the requirements for the award of Doctor of Philosophy in Meteorology and Climate Science of the Federal University of Technology, Akure, Nigeria.

September, 2019

DECLARATION

I hereby declare that this thesis was written by me and is a correct record of my own research work. It has not been presented in any previous application for any degree of this or any other University. All citations and sources of information are clearly acknowledged by means of references.

Candidate's name: KUMI, Naomi

Signature: ……… **Date: …….**

CERTIFICATION

We certify that this thesis entitled "Improving Seasonal Rainfall Prediction over West Africa using Dynamic Climate Models" is the outcome of the research carried out by Kumi, Naomi in the Department of Meteorology and Climate Science, the Federal University of Technology, Akure, Nigeria, in partnership with the West African Science Service Centre on Climate Change and Adapted Land Use (WASCAL).

Major Supervisor's name: ... Associate Professor Babatunde J. Abiodun……

Signature: ……. **Date:** ……

Co-Supervisor's name: ……Dr. Elijah A. Adefisan……

Signature: ……. **Date:** ……

ACKNOWLEDGEMENTS

My sincere appreciation goes to the German Federal Ministry of Education and Research (BMBF; Bundesministerium für Bildung und Forschung) and West African Science Centre on Climate Change and Adapted Land Use (WASCAL) for providing the scholarship and financial support for this programme. I am also grateful to WASCAL for sponsoring my research visit to the Climate Systems Analysis Group (CSAG), University of Cape Town (UCT), South Africa.

I am forever thankful to my supervisor, Associate Professor Babatunde J. Abiodun. You were not just a supervisor, but a father, an elder brother, a role model, a counsellor, a motivator, a friend and a great host (during my stay in Cape Town). Your patience, constructive criticisms, encouragement and support guided me throughout this programme. Your immense contribution towards my personal and professional career cannot be quantified. I cannot thank you enough!

My sincere gratitude also goes to my co-supervisor, Dr. Elijah A. Adefisan. Sir, thank you for collaborating to make this work a success. Thank you for your time, contribution, advice and all the corrections you made towards the accomplishment of this work.

I am thankful to the Directors and staff of WASCAL Head Office, Accra, Ghana and WASCAL Graduate Research Program in West African Climate System (GRP-WACS), Federal University of Technology Akure (FUTA), Nigeria for their strong support and encouragement throughout the period of study. I am also appreciative of Prof. A.A. Balogun, Head, and the staff of Meteorology and Climate Science Department, FUTA, Nigeria, for their assistance.

I appreciate the productive contributions and suggestions by the “peer review team” at the University of Cape Town, and I say thanks to you all. Thanks also to Mr. Phillip Mukwena (CSAG, UCT) for his friendliness and technical support during my research visit. I appreciate the friendliness and support from all my course mates especially Sawadogo Windmanagda, Abdoulaye Ballo and Abdou Latif Bonkaney who were with me during my research visit to UCT. A big thank you goes to my “West African Group” members of St. Paul’s AnHouse (Cape Town); Dr. Godwin Dziwornu, Kojo Sekyi Acquah, Henrietta Dede Attram, Constance Mawunyo Korkor and Nheoma Worugji. I really cherish the time we spent together, the love and care for each other.

Dr. Nana Ama Browne Klutse, I appreciate your advice and encouragement right from the very day I confided in you (during an ICTP workshop in Niger, 2015) that I wished to pursue a PhD degree. You kept sending me numerous websites to apply for admission/scholarship; one of them was WASCAL. Sister, I am sincerely grateful for your support despite your busy schedules. Dr. Evelyne Toure N'Datchoh, you have been a true sister, thank you for everything.

Many thanks to the Management of Ghana Meteorological Agency, for approving my application for study-leave with pay. I respectfully acknowledge all authors whose works served as a guide for this study.

I am highly indebted to my family and friends (Marvin and Adusei), my dear mums (Madam Martha Adwoa Kumi and Madam Fatima Afoko Mahama), my brothers (Justice, Roger and Essel), the Addo family (Accra-Ghana), the past and present class teachers of my daughter at St. Martin de Porres school (Dansoman, Accra-Ghana), Mrs. Ruth Abiodun (wife of my supervisor, Cape Town) and my friend/brother (Prophet Justice Essandoh) for their selfless support spiritually and physically.

I am thankful to the external examiner, Prof. J.A. Adedoyin (University of Botswana), representative of the School of Postgraduate Studies, Prof. E.O. Ogolo (FUTA) and other members of the examination panel, whose comments and suggestions strengthened the quality of this work.

Finally, with a joyous heart I give the biggest thanks to my lovely husband (Rev. Humphrey Teye Manso) and adorable daughter (Oforiwa Kumi Manso), for their prayers, support, love, endurance, tolerance and patience while mummy was far away from home. The journey has been tough, but we made it: Cheers!

I thank the Almighty God for His special grace and mercies in guiding me through this PhD journey. I am eternally grateful, Lord.

DEDICATION

To the cherished memory of my father, Mr. Amos Aworoh Frimpong. Unfortunately, you left at a young age, even before I started pre-school. Thirty-three years after your demise, I have obtained this PhD degree for you. I know you are very happy, wherever you are.

To my mother, Madam Martha Adwoa Kumi, who single-handedly funded my education to the university level: Your boundless sacrifices and efforts made it possible for me to reach this far.

To my husband Humphrey and daughter, Oforiwa.

ABSTRACT

Reliable prediction of seasonal rainfall is crucial for decision-making in various socio-economic sectors in West Africa, but obtaining reliable forecasts poses a big challenge to weather forecasters across the region, because their seasonal forecasts are mostly based on empirical models. While several recent studies are suggesting that the use of dynamic climates models may be a solution to the challenge, there is a dearth of information on how well these models simulate parameters like rainfall onset date (ROD), rainfall cessation date (RCD) and length of rainy season (LRS) over West Africa. The present study evaluates the performance of both global and regional climate models (GCMs and RCMs) in simulating these parameters over the study domain in the past and present climate. These datasets are from the China Meteorological Administration (CMA) Sub-seasonal to Seasonal (S2S) prediction, the UK Met Office Unified Model (MetUM), and 8 of RCMs that participated in the Coordinated Regional Climate Downscaling Experiment (CORDEX). The study also examines how a further modification of the Betts-Miller Janjic (BMJ) convective scheme in the Weather Research and Forecasting (WRF) model can improve the prediction of seasonal rainfall over West Africa. This study further assesses the potential impacts of 1.5°C and 2°C global warming levels (GWL15 and GWL20) on ROD, RCD and LRS in West Africa. Using common definitions within the sub-region, the simulated RODs, RCDs and LRS are compared with observation from satellite datasets, and the models' capability to reproduce the inter-annual variability of these parameters over the climatological zones in the sub-continent is statistically quantified. The impacts of GWL15 and GWL20 on each parameter were also quantified and compared. The outcomes of the study show that all the models have some biases in their simulations although they do produce convincing results. The

CMA model realistically simulates the observed spatial pattern and the interannual variability of RODs in the study area, as well as the observed seasonal movement of the West African Monsoon (WAM) and its associated rainfall patterns. The MetUM also reproduces the latitudinal progression of the observed RODs, RCDs and LRS over West Africa suitably, but performs poorly in simulating their inter-annual variability, even though there is improvement in the simulations of the new versions. It was also found that the CORDEX RCM ensemble correctly replicated and captured the essential features in the observed RODs, RCDs and LRS in the historical climate, and the RCM spread also enclosed the observed values. Most of the selected convection schemes reliably simulate the observed spatial distribution of RODs, RCDs, and LRS in the study area but overestimated the average monthly rainfall over the entire West African region. A new version of the BMJ scheme outperforms the default scheme in the sub-continent. The study project the western and eastern Sahel as hot-spots for a delayed ROD and reduced LRS in the 1.5°C and 2°C warmer climate under the Representative Concentration Pathway (RCP4.5 and RCP8.5) scenarios. The results of this study will be beneficial for agricultural and water resources planning decision-making and in reducing the impacts of global warming over West Africa.

TABLES OF CONTENTS

LIST OF TABLES

LIST OF FIGURES

LIST OF ACRONYMS

AEJ African Easterly Jet

AEJ-S Southern African Easterly Jet

AEW African Easterly Wave

ALADIN Aire Limitée Adaptation Dynamique Développement International (International Development for Limited-area Dynamical Adaptation)

AMMA African Monsoon Multidisciplinary Analysis

AOGCM Atmosphere Ocean General Circulation Model

BCC Beijing Climate Center

BM Betts-Miller

BMBF Federal Ministry of Education and Research the German Bundesministerium für Bildung und Forschung

BMJ Betts-Miller-Janjic

BoM Bureau of Meteorology

CAPE Convective Available Potential Energy

CCD Cold Cloud Duration

CCLM COSMO model in Climate Model

CDD Consecutive Dry Days

CFSR Climate Forecast System Reanalysis

CHIRPS Climate Hazard Group Infrared Precipitation with Stations

CHPC Centre for High Performance Computing

CMA China Meteorological Administration

CORDEX Coordinated Regional Climate Downscaling Experiment of Africa

CP Cumulus Parameterization

CRU Climate Research Unit

CSAG Climate Systems Analysis Group

CWD Consecutive Wet Days

DJFM December-February

DRR Disaster Risk Reduction

DEF Definition

ECMWF European Centre for Medium-Range Weather Forecasts

ERAIN ERA-Interim Reanalysis

ENSO El Niño Southern Oscillation

EPS Ensemble Prediction System

EUMETSAT European Organisation for the Exploitation of Meteorological Satellites

FCFA Future Climate for Africa

FUTA Federal University of Technology, Akure

GCM General Circulation Mode

GHG Greenhouse Gas

GPCC Global Precipitation Climatology Centre

GPCP Global Precipitation Climatology Project

GRP-WACS Graduate Research Program in West African Climate System

GTS Global Telecommunication System

GWL Global Warming Level

GWL15 Global Warming Level at 1.5°C

GWL20 Global Warming Level at 2°C

HadGEM Hadley Centre General Environmental Model

HIRHAM High Resolution Hamburg Model

ICTP International Centre for Theoretical Physics

IMPALA Improving Model Processes for African Climate

IPCC Intergovernmental Panel on Climate Change

IR Infrared

IRP IR Precipitation

ITCZ Inter-Tropical Convergence Zone

ITD Inter-Tropical Discontinuity

ITF Inter-Tropical Front

JJAS June July August September

KF Kain-Fritch

LLJ Low-Level Jet

LRS Length of the Rainy Season

LW Longwave

MetUM UK Meteorological Office Unified Model

MOSES Met Office Surface Exchange Scheme

MTJ Mid-tropospheric Jet

MYJ Mellor-Yamada-Janjic

NH Northern Hemisphere

NWP Numerical Weather Prediction

PBL Planetary Boundary Layer

PC2 Prognostic Condensate

RACMO Regional Atmospheric Climate Model

RCA Rossby Centre Regional Atmospheric Model

RCD Rainfall Cessation Date

RCM Regional Climate Model

RCP Representative Concentration Pathway

REMO Regional Model

RFE2 Rainfall Estimation Algorithm Version 2

RMSE Root Mean Square Error

ROD Rainfall Onset Date

RRTMG Rapid Radiative Transfer Model for Global models

S2S Sub-seasonal to Seasonal

SST Sea Surface Temperature

SW Shortwave

TC Tropical Cyclone

TEJ Tropical Easterly Jet

TKE Turbulence Kinetic Energy

TRMM Tropical Rainfall Measuring Mission

UCT University of Cape Town

UK United Kingdom

WAM West African Monsoon

WAMEX West African Monsoon Experiment

WASCAL West African Climate Service Centre on Climate Change and Adapted Land Use

WCRP World Climate Research Program

WMO World Meteorological Organisation

WRF Weather Research and Forecast

WWRP World Weather Research Program

CHAPTER ONE

INTRODUCTION

1.1 BACKGROUND TO THE STUDY

Rainfall plays a crucial role in the socio-economic activities of West Africa. In this region, major socio-economic activities, such as agricultural practices, hydro-electric power generation, and water-resource management are mainly rain-fed. So, decisions that are made in these socio-economic sectors depend primarily on rainfall characteristics, especially during the rainy season. For example, the scheduling of agricultural activities (from land preparation to crop selection, planting and harvesting) depends on the onset and cessation of the rainy season, as well as on the amount and distribution of the rainfall during the rainy season (Amekudzi *et al.*, 2015). The wrong timing of the onset of the rainy season or insufficient rainfall during a season pose a major risk to crop yields and can lead to food scarcity and famine (Nicholson *et al.,* 2000; Omotosho *et al.,* 2000; Abiodun *et al.,* 2008). In addition, most West African countries depend on hydro-electric power generation, meaning that any rainfall deficit in the seasonal rainfall amount may decrease the amount of energy supply for both domestic and industrial uses. A typical example of this occurred in Ghana in 2012 and 2015, when a reduction in the water level of the Akosombo hydropower systems led to severe power rationing and ultimately to the collapse of various companies in the country (GhanaWeb Opinions of Friday, 27 February 2015; Boakye *et al*. 2016; Abeberese *et al.* 2017). This led to a spike in unemployment in the country. Other impacts of rainfall deficit in West Africa include water conflicts and migration, as seen, for example, in the conflicts between the Fulani herdsmen and the people of Asante Akim North District in Ghana (Kuusaana and Bukari, 2015).

However, despite the importance of seasonal rainfall for socio-economic activities in West Africa, there is no reliable system for predicting the characteristics of seasonal rainfall over the region (Omotosho and Abiodun, 2007).

Most of the existing seasonal forecasting in many meteorological organizations is based on statistical and empirical equations derived from past seasonal climate data. Given the strong relationship between temperature and rainfall variability, there is a concern that ongoing global warming may further alter the characteristics of seasonal rainfall in the future. This could make the statistical forecasting of seasonal rainfall even less reliable in the future, when the empirical equation upon which the models are built may become even less reliable than they are at present. Hence, there is a strong need to use dynamic climate models for forecasting seasonal rainfall over West Africa. This thesis intends to improve knowledge in this area by assessing the capability of both global and regional dynamic climate models (GCMs and RCMs) to predict rainfall characteristics over the study domain; it also examines how further development of a convective scheme in RCM can improve the prediction of seasonal rainfall.

1.2 THE WEST AFRICAN CLIMATE

West Africa is characterized by two main seasons: the dry season (November-March, also known as the Harmattan period) and the rainy season (April-October, also known as the monsoon season). The dry season is dominated by hot and dry continental air masses (the north-easterly winds), which originate from the high-pressure system above the Sahara Desert and transport dust across the sub-continent. The rainy season

is dominated by the moisture-laden, tropical maritime or equatorial air masses, which produce south-westerly winds originating from the Atlantic Ocean (Nicholson, 2013). West African annual rainfall is almost constant along each latitude, but it decreases sharply from the south to the north. Based on the spatial distribution of the annual rainfall, this region is usually divided into three zones along the latitudes, namely: the Guinea (4°N–8°N), Savanna (8°N–12°N) and Sahel (12°N–20°N) zones (Figure 1.1). The Guinea zone, which is bordered by the Atlantic Ocean to the south, has a bimodal rainfall regime with a major season from March to June and a minor season from September to November. The Savanna, which is located north of Guinea Coast, has a unimodal rainfall regime. The Sahel zone also exhibits a unimodal regime from June to September. The annual rainfall ranges from between 1250 and 1500mm over the Guinea zone, between 750 and 1250 mm over the Savanna zone, and about 750mm over the Sahel zone. Hence, Guinea zone is the most humid of the three, and thus the most favourable zone for agriculture.

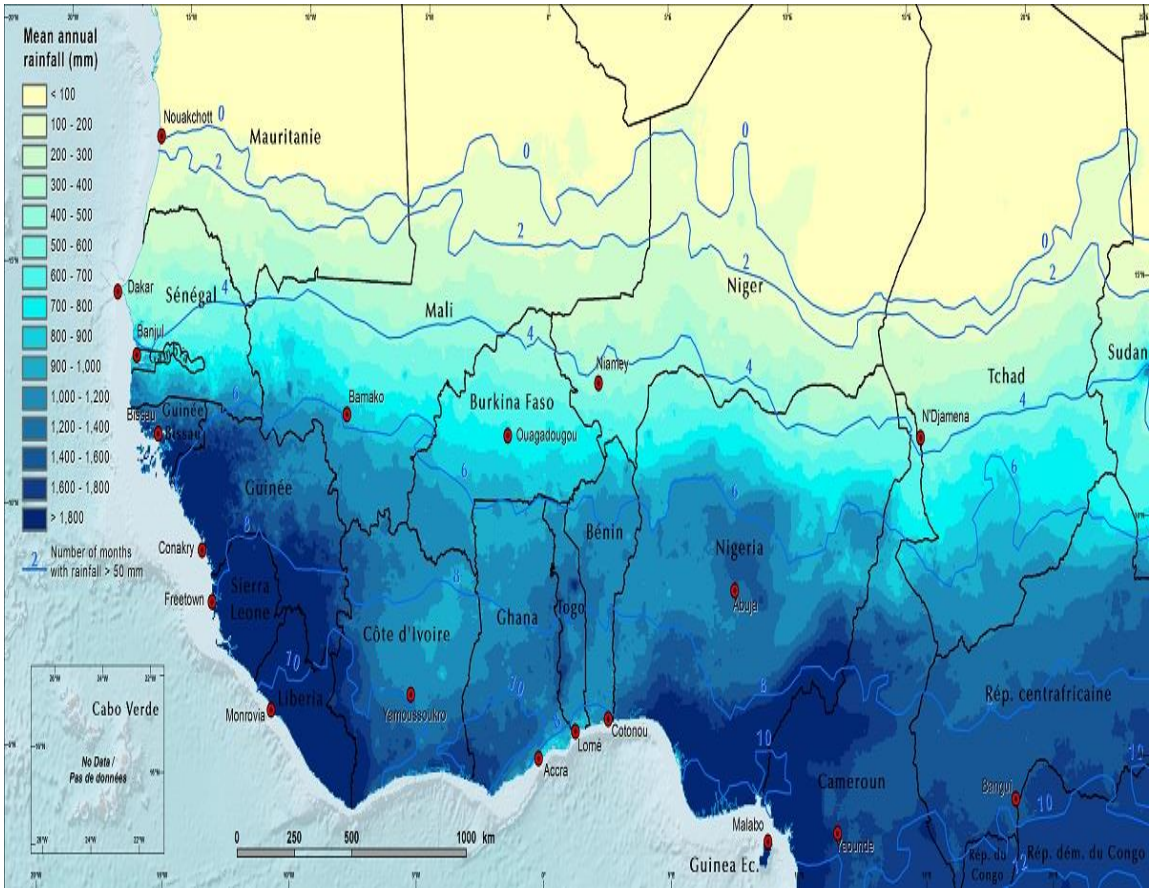

Figure 1.1: Map of West African Showing Mean Annual Rainfall.

Source: https://eros.usgs.gov/westafrica/node/157

1.3 CHARACTERISTICS OF SEASONAL RAINFALL THAT ARE IMPORTANT FOR AGRICULTURAL PRACTICES IN WEST AFRICA

In West Africa, seasonal rainfall has many characteristics that are crucial for socio-economic activities of the countries that make up this region. The most essential characteristics relevant for agricultural practices in West Africa are the rainfall onset date (ROD), rainfall cessation date (RCD), length of rainy season (LRS), consecutive wet days (CWD), consecutive dry days (CDD), wet spells, dry spells, extreme rainfall event and the total rainfall (RTOT). The description of these parameters are summarized in Table (1.1).

Table 1.1: Description of Important Seasonal Rainfall Characteristics for Agriculture.

Parameter	Description and Importance/Effect
Rainfall Onset Date (ROD)	ROD is the start or beginning of the rainy season. This is an event that occurs once in a year. Knowing ROD is important for planning farming activities across West Africa. It guides farmers in preparation of their farmlands, selection of crops or seeds, and for determining the optimal planting time (to avoid the risk of planting too early or too late).
Rainfall Cessation Date (RCD)	RCD is the end of the rainy season. It helps farmers to determine the type of seed to plant (e.g., long or short-lived plants, drought-resistant plant, etc).
Length of the Rainy Season (LRS)	LRS is the duration of the rainy season. It is usually obtained as the period between the RCD and ROD (i.e. RCD minus ROD). It is important for agriculture practice. A long LRS is good for food production and security, because many farmers take advantage to cultivate the old harvest and plant new crops within same season.
Consecutive Wet Days (CWD)	CWD is the maximum number of consecutive days with rainfall amount more than 1 mm. This information is good in selecting crops (or seed variety), because while some crops enjoy continuous rain (large CWD), some do not. Large CWD may be good in the beginning of the rainy season (because it softens the

	soil for effective crop germination), but it is not good in the flowering and harvesting stages.
Consecutive Dry Days (CDD)	CDD is the maximum number of consecutive days with rainfall amount less than 1 mm. It is a useful indicator for short drought period. Large CDD is not good in the beginning of the rainy season when continuous rainfall is needed to soften the soil for effective crop germination, but it is not good in the harvesting period.
Wet Spells	This is a period of 7 or more consecutive days of rainfall (at least 0.1mm) immediately preceded and followed by consecutive dry days. The duration of a wet spell is thus defined as the number of days between the two consecutive dry days. Wet spells are important between the time of sowing and the germination stage to aid crop survival.
Dry Spells	This is a period of more than 7 consecutive days of no rainfall within the rainy season. This is usually shorter and not as severe as a drought. Dry spells are useful in agriculture when crops are in the maturing stage because most crops do not need too much water. However, it causes serious crop failures.

Extreme Rainfall Event	An extreme rainfall event is said to occur when the rainfall amount in a day exceeds a given threshold (known as extreme rainfall threshold). The extreme rainfall threshold for an area can be a fixed value (e.g. 20 mm day^{-1}) or certain percentile (e.g. 90th or 95th) of daily rainfall for the area. Extreme rainfall is not good for agriculture. It can cause soil erosion and carry the soil away. This will loosen the roots and crops will fall down, affecting the growth and causing damage to the crops. It can also lead to flooding, loss of crops and livestock.
Total Rainfall (RTOT)	This is the accumulated rainfall amount over the rainy season. Given that the most West African rain occurs during the rainy season, the RTOT is almost the same as the annual total rainfall. However, RTOT determines the amount of water available for crop growth during the rainy season. Rain water that is not absorbed by the soil and plant roots runs into streams and rivers. Farmers can use such water to irrigate their crops later when there is not enough rain for their crops to grow.

1.4 PROCESSES INFLUENCING THE CHARACTERISTICS OF WEST AFRICAN RAINFALL

The West African rainfall regime is influenced by many processes. While some of these processes are located in West Africa, others are located outside the subcontinent. However, the influence of the remote processes (e.g., the African easterly jet, the tropical easterly jet and sea surface temperatures) on West African rainfall usually

comes through that of the local processes (e.g., the West African monsoon and the intertropical convergence zone). A brief description of some of these features (both local and remote) and how they influence the characteristics of rainfall are given below.

1.4.1 The West African Monsoon

The West African Monsoon (WAM) is a large-scale atmospheric circulation characterized by a seasonal reversal of winds, primarily due to the differential heating of the ocean and the land surface during the boreal summer (Afiesimama *et al.,* 2006; Sylla *et al.,* 2013a). This differential heating leads to a continent-maritime temperature gradient, which advects cool moist air (referred to as the monsoon) from the Gulf of Guinea onto the hot dry continent (Figure 1.2). The moist air, which is the main source of moisture over the sub-continent, produces a rain-band that travels from the Guinea Coast to the Sahel (from March to August) and retreats southward (from August to September) (Klein *et al.,* 2015). The northward progression of the monsoon with its high moisture content determines the rainfall onset date (ROD) over the subcontinent (Figure 1.2, left panel), while the southward retreat (Figure 1.2, right panel) influences the rainfall cessation date RCD. Hence, in order for a climate model to accurately simulate ROD, RCD and length of rainy season (LRD) over West Africa, the model must capture the meridional movement of the monsoon and the associated moisture transport. The present study investigates how well some contemporary models replicate the monsoon.

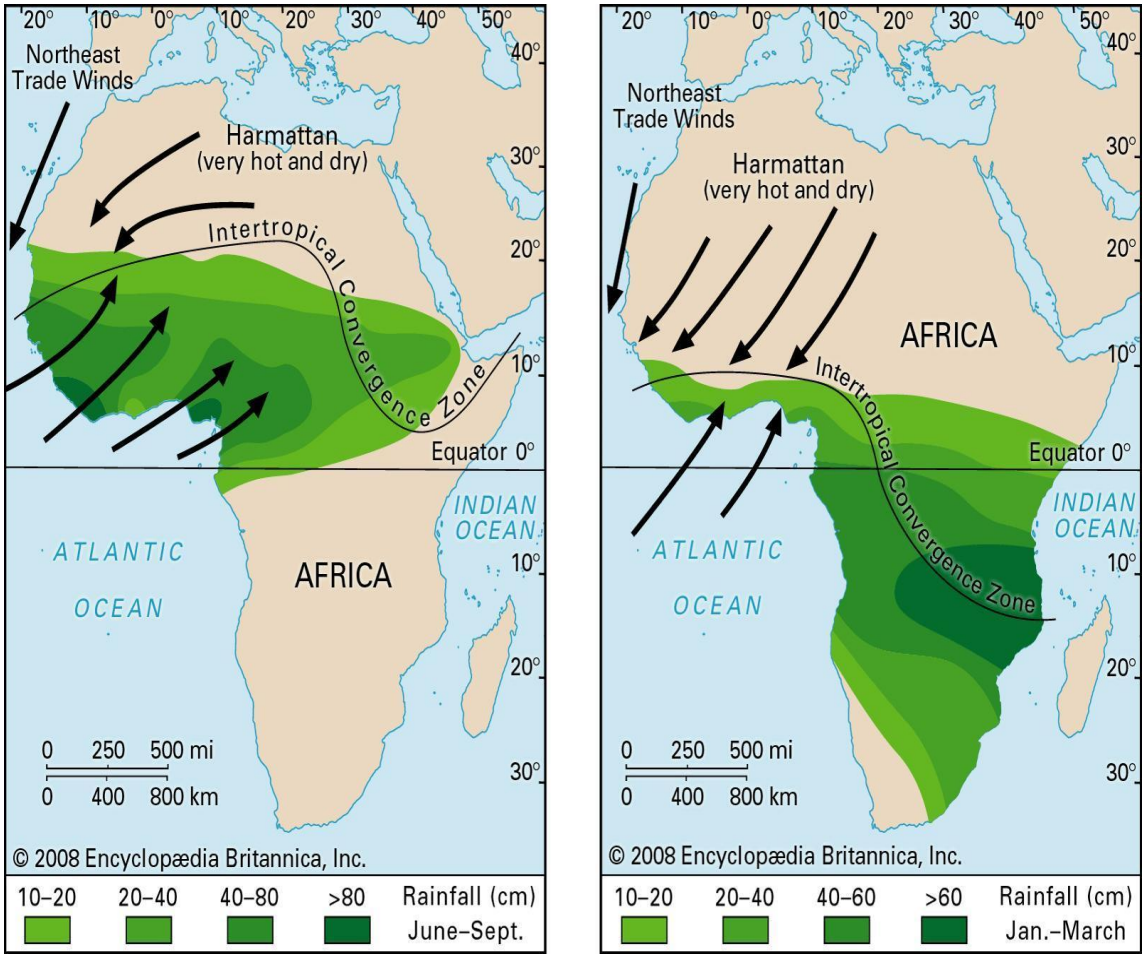

Figure 1.2: The West African Monsoon. The Left and Right Panels Describe the Wet and Dry Seasons Respectively, over West Africa.

Source: https://www.britannica.com

1.4.2 The Inter-Tropical Convergence Zone (ITCZ)

The intertropical convergence zone (ITCZ), a fundamental atmospheric feature over West Africa, is a line that separates the warm moist southwesterly monsoon flow (off the tropical Atlantic) from the much hotter and very dry northeasterly wind from the Sahara Desert (Issa Lélé and Lamb, 2010). The wet southwesterly monsoon flow forms a wedge into the dry northeasterly wind. The obvious consequence of this arrangement is the creation of a more or less pronounced 'humidity discontinuity' (Ilesanmi, 1971). Different names have been given to this boundary by researchers and weather forecasters working in the tropics. Some refer to it as the Inter-Tropical Convergence Zone (ITCZ; Figure 1.2), others call it the Inter-Tropical Discontinuity (ITD) or the Inter-Tropical Front (ITF), which accounts for the structure and behaviour of the boundary on both land and water. This boundary is, primarily, regarded as a region of 'maximum surface gradient'; a humidity discontinuity (Ilesanmi 1969). The term ITD is used to describe this moisture boundary on land (as proposed by the World Meteorological Organization's (WMO) Provisional Guide to Meteorological Practices. Rainfall over West Africa occurs a few hundred kilometres south of the ITD, where the monsoon wedge is deeper. However, the ITCZ (or ITD or ITF) migrates with the meridional movement of the monsoon flow. As rainfall over West Africa occurs a few hundred kilometres south of the ITD, where the monsoon wedge is deeper, the location of the ITD can be used to determine the ROD over West Africa.

1.4.3 The African Easterly Jet

The African easterly jet (AEJ) is an easterly wind maximum found around the middle troposphere over West Africa (Figure 1.3). The AEJ has been given different names by different authors. For example, Hastenrath (1996) described it as the West African mid-tropospheric jet (MTJ). During the West African monsoon experiment (WAMEX, 1978), it was referred to as a low-level jet (LLJ) because of its position relative to the upper-level tropical easterly jet (TEJ). The AEJ is a prominent feature of the complicated zonal wind structure that forms over northern Africa in summer (Cook, 1999). It is visible throughout the year but becomes relatively weak when located around 0°–5°N during the Northern Hemisphere (NH) winter. However, it strengthens during the NH summer and shifts to 10°–12°N, and the core speeds range from about 8m/s in October–March to 12m/s in June (Nicholson and Grist, 2003). The altitude of the core also changes during the year; it is at 600mb in April–September when the jet is relatively strong, and closer to 700mb during the months of October–March, when the AEJ is relatively weak.

The AEJ has been associated with deep convective activities, such as squall lines and thunderstorms over West Africa. The location and strength of the jet are some of the features for determining the rainfall pattern over West Africa (Afiesimama, 2007). It is noted that the rain-belt (especially over the Sahel) is most intense when the AEJ is well developed, so it appears that the jet modulates the development of the rainy season (Nicholson and Grist, 2003). The clearest example of this is the fact that the AEJ controls the development and organization of rain-bearing systems via the generation of waves. Since the jet has similar characteristics to the ITD in its annual cycle, whose position determines the different weather zones of the region, the jet's meridional oscillation and strength need to be examined carefully for accurate

prediction of weather and climate (e.g., onset and cessation of rainfall, total rainfall, wet spells, dry spells, etc). This study evaluates the ability of some of the dynamic models (specifically the ones used in this thesis - see Section 4.3.2) to simulate the AEJ in relation to RODs.

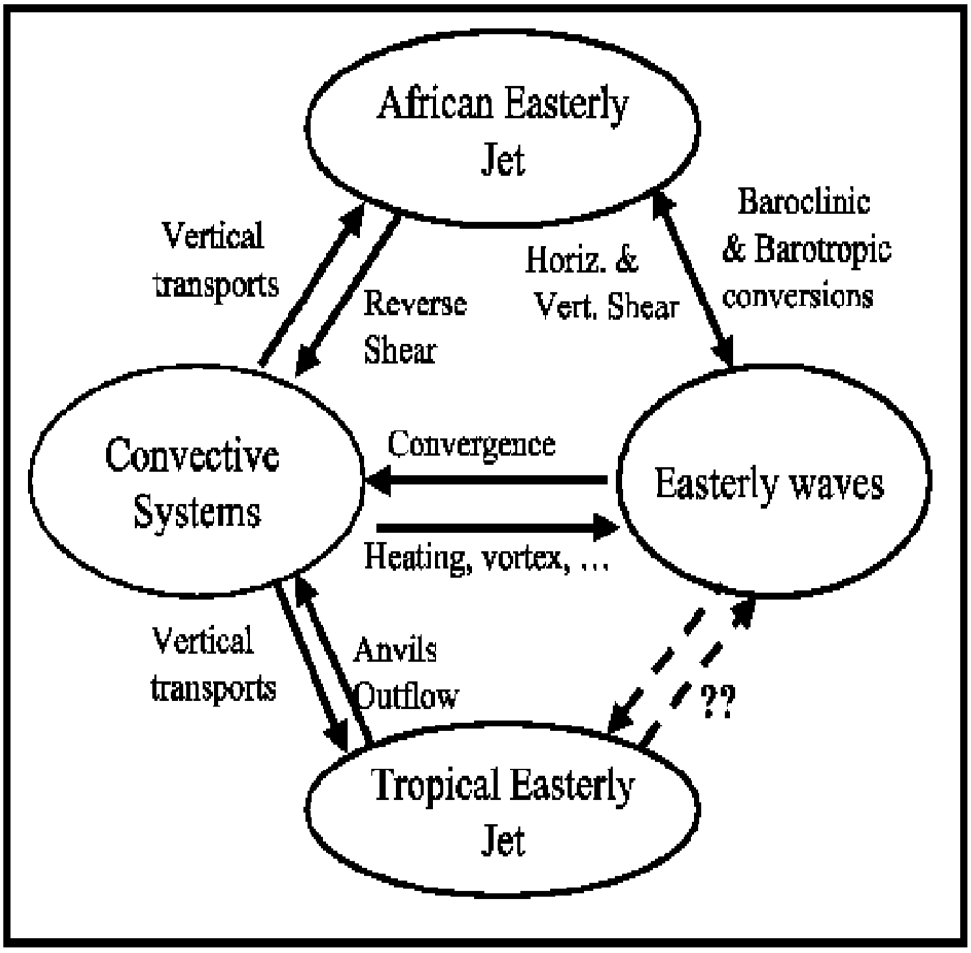

Figure 1.3: Interactions between the Main Atmospheric Features observed over West Africa. Source: Redelsperger et al. 2002.

1.4.4 The Tropical Easterly Jet

The tropical easterly jet (TEJ) stream (Figure 1.3) is one of the most intense circulation features over Africa (Nicholson *et al.*, 2007), and is one of the features of the WAM system. The TEJ is produced as a result of the strong upper tropospheric anticyclone above the Tibetan plateau. It is a summer-time upper-tropospheric (100-200 hPa) easterly wind between 5° and 20°N (Lemburg *et al.*, 2017). This jet lies in the upper troposphere and originates in the South Asian Monsoon system over the Bay of Bengal; it extends westwards to Africa and decays over the tropical Atlantic, reaching core speeds of more than 35m/s (Nicholson *et al.*, 2007). The TEJ core strengthens from May to September, with a maximum intensity during the regional rainy season-summer months of June-September (JJAS). Starting from May, the tropical easterlies increase promptly as the jet stream moves northward. The jet is intense between latitudes 13°N and 3°S in the months of June through September (Okonkwo *et al.*, 2014), before weakening and disappearing in October. There is a positive correlation between Sahel rainfall and the strength of the West-African TEJ in the seasonal mean. It was suggested (Grist and Nicholson, 2001; Lemburg *et al.*, 2017) that a strong TEJ can enhance rainfall (e.g., total rainfall, wet spells and consecutive wet days) by increasing upper-level divergence. However, it is also possible that a TEJ anomaly is a consequence of increased rainfall (e.g., extreme rainfall events) or that both TEJ anomalies and extreme rainfall events are governed by an external quantity (Lemburg *et al.*, 2017). Grist and Nicholson (2001) believe that the TEJ tends to be viewed as a passive system over Africa, even though its intensity is one of the strongest contrasts between wet and dry years in West Africa. Hence, the TEJ may be a critical factor in the development of the rainy season and the overall climate in West Africa (Nicholson *et al*. 2007). There is therefore a need to study its dynamics and the

ability of the dynamic models to simulate the TEJ in relation to the WAM characteristics.

1.4.5 Sea Surface Temperatures

Sea Surface Temperature (SST) anomalies have a significant influence on West African rainfall. Global SST anomalies have been statistically associated with dryness over Sahelian Africa (Ward, 1998; Vizy and Cook, 2001). It is documented that there is a relation between Sahel droughts and El Niño Southern Oscillation (ENSO) anomalies through upper and lower tropospheric dynamics (weakened TEJ and enhanced north-easterlies), as well as with the South Atlantic SST through lower tropospheric dynamics (weakened monsoon flow). Droughts (e.g., consecutive dry days) and floods (e.g., consecutive wet days) over West Africa have also been associated with SST anomaly patterns (Fontaine and Janicot, 1996). Although many studies have emphasized the important role of SSTs on West African rainfall, Camberlin *et al*. (2001) admitted in their study that the rainfall variance explained by large-scale SST anomalies seldom reaches 50%, and that other regional or large-scale features must be considered too.

The influence of these climate drivers (and many others) on the West African rainfall characteristics contributes to some of the challenges faced when attempting to make reliable predictions of rainfall onset and cessation dates in this region. The ability of contemporary climate models to simulate these characteristics will be investigated in the present study.

1.5 JUSTIFICATION FOR THE STUDY

West African rainfall, which plays a crucial role in the socio-economic activities of many countries in that region, exhibits high inter-annual and decadal variability due to complex interactions among many processes induced by atmosphere-ocean coupling, topography, and atmosphere-biosphere exchanges. In addition, due to ongoing global warming, West Africa has experienced significant changes in rainfall patterns in recent times, and there are indications that such changes may continue into the future, as global warming persists. The variability of rainfall and changes in rainfall patterns pose particular challenges to agriculture (which is the backbone of many economies in the region) and energy supply across many of the countries in this region. The reliable prediction of seasonal rainfall characteristics will reduce the vulnerability of agriculture to rainfall variability and changes, as it will assist farmers to adjust their management decisions in order to increase their yields or incomes, and also to increase the efficiency of agricultural inputs (Hansen, 2002, 2005; Ingram *et al.*, 2002; Jagtap *et al.*, 2002; Nelson *et al.*, 2002; Philips *et al.*, 2002; Podestá *et al.*, 2002).

While there are several seasonal forecasting models (based on both empirical and dynamic models), only a few studies have examined their ability to simulate the characteristics of West African rainfall accurately and to link them to associated features that influence the rainfall characteristics (Sarria-Dodd and Jolliffe, 2001; Ati *et al.*, 2002; Omotosho *et al.*, 2000). Also, several advances have been made with regard to further developing GCMs to improve the prediction of seasonal rainfall, but there is still a dearth of information as to how the development efforts are able to improve the simulation of seasonal rainfall characteristics in West Africa. A comprehensive evaluation of the old and the new versions of the climate models is thus needed.

1.6 AIM AND OBJECTIVES

The aim of this study is to improve the prediction of seasonal rainfall over West Africa using dynamic climate models.

Objectives:

The main objectives of this study are to:

a) evaluate the capability of the CMA S2S model (GCM) to simulate seasonal rainfall characteristics over West Africa;

b) examine how a further development of the MetUM (GCM) is able to improve the simulation and prediction of seasonal rainfall over West Africa;

c) assess how well the contemporary RCMs simulate the characteristics of seasonal rainfall over West Africa;

d) determine the sensitivity of seasonal rainfall characteristics to convective schemes in the WRF model (RCM);

e) examine how a further modification of a convective scheme could improve the prediction of seasonal rainfall by the WRF model (RCM); and

f) assess the impact of climate change on the characteristics of seasonal rainfall over West Africa.

1.7 RESEARCH QUESTIONS

To contribute towards improving the prediction of seasonal rainfall over West Africa, this thesis seeks to address the following questions:

a) How well does a modern-day GCM simulate rainfall characteristics in West Africa?

b) How well does a further development of the MetUM improve the simulation of seasonal rainfall predictions in West Africa?

c) How well do frequently used RCMs simulate rainfall characteristics in West Africa?

d) How sensitive is the simulation of rainfall characteristics to different convection schemes in the WRF model?

e) To what extent can alterations in the convection scheme of the WRF model improve the simulation of rainfall characteristics over West Africa?

f) What are the potential impacts of climate change on the rainfall characteristics over West Africa?

1.8 STRUCTURE OF THE THESIS

The chapters in the thesis are structured as follows:

Chapter 2 reviews the literature on the following relevant topics: (1) prediction of seasonal rainfall over West Africa; the use of GCMs and RCMs, (2) international experiment of climate models over West Africa, (3) improvement and application of climate models over West Africa, (4) challenges in respect of the prediction of rainfall over West Africa, (5) the impacts of climate change and global warming on West African rainfall characteristics.

Chapter 3 provides information on the different datasets and methodology used in the study. The definitions used to classify rainfall onset and cessation dates, as well as the length of the rainy season, are outlined in this chapter.

Chapter 4 presents the results of this study and discusses the findings from Chapter 3, giving a detailed analysis of the findings from each of the specific objectives of this thesis, as articulated in Section 1.6 above.

Chapter 5 presents the summary and conclusions of the study, as well as making recommendations and suggestions with regard to future work in the study domain.

CHAPTER TWO

LITERATURE REVIEW

This chapter reviews previous studies on the dynamic modelling of rainfall characteristics over West Africa. The chapter also reviews several related studies on seasonal climate prediction, challenges in generating such forecasts and the impact of climate change and global warming on the rainfall characteristics of West Africa.

2.1 PREDICTION OF SEASONAL RAINFALL OVER WEST AFRICA

Several studies have documented different methods used for forecasting seasonal rainfall over West Africa (e.g., Omotosho, 1990, 1992; Roncoli *et al.*, 2002; Omotosho and Abiodun, 2007; Mounkaila *et al.*, 2014). Some of these studies (e.g. Roncoli *et al.*, 2001a; Roncoli *et al.*, 200lb; Ingram *et al.*, 2002; Roncoli *et al.*, 2002) discussed the use of so-called 'traditional method' by most farmers in West Africa. With traditional methods, for instance, local rainfall forecasts rely on the observation and interpretation of specific phenomena. These phenomena may be features in the surrounding landscape (e.g., trees, animals, and sky) or spiritually manifested in the form of divination, visions, or dreams. For example, Roncoli *et al*. (2001a) showed that farmers use the fruit production of certain trees as an indicator for the onset of the rainy season and for an indication of temperatures (either high or low) during the dry season. Similarly, Roncoli *et al*. (2002) indicated that farmers also observe the intensity and direction of winds, and the behaviour of birds and insects throughout the year. However, farmers are also eager to receive scientific information, because

forecasts from traditional method are becoming less reliable due to increasing climate variability (Roncoli *et al.,* 2002).

Most studies have used or adopted statistical methods or empirical models for seasonal forecasting over West Africa (e.g., Omotosho, 1990, 1992; Janicot *et al.,* 1998; Omotosho *et al.,* 2000; Sarria-Dodd and Jolliffe, 2001; Ati *et al.,* 2002; Leduc-Leballeur *et al.,* 2013). In these methods, the seasonal prediction models are built on the empirical relationship between rainfall and other climate variables (e.g., sea surface temperature, African easterly jet, tropical easterly jet, Saharan heat low), which are known to influence the onset of rainfall. For example, Omotosho *et al.* (2000) used surface data (e.g., daily mean values of surface pressure, temperature and relative humidity) to predict the onset and cessation of the rainy season and the total rainfall amount for the season over West Africa. Leduc-Leballeur *et al*. (2013) also used SST, surface wind vectors and daily rainfall data to investigate the role of air-sea interaction mechanisms in the coastal precipitation of the Gulf of Guinea. However, these authors also acknowledge the limitations of using empirical methods for seasonal prediction, which includes the inability to quantify or account for the effect of various atmospheric processes (as stated in Section 1.4 above) that influence precipitation or the start of the monsoon season over West Africa. Hence, the predictive skills of empirical models in forecasting rainfall characteristics are usually low.

To overcome the shortcomings of the empirical models, recent studies are now adopting the use of dynamic models for seasonal forecasts over the sub-continent (e.g., Cook and Vizy, 2006; Djiotang *et al.,* 2010). The use of the dynamic approach for

seasonal forecasting can be divided into two groups: the global climate model group and the regional climate model group.

2.1.1 Seasonal Prediction using Global Climate Models

Several studies have adopted the use of GCMs to simulate rainfall characteristics, both globally and regionally. For example, Piedelievre (2000) evaluated the potential predictability of seasonal and monthly time-scales of some GCM predictions globally and found that the models' performance could be improved by increasing the ensemble size and by merging different models. Kulkarni *et al*. (2012) also used GCMs to generate probabilistic predictions of the Indian summer monsoon rainfall. Although they found improvements in the skill of the probabilistic forecasts, they also acknowledged that the skill and accuracy of these predictions was too low. They thus suggested that predictions from such modelling systems could be made more useful by developing appropriate probabilistic schemes, in order to provide the user community with uncertainties in the predictions. Cook and Vizy (2006) simulated the WAM system for the 20^{th} and 21^{st} centuries using some coupled GCMs and found that most of the GCMs failed to capture the precipitation maximum of the WAM system. Similarly, Kim *et al*. (2010) investigated the effects of aerosol-radiative forcing on the diurnal and seasonal cycles of precipitation over West Africa and the eastern Atlantic Ocean using GCM simulations. The authors concluded that their results were useful because they agreed with other modelling results, although there were notable biases. However, GCMs usually have a coarse horizontal grid resolution and therefore cannot represent the influence of mesoscale features (such as isolated reliefs, lakes, coastlines and sharp variations in vegetation, temperature and soil moisture) on the climate systems very accurately (Pohl and Douville, 2011).

2.1.2 The use of Regional Climate Models over West Africa

To address the limitations of the GCMs with regard to their low resolution, many studies downscale GCM simulations with RCMs which have a higher resolution. Many authors have used RCMs to simulate the intra-seasonal, inter-annual and decadal variability of rainfall, as well as the characteristics of the WAM system (e.g., Afiesimama *et al.*, 2006; Omotosho and Abiodun, 2007; Sylla *et al.*, 2009; Pu and Cook, 2010; Meynadier *et al.*, 2010; Abiodun *et al.*, 2012). Typical among such studies is that of Afiesimama et al. (2006), which examined the ability of the International Centre for Theoretical Physics (ICTP) RegCM3 to capture the mean climate characteristics of the West African climate system with an emphasis on the rainy season. Their study focused on the period 1981–1990, during which there was anomalously low rainfall over West Africa, in fact, rainfall was below the long-term means nearly everywhere in several individual years. They concluded that the simulation produced encouraging results and suggested that there was a good potential for using this regional climate model (RegCM) to study climate variability and physical processes over West Africa. Nevertheless, their study also found a few discrepancies between the model output and the observations; the simulations tended to overestimate rainfall along the Guinea Coast and to underestimate rainfall in the Sahel. In other words, the model produced more frequent rains over the coast than was actually the case. Temperatures along the Guinean coast were also comparatively lower in the model by about 1-2°C than they were in reality.

Omotosho and Abiodun (2007) used an RCM to simulate the characteristics of the moisture build-up and rainfall over West Africa. They examined the mechanism and variability of the influx of moistness over West Africa over a 21-year period (1980 - 2000), using the ICTP regional climate model known as RegCM3. Their results

showed that the RegCM3 model is good at reproducing rainfall and moisture patterns over West Africa, particularly over the Sahel and Savanna zones. However, they also discovered some discrepancies in the RCM simulations, which suggest that it is necessary to improve the model for better prediction of the onset of the rainy season in West Africa.

Other studies have used RCMs to simulate the characteristics of West African climate (Sylla *et al.,* 2009; Pu and Cook, 2010; Meynadier *et al.,* 2010), as well as the entire African climate (Sylla *et al.,* 2010); all of them have concluded that the RCMs used in their respective studies showed a relatively good performance over West Africa as well as over the larger African domain. Abiodun *et al*. (2012) also used an RCM (specifically RegCM3) to model the impacts of reforestation on the future climate (2031 - 2050) of West Africa. In their conclusion, they asserted that the RegCM3 model gave a credible simulation of the West African climate, in agreement with previous studies. Despite such positive findings, almost all the authors mentioned above recommended improvements in these RCMs (particularly the convection schemes) over West Africa. The present study thus adopts and evaluates both GCM and RCM methods to study the characteristics of seasonal rainfall over West Africa.

2.2 INTERNATIONAL EXPERIMENT OF CLIMATE MODELS OVER WEST AFRICA

Various international experiments have been conducted to improve rainfall prediction over Africa, and especially over West Africa. Some of these experiments are reviewed in this section.

2.2.1 African Monsoon Multidisciplinary Analysis (AMMA) Experiment

The African Monsoon Multidisciplinary Analysis (AMMA) was one of the biggest programmes of research into environment and climate ever attempted in Africa (e.g., Level *et al.,* 2010; Bechara *et al.,* 2010). The AMMA program aimed to provide a better understanding of the WAM and its underlying physical, chemical and biological processes (Janicot *et al.,* 2008). This intensive field campaign took place during the summer of 2006 to better document specific processes and weather systems at various key stages of that year's monsoon season. Moreover, the campaign was embedded within a longer observation period that documented the annual cycle of surface and atmospheric conditions between 2005 and 2007. Other field work also took place under the AMMA project. For instance, Mari *et al.* (2008) described a forecasting tool that was developed to predict the intrusions of the southern hemispheric fire plumes into the Northern Hemisphere during the fourth airborne campaign of the AMMA. The authors found that the footprint of the biomass burning plumes over the Gulf of Guinea showed clearly marked intraseasonal variability. The study thus emphasised the role of the Southern African easterly jet (AEJ-S) in the transport of the southern hemispheric biomass burning plumes during the wet summer-season in West Africa, which leads to the accumulation of pollutants over the continent. The authors concluded that continental circulation increased the possibility for the biomass burning plumes to reach the convective regions located further north. Sow *et al*. (2009) also analysed three major dust events during the 2006 and 2007 AMMA special observation periods in order to study the potential impact of wind speed on the initial size distribution of emission fluxes in Niger. The individual experiments under the AMMA project contributed significantly towards an understanding of the West African climate system.

2.2.2 Coordinated Regional Climate Downscaling Experiment (CORDEX)

An earlier study (Giorgi *et al.*, 2009) described the CORDEX program as an international coordinated framework that was sponsored by the World Climate Research Program (WRCP). According to Giorgi *et al*. (2009), the Phase 1 experiment of CORDEX had a two-fold purpose. Firstly, to provide a framework to evaluate and benchmark the performance of climate models (i.e., the model evaluation framework), and secondly, to design a set of experiments to produce climate projections for use in impact and adaptation studies (i.e., the climate projection framework), as shown in Figure 3.1. With its goal of providing a framework that would be accessible to the broader scientific community with the maximum use of results, the CORDEX domains therefore encompassed the majority of the world's land areas, with a standard horizontal resolution of ~50 km (or 0.5 degrees). The CORDEX experiment covered five regional domains, namely, the entire African, Australian, South American, North American and European continents (Giorgi *et al.*, 2009).

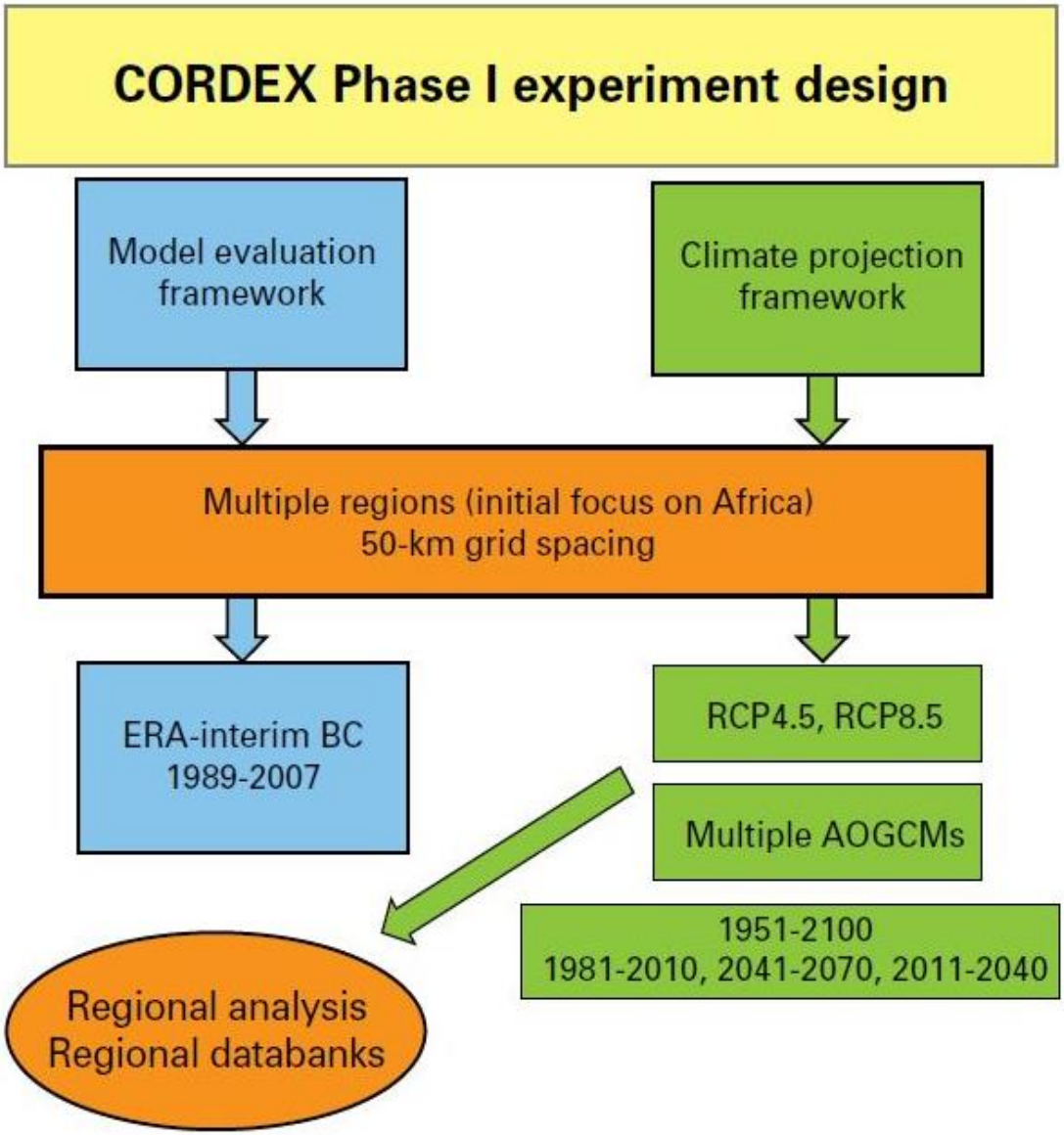

Figure 2.1: Schematic Depiction of the first Phase of CORDEX Experiment Set-up.

Adopted from Giorgi *et al.*, 2009.

In order to achieve the goals of the CORDEX experiment, it was useful to test the framework for a single region in order to assess its strengths and weaknesses before applying it worldwide. The African continent (about 25°W-60°E and 44°S-42°N; Figure 2.2) was thus selected as the first target region for several reasons: its vulnerability to climate variability and climate change, its low adaptive capacity and the projected impact of climate change on its economies (Giorgi *et al.*, 2009, Nikulin *et al.*, 2012). The sub-region in the ten boxes (Figure 2.2) shows the evaluation zones in Africa (e.g. East Africa (EA), Central Africa (CA), West Africa (WA) and South Africa (SA)). (Adopted from Mounkaila's thesis, 2015).

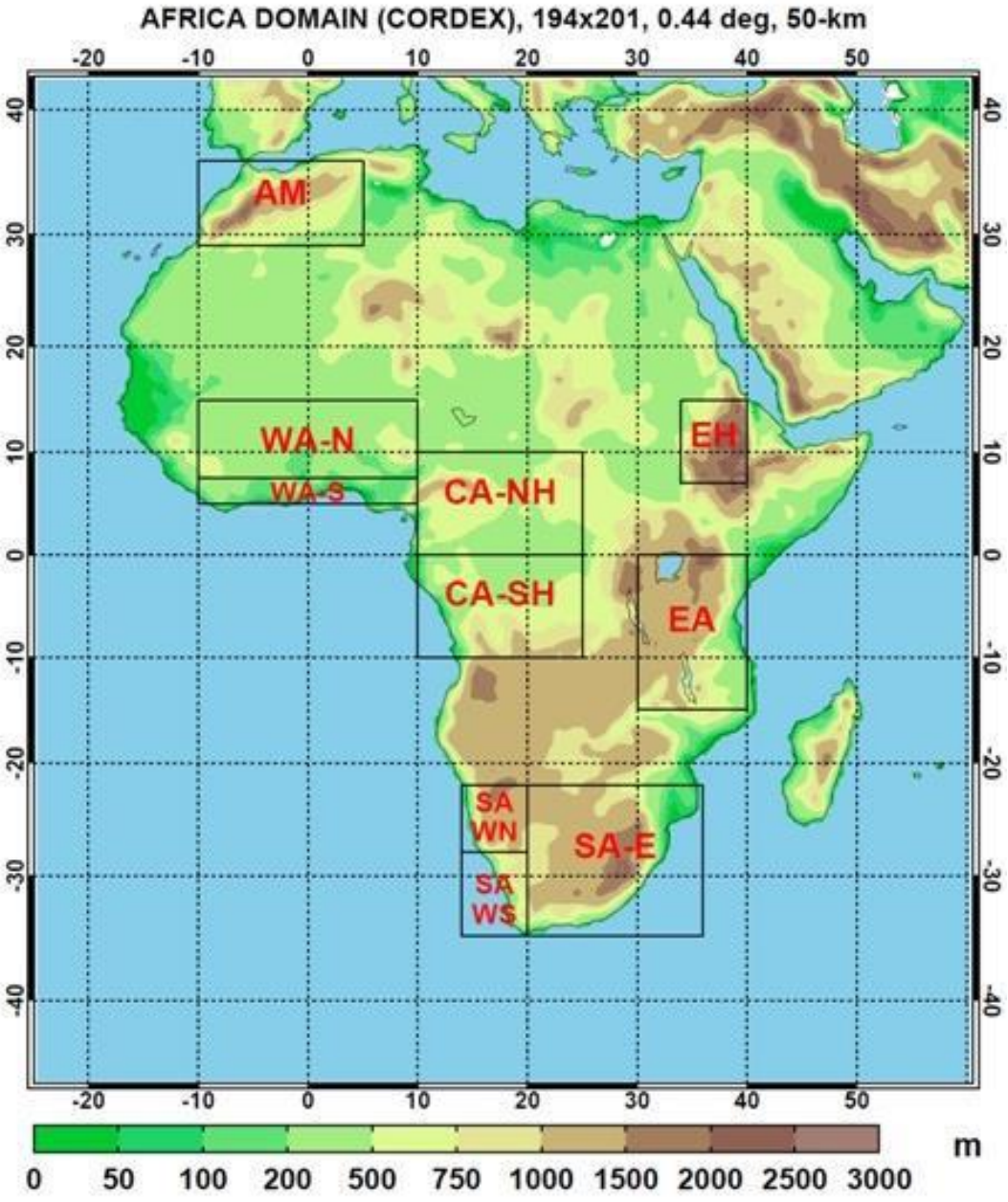

Figure 2.2: Orography (in meter) of the CORDEX Africa Evaluation Domain.

Several studies have analysed the CORDEX datasets over West Africa for the past, present and future climates. For example, Nikulin *et al*. (2012) used the CORDEX data to study precipitation climatology over the African domain (including West Africa); the results showed that the ensemble mean presented the best simulated WAM precipitation albeit with some biases. Abiodun *et al*. (2017) also used CORDEX data to simulate the potential impacts of climate change on extreme precipitation over four coastal African cities (namely, Cape Town, Maputo, Lagos and Port Said). They concluded that the CORDEX simulations were correctly able to reproduce the characteristics of extreme precipitation over the cities selected for their study, with biases within the observation uncertainties. Similarly, Klutse *et al*. (2016) simulated the daily characteristics of the West African summer monsoon using the CORDEX simulations and concluded that the study produced encouraging results. As part of the research for the present PhD study, Kumi and Abiodun (2018) used the CORDEX data to simulate the potential impacts of global warming on the RODs, RCDs and LRS in West Africa. The results of their study and an additional analysis done in this geographical area will be presented in the results and discussion chapter (Chapter 4).

2.2.3 Sub-seasonal to Seasonal (S2S) Prediction Project

Many researchers see the Sub-seasonal to Seasonal (S2S) model dataset as a new frontier for atmospheric research. Olaniyan *et al*. (2018) indicated that the increasing demand for reliable forecasts around the globe has led to various seasonal climate prediction datasets being made publicly available for evaluation. An example of such a dataset is the European Centre for Medium Range Weather Forecasting (ECMWF) S2S model output data. Researchers in different areas of the world have examined the

predictive skills of the S2S models for different purposes. For instance, Lynch *et al*. (2014) found that the ECMWF S2S model had statistically significant skill in predicting the weekly mean wind speeds over various areas of Europe at lead times of at least 14–20 days. Over Australia, White *et al*. (2015) used forecasts from the Australian Bureau of Meteorology's (BoM) S2S timescales to examine how the forecasting of flood events across a range of prediction timescales could be beneficial in Australia for disaster risk reduction (DRR) activities, emergency management and response, and strengthening community resilience. Across Africa, Tompkins and Giuseppe (2015) used the ECMWF S2S rainfall and temperature data to investigate the forecasting of advanced warnings with regard to the spread of malaria in an idealized experiment. Based on their preliminary examination of the forecasts, they found that, the ECMWF S2S data were able to predict the years during the last two decades in which documented malaria outbreaks occurred in Uganda and the highlands of Kenya.

Some studies have also been done over West Africa using the ECMWF S2S data (e.g., Tompkins and Feudale, 2010; Olaniyan *et al.,* 2018). Tompkins and Feudale (2010) evaluated the ECMWF operational Seasonal Forecast System (SYS3) at a lead-time of 2-4 months in a 49-yr hindcast dataset, to simulate the WAM precipitation. The authors found that the SYS3 reproduces the progression of the WAM, albeit with some differences in respect of the climatology. Olaniyan *et al*. (2018) also evaluated the predictive skill of the ECMWF-S2S precipitation forecasts during the peak of the WAM in Nigeria, using station data and a 10-member ensemble of the ECMWF S2S forecasts, from the Ensemble Prediction System (EPS) version of the ECMWF. They concluded that the model was incapable of accurately predicting wind strength at the 700mb level to depict the AEJ, but that it was capable of adequately and reliably

predicting the latitudinal positions of the ITD, as well as the mean sea level pressure component of the thermal lows and the SST anomalies over the Pacific and Atlantic Oceans. So far, however, no study has investigated the ability of the S2S model output data to accurately predict the onset of rainfall in lead-time in the West African region.

2.2.4 Improving Model Processes for African Climate (IMPALA) Project

The IMPALA (Improving Model Processes for African cLimAte) project is part of the Future Climate for Africa (FCFA) program (James *et al.*, 2018). "The aim of the project was to deliver a step change in global model climate prediction for Africa on the 5-40 year timescale by delivering reductions in systematic model errors, resulting in reduced uncertainty in respect of predictions of African climate and enabling improved assessment of the robustness of multi-model projections for the continent" (FCFA IMPALA Interim Progress Report, 2016). The project focused on the UK Met Office Unified Model (MetUM), "at the beginning of a four-year effort to improve its ability to simulate the African climate" (James *et al.*, 2018). James *et al*. (2018) saw the MetUM as a "fitting example, since it was already subject to well-established evaluation procedures, and there was a good baseline understanding of the model's performance, yet important gaps exist in the analysis of the processes that matter for Africa".

Davies *et al.* (2005) described the MetUM as a numerical model of the atmosphere that could be used for both weather and climate applications. It is in continuous development by the Met Office and its partners, which are adding state-of-the-art understanding of atmospheric processes to new releases (the UK Met Office, https://www.metoffice.gov.uk). "This is designated as the global numerical weather

prediction (NWP) cycle G53. Its dynamical core uses a semi-implicit semi Lagrangian formulation to solve the non-hydrostatic, fully compressible deep atmosphere equations of motion discretized onto a regular longitude/latitude grid. The radiation scheme employed is the two-stream radiation code of Edwards and Slingo (1996) with six and nine bands in the shortwave (SW) and long-wave (LW) parts of the spectrum respectively. The atmospheric boundary layer is modelled with the turbulence closure scheme of Lock *et al*. (2000) with modifications described in Lock (2001) and Brown *et al*. (2008), whilst the land surface and its interaction with the atmosphere are modelled using the Met Office Surface Exchange Scheme (MOSES, Cox *et al.*, 1999). Convection is represented with a mass flux scheme based on Gregory and Rowntree (1990) with various extensions to include down-draughts (Gregory and Allen, 1991) and convective momentum transport. Large-scale precipitation is modelled with a single-moment scheme based on Wilson and Ballard (1999), whilst cloud is modelled using the prognostic cloud fraction and prognostic condensate (PC2) scheme (Wilson *et al*. 2008a, b). The horizontal grid spacing used is 0.375° ×0.5625°, which corresponds to a resolution of approximately 40 km in the mid-latitudes" (Mulcahy *et al.*, 2014: page 4751).

2.3 IMPROVEMENT AND APPLICATION OF CLIMATE MODELS OVER WEST AFRICA

Many researchers have studied different components of climate models and have shown that cumulus (convective) parameterization is a major source of errors in models (both GCM and RCM); (Leung *et al.,* 2004; Im *et al.,* 2008). These studies showed that convective parameterization (CP) is one of the most important physical

processes in climate models when simulating monsoon rainfall. Flaounas *et al*. (2011), who examined the impact of various physical schemes in the Weather Research and Forecasting (WRF) model, argued that CP schemes strongly influence the dynamics and the variability of precipitation. Skamarock *et al*. (2005) described CP schemes as being responsible for the sub-grid-scale effects of convective and/or shallow clouds. According to them, convection schemes are intended to represent vertical fluxes due to unresolved updrafts and downdrafts and compensating motion outside the clouds. They thus stated that cumulus parameterizations are theoretically only valid for coarser grid sizes, (e.g., greater than 10 km), where they are necessary to properly release latent heat in the convective columns at a realistic time scale. Sometimes these schemes have been found to be helpful in triggering convection in 5–10 km grid applications. Previous studies (e.g., Fonseca *et al.*, 2015) have shown that there are essentially two widely used types of CP schemes in weather and climate models: firstly, mass-flux or moisture convergence schemes (e.g., Arakawa and Schubert, 1974; Kain and Fritsch, 1990, 1993; Kain, 2004; Emanuel, 2001), and secondly, adjustment schemes (e.g., Betts, 1986; Betts and Miller, 1986; Janjic, 1994). In the former (mass-flux schemes), a one-dimensional cloud model is used to compute the updraft and downdraft mass fluxes, and processes such as entrainment and detrainment are also normally considered. In contrast to these increasingly complex parameterizations, which can involve detailed models of cloud processes, convective adjustment schemes take an 'external' view of convection and simply relax the large-scale environment towards reference thermodynamic profiles. This study examines some of the convection schemes in the WRF model and further assesses how altering some of the parameters in the Betts-Miller-Janjic (BMJ) scheme will influence the prediction of rainfall characteristics.

2.3.1 The Kain-Fritch Convective Scheme

Some authors have responded to the recommendations that CP schemes in RCMs need to be improved and have conducted studies in that direction. For example, there have been some modifications to the Kain-Fritch (KF) scheme (e.g., Kain, 2004) in the last decade. Nonetheless, several authors have suggested that further improvements to the KF scheme were still possible, although this scheme did appear to be more accurate in simulating rainfall (Ma and Tan, 2009; Huang and Gao, 2017; Stergiou *et al.*, 2017). According to Kain (2004), the KF scheme was a mass-flux parameterization, which used the Lagrangian parcel method (e.g., Simpson and Wiggert, 1969; Kreitzberg and Perkey, 1976), including vertical momentum dynamics (Donner, 1993), to estimate whether instability existed, whether any existing instability would become available for cloud growth, and what the properties of any convective clouds might be. Kain (2004) thus divided the KF scheme into three parts: the convective trigger function, the mass-flux formulation, and the closure assumptions. In response to feedback from numerical modellers who used the scheme, Kain (2004) made changes to the updraft, the downdraft formulation, and the closure assumption. The new updraft algorithm had a specified minimum entrainment rate and formulations to allow variability in the cloud radius and cloud-depth threshold for activation of deep (precipitating) convection. Furthermore, the effects of shallow (non-precipitating) convective clouds had been included. In the new downdraft algorithm, downdraft mass-flux was estimated as a function of the relative humidity and stability just above the cloud base and no longer related to vertical wind shear. Finally, the new closure assumption was based on the convective available potential energy (CAPE) for an *entraining (diluted)* parcel rather than one that ascended without dilution. Kain (2004) asserted that this approach provided reasonable rainfall rates for a broad range of convective

environments. Despite these improvements, however, Kain (2004) suggested that it was necessary to develop parameterizations for higher-resolution models, particularly for models with grid a spacing in the order of 1 - 10 km.

Another study that contributed to improving the KF scheme's CP was that of Ma and Tan (2009), who, according to the title of their paper, worked on "Improving the behavior of the cumulus parameterization for tropical cyclone prediction: Convection trigger". The main parameters that were re-examined by them were the original trigger function, for its role in convection initialisation (Kain, 2004), and the temperature perturbation, for its crucial role in determining the prerequisites for a parcel to move upward and to trigger convection. To avoid the convergence-related controversy, Ma and Tan (2009) proposed a new formula to redefine the convective temperature perturbation, in which the role of moisture advection was considered. In this new algorithm, the relationship between environmental forcing (e.g., the grid-scale temperature anomaly due to moisture and temperature advection) and local disturbance was explicitly established. Preliminary experiments were conducted to verify this new algorithm and showed that the distribution as well as the intensity of convective rainfall were significantly improved. The new algorithm also contributed to tropical cyclone (TC) track simulation (about 10%). According to Ma and Tan (2009), the new trigger scheme could reasonably eliminate convective instability under weak synoptic forcing. They concluded that their study provided convincing evidence of the advantages of the new trigger algorithm, but also suggested that further detailed examination was required to extend the understanding of the physics behind the scheme.

2.3.2 The Betts-Miller-Janjic Convection Scheme

Fonseca et al. (2015) described the Betts-Miller-Janjic (BMJ) convection scheme as an adjustment scheme whose essential principle was the relaxation of the temperature and humidity profiles towards reference thermodynamic profiles; precipitation was thus obtained as a necessary consequence from the conservation of water substance. According to Janjic (1994), the BMJ scheme differed from the BM (Betts and Miller, 1986) scheme in several important respects: the deep convection profiles and the relaxation time were variable and depended on the cloud efficiency, which was a non-dimensional parameter that characterised the convective regime. The cloud efficiency in turn depended on the entropy change, precipitation, and mean temperature of the cloud. The shallow convection moisture profile was derived from the requirement that the entropy change be small and non-negative. Attempts have been made (Janjic, 1994) to refine the scheme for higher horizontal resolutions, primarily by modifying the triggering mechanism. In particular:

- A floor value for the entropy change in the cloud was set up, below which the deep convection was not triggered;
- In searching for the cloud top, the ascending particle mixed with the environment; and
- The work of the buoyancy force on the ascending particle was required to exceed a prescribed positive threshold.

The new modification by Janjic (1994) was made in response to several problems identified in the original BM scheme, where:

- The eta model was occasionally producing heavy spurious precipitation over warm water, as well as widespread light precipitation over the oceans;

- The convective forcing, particularly the shallow type of forcing, could lead to negative entropy changes.

However, Janjic (1994) concluded that, despite the successes of the newly designed convection and viscous sublayer schemes, the episodes of excessive precipitation and over-developments of the associated systems over warm water had not been eliminated entirely. Excessive precipitation by the BMJ cumulus scheme was also reported by Fonseca *et al*. (2015), who run the WRF with the default BMJ CP scheme over the Indo-Pacific region, and subsequently suggested that the scheme needed to be modified. Mugume *et al*. (2017), who assessed the performance of the WRF model in simulating rainfall over western Uganda, also reported that the BMJ scheme over-estimated rainfall. Conversely, Gilliland and Rowe (2007) found that the BMJ scheme produced less rain water when the WRF was run in an idealised simulation over South Dakota and Nebraska to simulate a warm-season convective system. They asserted that, although moisture in the environment was an important variable in the BMJ scheme, and even though the sounding had a deep moist layer, the BMJ scheme was not able to realize this moisture in the form of precipitation. In a real-case simulation over the same region, Gilliland and Rowe (2007) claimed that the BMJ simulation was unable to represent any significant convective precipitation. They then concluded that, since the BMJ scheme depended on a deep layer of available moisture, its effectiveness was limited in a region with little moisture, even when moderate CAPE was available. This present study modified certain parameters in the BMJ convection scheme in order to improve the simulation of this scheme over West Africa.

Fonseca *et al*. (2015) also worked on improving the BMJ CP scheme to improve the simulation of precipitation in the tropics. As reported by other researchers, Fonseca *et*

al. (2015) too found that the default WRF-BMJ implementation scheme produced excessive rainfall over Southeast Asia, and thus developed a new version of the scheme, one in which the humidity reference profile was moister. They chose this approach because a moister humidity reference profile would lead to a smaller amount of precipitation being generated by the scheme (Fonseca *et al.,* 2015). They also investigated the sensitivity of the precipitation produced by the BMJ scheme to changes in the "instability parameter, α", which was found in the definition of the potential temperature reference profile; the "factor of proportionality, F_S", used in the definition of the humidity reference profile for deep convection; the "cloud efficiency, E" and the "convective adjustment or relaxation timescale, τ" (Fonseca *et al.,* 2015: 2919). The model's performance was assessed with different verification diagnostics, including the model bias, normalised bias, correlation, variance similarity and normalised error variance. Different diagnostic tests were run for 1 day, 1 month, and 4 months over Southeast Asia. Finally, the modified BMJ scheme was assessed over the entire tropics for 11 months, focussing on the boreal summer monsoon seasons, June to September (JJAS) 2008, and the winter monsoon season, December to February (DJFM), which straddled 2008 and 2009. In conclusion, Fonseca *et al*. (2015) found in the 1 day runs that the precipitation produced by the BMJ scheme was not sensitive to changes in the cloud efficiency E and F(E) but that it varied greatly when the humidity and temperature reference profiles were modified (α and F_S, respectively). It was also found in the 1 month experiment that, out of the different options considered, the best agreement with the Tropical Rainfall Measuring Mission (TRMM) was obtained when F_S was set to 0.6, the value recommended by Janjic (1994), corresponding to a moister humidity reference profile, while keeping α at its default value of 0.9. Fonseca *et al.'s* (2015) conclusion on the 4 and 11 month

experiments was that it was crucial to properly represent the water vapour mixing ratio in the tropics in order to simulate the observed precipitation. Also, any changes made to the BMJ scheme would only have an impact on the precipitation if some form of nudging was applied in the interior of the model domain. This meant that the advantage of modifying the BMJ scheme to produce better rainfall estimates lay in the final dynamic consistency of the rainfall with other dynamic and thermodynamic variables of the atmosphere.

There is therefore a need to improve some of these CP schemes and see how to optimise them for simulations over West Africa; and part of this study lies in that direction.

2.4 CHALLENGES IN RAINFALL PREDICTION OVER WEST AFRICA

Some previous studies have documented several of the challenges of generating reliable seasonal rainfall predictions over West Africa. For example, Omotosho *et al.* (2000) found that one of the challenges might be the complexity of the West African climate system. In other words, the irregularities in the rainfall distribution, both in time and in space, serve as a hindrance in predicting rainfall (e.g., onset and cessation dates) within that region. Fontaine and Bigot also (1993) also linked West African rainfall to the south-west monsoon circulation during summer because of the particular geometry of the West African continent, which increases the strong sea-land contrasts westwards of about 20°E. Fontaine and Bigot (1993) have argued that the low latitudes (less than 18°N) of the sub-region were the basis for mean flows to play an important role, which made oceanic and continental surface conditions **(**SST**,** albedo, soil wetness and vegetation, surface roughness) influence the climatic evolution and

particularly the rainfall variability on monthly and seasonal time-scales (Folland *et al.*, 1991). Fontaine and Bigot (1993) found a rainfall departure character in the Sahel zone and at the Guinea Coast that manifested itself as a dipole and was thus classified into two West African rainfall types: in the first, a negative departure occurs over the Sahel zone and a positive departure over the Guinea Coast, and in the second, this was reversed. These rainfall departures make it difficult, however, to apply a particular ROD definition or tool that would fit the entire sub-continent.

It is documented that there are about 18 distinct ROD definitions over West Africa in publications (Fitzpatrick *et al*., 2015). However, in recent times, some of these definitions have become common among researchers and forecasters across the sub-continent. This study employed two of the commonly used ROD definitions based on the findings of some recent studies. For instance, Mounkaila *et al.* (2014) used four of the prominent ROD definitions; AGRHYMET (1996), Stern *et al.* (1981), Sivakumar (1988) and Omotosho *et al.* (2000). Mounkaila *et al.* (2014) concluded that although the four definitions produced different RODs over each zone in West Africa, AGRHYMET (1996) consistently produced the earliest ROD, while Omotosho *et al.* (2000) gave the latest RODs. In most years, the authors asserted that Stern *et al.* (1981) and Sivakumar (1988) produced RODs which fell within those of AGRHYMET (1996) and Omotosho *et al.* (2000). They claimed the maximum difference between Stern *et al.* (1981) and Sivakumar (1988) was less than 5 days, and ascribed the strong agreement between the two definitions to the fact that they use the same criteria for identifying false ROD (Stern *et al.*, 1981). However, Mounkaila *et al.* (2014) claimed AGRHYMET (1996) was an outlier in most cases. Hence, this study chose the definitions by Stern *et al.* (1981) and Omotosho *et al.* (2000) to evaluate

their performances using different observation and model datasets based on the findings of Mounkaila *et al.* (2014).

The adoption of appropriate datasets by forecasters and researchers in the sub-region also posed a challenge. For instance, Tompkins and Adebiyi (2012) asserted that the onset of rainfall could be diagnosed either from satellite data or local *in situ* observations, such as rain gauges; they concluded that satellite data were generally more complete but might show substantial biases. Fitzpatrick *et al*. (2015) similarly argued that data from rain gauges were usually a more accurate representation of localised rainfall. However, other studies (e.g., Ali *et al.*, 2005; Roca *et al.*, 2010) emphasised that the coverage of *in situ* observations across West Africa was not spatially consistent, and that there were many regions in which observations were very sparse. Meanwhile, studies have been conducted across the entire sub-region on the use of different observed and model data (e.g., Global Precipitation Climatology Project [GPCP], Tropical Rainfall Measuring Mission [TRMM], ERA Interim Reanalysis [ERAIN], CORDEX data) in predicting the onset of the rains; the results of these studies have been very helpful (e.g., Vellinga *et al.*, 2012; Mounkaila *et al.*, 2014). The findings from these studies suggested that observed (gridded) data covered wider areas even within a particular country, and that they thus had a greater advantage over station (gauge) data in predicting rainfall onset in the past, present and future climate over West Africa. Applying different observation datasets (predictands, e.g., rainfall data) and model simulations to generate seasonal forecast increased confidence in the output. Unfortunately, this approach (of applying different observation datasets) is not very common in most meteorological service departments, although different predictors (e.g., SST, OLR) are used. This present study thus aims to use different observations (i.e., gridded satellite data) and model data to simulate

rainfall characteristics over the study domain. Since understanding the characteristics of onset and cessation of the rainy season is important for socio-economic development in West Africa, there is a strong need to examine how the ongoing global warming may affect these parameters in the future.

2.5 IMPACT OF CLIMATE CHANGE ON WEST AFRICAN CLIMATE

Several studies have shown how ongoing global warming may affect the West African climate (e.g., Abiodun *et al.,* 2012; Seth *et al.,* 2013; Sylla *et al.,* 2015; Diallo *et al.,* 2016; Tall *et al.,* 2017; Klutse *et al.,* 2018). For instance, Diallo *et al.* (2016) projected a decrease in mean precipitation over the western Sahel, and an increase over the central and/or eastern Sahel in the near future, which suggested projected dry conditions over the western Sahel that were likely to affect agriculture and water resource management. A study by Abiodun *et al*. (2012) projected that, in 2031 - 2050, the West African climate would be warmer throughout the whole year, with less (i.e., lower temperatures) during the rainy months (April to September) but more (i.e., higher temperatures) during the dry-wet and wet-dry transition months (March and October, respectively). They concluded that, during the summer months (JJA), the warming and drying would be more pronounced in the western part of the Sahel than in the eastern part, because the monsoon flow would be stronger, deflecting cool and moist air from the west to the east. Similarly, Mariotti *et al*. (2014) projected a forward shift (i.e., from earlier in the year to later in the year) of the monsoon season over West Africa and the Sahel, in agreement with previous studies by Seth *et al*. (2013). They also projected a more widespread decrease in precipitation throughout the

monsoon season, mostly associated with a reduction of activity by the African easterly waves (AEWs).

Klutse *et al*. (2018) also projected a reduction in mean rainfall across the region as a result of enhanced global warming. They found an increase in consecutive dry days (CDD) over the Guinea Coast, which might adversely influence future crop yields, thereby increasing the risk of food insecurity in the region. In their work, Sylla *et al*. (2015) projected an increased risk of both drought and flood events towards the late 21st Century, especially during the onset and early mature monsoon phases, which are critical in determining the evolution and quality of the crop season in West Africa. In relation to hydrology and irrigation practices on the sub-continent, Tall *et al*. (2017) found that climate change would substantially affect the hydroclimate (especially in Senegal, where they focused on Lake Guiers) in the near future, by resulting in a lesser surface water amount (due to a decrease in surface runoff and an increase in evapotranspiration) and in a generalised decrease of water availability during the late 21st century.

However, there is a dearth of information on how climate change may impact the RODs, RCDs and LRS over West Africa in the future. Understanding these impacts will assist policy makers in making relevant decisions with regard to minimising the associated risks. Hence, a section of this study (Section 4.7) examines and compares the future impacts of 1.5°C and 2°C global warming levels (GWLs) on RODs, RCDs and LRS in West Africa under two future climate forcing scenarios (RCP4.5 and RCP8.5).

This chapter has presented a review of literature on the prediction of seasonal rainfall over West Africa using GCMs and RCMs, the international experiment of climate

models over West Africa and the improvement and application of climate models over West Africa. The chapter also reviewed several studies on the challenges in respect of the prediction of rainfall over West Africa. Finally, a review of literature was done on the impacts of climate change and global warming on West African rainfall characteristics. Having looked at these factors, the next chapter presents and discusses the data and methodology used in this study.

CHAPTER THREE

DATA AND METHODOLOGY

This chapter presents the datasets used in the thesis and describes the methods used to analyse these datasets. The chapter also provides the definitions used in calculating the characteristics of rainfall in West Africa that were applied in this study.

3.1 STUDY AREA

The domain for this study is West Africa (0°N-20°N; 20°W-20°E), with the three main rainfall zones designated as Guinea, Savanna and Sahel. The designation of the study area follows that of previous studies (e.g., Abiodun *et al.,* 2012; Diasso and Abiodun, 2015; Kumi and Abiodun, 2018). The Sahel zone usually has a short rainy season and an extended dry season, which makes it vulnerable to severe droughts. This zone covers Senegal, Niger, and the northern parts of Guinea-Bissau, Guinea, Mali, Burkina Faso and Nigeria (Figure 3.1). The vegetation is mostly grassland and the main activity of the people is pastoral farming which involves the rearing of cattle, goats and sheep. The Savanna zone has a relatively similar rainfall season as the Sahel. The vegetation is mainly grassland with some shrubs and acacia trees, although the southern parts of this zone have some forests. Both agriculture and pastoral farming are practised by the inhabitants. Some of the major crops that are cultivated are millet, sorghum, groundnuts, maize, cotton, shea butter, rice and beans. This zone covers the most parts of Guinea, Sierra Leone, Ghana, Togo, Benin, Nigeria, southern parts of Guinea-Bissau, Mali and Burkina Faso, and the northern parts of Liberia and Cote d'Ivoire. Lastly, the Guinea zone is usually regarded as the wettest region of West

Africa because of its bimodal rainfall regime and large annual rainfall amounts. The climate of this zone makes intensive agricultural practices such as cash and food crops, possible. Some of the major crops that are grown in this area are, among others, cocoa, coffee, mango, citrus, oil palms, rubber, yam, plantain, cassava and banana. This zone covers the southern parts of Sierra Leone, Guinea, Liberia, Cote d'Ivoire, Ghana, Togo, Benin and Nigeria.

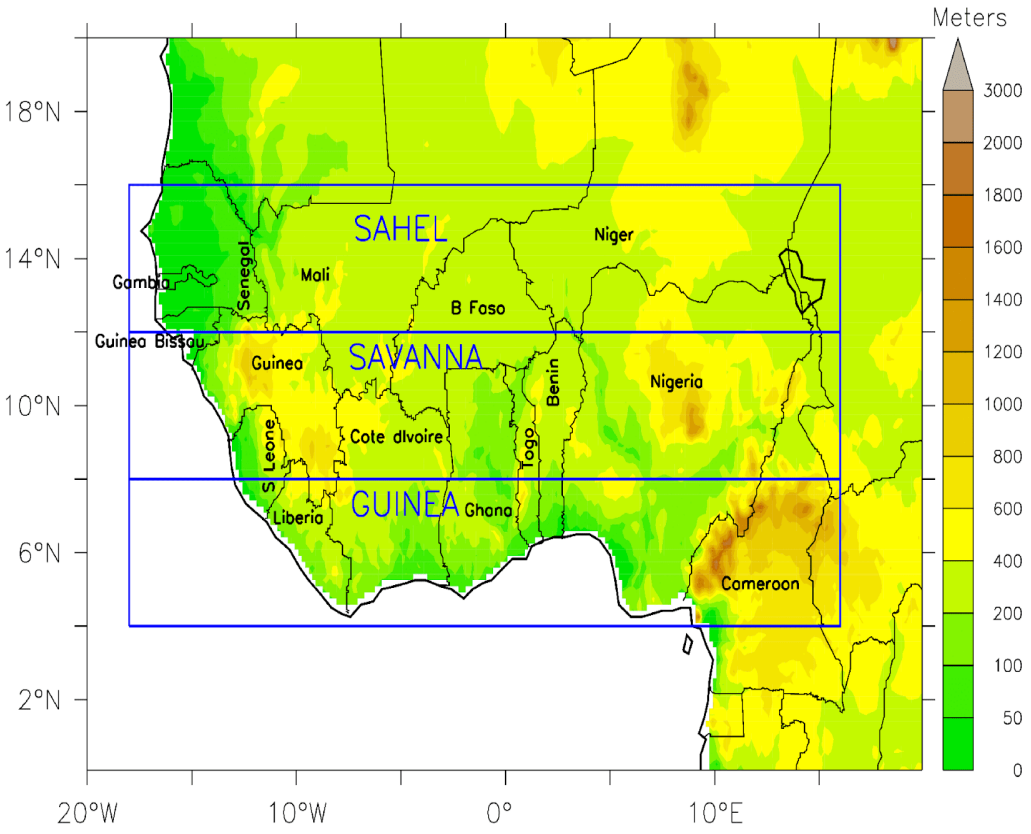

Figure 3.1: West African Domain Showing the Topography and Regions Designated as Guinea, Savanna and Sahel Zones.

3.2 DATA

The types of datasets used in this study were: observations, reanalysis and model simulations.

3.2.1 Observation Data

The two rainfall observation datasets used in this study were the African Rainfall Climatology version 2 (ARC2) of 1983 - 2012 (Novella and Thiaw, 2013) and the Climate Hazard Group Infrared Precipitation with Stations (CHIRPS) of 1981 - 2015 (Funk *et al.,* 2014, 2015). These observation datasets were used to evaluate the simulated rainfall datasets.

The newly operational ARC2 dataset consists of daily gridded 0.1° x 0.1° rainfall estimates with a spatial domain of 40°S–40°N and 20°W–55°E, encompassing the African continent from 1 January 1983 to the present and forward into the future. "Like the operational Rainfall Estimation algorithm version 2, (RFE2), ARC2 uses inputs from two sources: 1) 3-hourly geostationary infrared (IR) data centered over Africa from the European Organisation for the Exploitation of Meteorological Satellites (EUMETSAT) and 2) quality controlled Global Telecommunication System (GTS) gauge observations, reporting 24-h rainfall accumulations over Africa" (Novella and Thiaw, 2013: 588). "One main advantage of the new ARC2 dataset is that it is easily applied to operational climate monitoring. The daily availability of the ARC2 has furthermore allowed the generation of numerous products that provide important insight into the evolution of rainfall totals and anomalies at weekly, dekadal (10 -day), monthly, and seasonal time scales, all of which are critical to decision making in agriculture, water resources, and food security" (Novella and Thiaw, 2013: 597). "Despite its shortcomings (e.g., it tends to underestimate precipitation in certain

areas), the value of ARC2 lies in its availability in real time, which makes it convenient not only for climate studies but also for real-time climate monitoring. The fact that it is continuous and delivers the daily rainfall climatology at a high resolution, helps users to better understand the fine-scale evolution and character of monsoonal precipitation over many remote regions of Africa" (Novella and Thiaw, 2013: 604).

CHIRPS is a new quasi-global (50°S-50°N), high resolution (0.05° x 0.05°), daily, pentadal, and monthly precipitation dataset. "CHIRPS incorporates station data in a two-phase process, producing two unique products. In the first phase, which yields a preliminary rainfall product with 2 -day latency, the sparse gauge data from the Global Telecommunication System (GTS) of the World Meteorological Organization (WMO) are blended with Cold Cloud Duration (CCD) derived rainfall estimates at every pentad. In the second phase, which yields a final product with a ~3 week latency, the best available monthly (and pentadal) station data are combined with monthly (and pentadal) high resolution CCD-based rainfall estimates to produce fields that are similar to gridded monthly station products, such as those produced by the Global Precipitation Climatology Centre (GPCC) or the University of East Anglia's Climate Research Unit (CRU). Thus, the CHIRPS falls somewhere between heavily curated interpolated gauge datasets like the GPCC and sparse gauge plus satellite products like the RFE2" (Funk *et al.*, 2015: 2). In general, CHIRPS is the product of a two part process. "First, IR Precipitation (IRP) pentad rainfall estimates are created from satellite data by calculating the percentage of time during the pentad that the IR observations indicate cold cloud tops (<235° K) and converting that value into millimetres of precipitation by means of previously determined local regression with TRMM 3B42 precipitation pentads. In the second part of the process, stations are

blended with the CHIRP data to produce the final product, CHIRPS" (Funk *et al.*, 2014: 2).

3.2.2 Reanalysis Data

The reanalysis datasets were from the ECMWF Interim Reanalysis (ERA-Interim) of 1979 - 2015 (Dee *et al.,* 2011). The datasets were daily precipitation, meridional and horizontal winds at surface and pressure levels, and specific humidity data, at 0.75° x 0.75° horizontal grid resolution.

ERA-Interim is the latest global atmospheric reanalysis produced by the ECMWF. The ERA-Interim project was conceived to serve as a bridge between the highly successful ERA-40 atmospheric reanalysis, completed in 2002, and future generations of reanalyses to be produced at the ECMWF. A key objective was to address several difficult data assimilation problems encountered in ERA-40, mostly related to the use of satellite data. Good progress was achieved in this regard; for instance, the ERA-Interim precipitation estimates do not show the excessive rainfall seen in ERA-40 (Dee *et al.*, 2011). "The impact of satellite observations on the reanalysis of precipitation is most directly felt over the oceans. Over land, the information used by the model to generate rain is more strongly constrained by *in situ* measurements of temperature and humidity from radiosondes and land stations. The quality of the precipitation estimates from reanalyses therefore tends to be better over well-observed land locations than over oceans" (Dee *et al.,* 2011: 580). All observations used in ERA-Interim are subject to a suite of quality control and data selection steps. Various preliminary checks serve to detect errors that can occur when measurements are recorded or transmitted. These include checks for completeness of reports, physical

feasibility, integrity of ship routes and aircraft flight tracks, hydrostatic consistency of radiosonde profiles, and the occurrence of duplicate reports. Observations that fail any of these checks are flagged for exclusion from further analysis. Quality information generated prior to and during the analysis, along with data departures, are stored with the observations and can be made available for later. The ERA-Interim reanalysis continues to be updated in near-real time, closely following data usage of the ECMWF operational forecasting system investigation (Dee *et al.*, 2011).

Nikulin *et al*. (2012) compared precipitation from ERA-Interim to that of the RCM results and observations in the framework of CORDEX-Africa. Although there are several ways to derive ERA-Interim precipitation (e.g., different spin-up, base time, and forecast steps), Nikulin *et al*. (2012) tested two methods (with and without spin-up) to derive the 3-hourly and daily precipitation; the results showed only minor differences between the two methods. Given the uncertainty as to which method is most appropriate, Nikulin *et al*. (2012) thus suggested using the simplest method, i.e., without spin-up, with the base times of 0000 and 1200 and forecast steps 3, 6, 9, and 12 h for 3-hourly precipitation, and the base times 0000 and 1200 and forecast steps of 12 h for daily precipitation. Monthly means are calculated by averaging the daily means.

3.2.3 Global Climate Model Simulation Data

3.2.3.1 The China Meteorological Administration (CMA) Data

The global model output dataset was from the ECMWF S2S data portal (http://apps.ecmwf.int/datasets/data/s2s/) and supported by the WMO through the

World Weather Research Program (WWRP) and World Climate Research Program (WCRP). The S2S portal consists of 11 datasets from different global climate centres. For this study, the ensemble data produced by the China Meteorological Administration (CMA) was analysed. The CMA model was chosen because it has daily data and fix reforecasts of up to 60-days (the highest number of reforecast days), which is needed to fulfil part of the goal of this study (namely, assessing the ability of the CMA S2S data to predict ROD in lead-time). The CMA ensemble data are from the Beijing Climate Centre's (BCC) Climate Prediction System version 1 and are coupled to the ocean. Operationally, the forecast systems are typically composed of coupled land, ocean and atmosphere components (White *et al.,* 2015). These are six-hourly instantaneous and accumulated hind-casts and fix reforecasts precipitation data from 1994 to 2014 (i.e., 21 years). The reforecasts cover up to sixty (60) days, and the data consist of four ensemble members. The data have a horizontal grid resolution of 1.5° x 1.5° and is re-gridded to the resolution of the observed datasets (0.44° x 0.44°) to enable easy comparison with the observed data. More details on the CMA simulations are available at http://s2sprediction.net/.

3.2.3.2 The Met Office Unified Model (MetUM) Data

The MetUM data are developed and used at the UK Met Office. The old (GA6/GC2) and new (proto-GA8/GC4) versions of the coupled atmosphere-ocean GCM from the Hadley Centre's Global Environment Model are used in this study. The datasets have horizontal resolution of 0.83° x 0.55° and were regridded to 0.44° x 0.44° (about 50km) over West Africa. Data from the atmosphere-only (GA6 and GA8) simulation,

forced with observed SSTs as well as the coupled (GC2 and GC4) simulation were analysed for 1989-2008 (i.e., 20 years).

3.2.4 The Coordinated Regional Climate Downscaling Experiment (CORDEX) Data

The simulated rainfall datasets were from the Coordinated Regional Climate Downscaling Experiment (CORDEX) (Nikulin *et al.*, 2012). They are 19 multi-model simulation datasets produced by eight CORDEX RCMs, namely: ALADIN (Aire Limitée Adaptation Dynamique Développement International (International development for limited-area dynamical adaptation), RCA (Rossby Centre regional Atmospheric model), CCLM (COSMO model in CLimate Mode), RACMO-V1 (Regional Atmospheric Climate Model version 1), HIRHAM (High Resolution Hamburg Model), REMO (REgional MOdel), RACMO-V2 (Regional Atmospheric Climate Model version 2), and WRF (Weather Research and Forecast). The RCMs and the GCMs they downscaled are given in Table 3.1. For more detailed information on the dynamics and configuration of the CORDEX RCMs, as well as the CORDEX projections, readers are referred to Nikulin *et al*. (2012; 2018). The simulation datasets cover the CORDEX-African domain at 0.44° x 0.44° horizontal resolution and provide climate data for past and future periods (1951-2100) under two climate forcing scenarios (RCP4.5 and RCP8.5, i.e., the middle- and high-level emission scenarios). The relevant periods are shown in Table 3.1; how the periods were obtained is described in Déqué et al. (2017).

Table 3.1: The 30-year Periods of 1.5˚C and 2˚C Global Warming Levels (GWL15 and GWL20) in RCP4.5 and RCP8.5.

RCMs	GCMs	RCP4.5		RCP8.5	
		GWL15 Period	**GWL20 Period**	**GWL15 Period**	**GWL20 Period**
RCA	CCCMA	2002 – 2031	2017 - 2046	1999 – 2028	2012 - 2041
	CNRM	2021 – 2050	2042 - 2071	2015 – 2044	2029 - 2058
	CSIRO	2020 – 2049	2033 - 2062	2018 – 2047	2030 - 2059
	ICHEC-r12	2010 – 2039	2031 - 2060	2005 – 2034	2021 - 2050
	HADGEM	2016 – 2045	2032 - 2061	2010 – 2039	2023 - 2052
	IPSL-MR	2002 - 2031	2020 – 2049	2002 – 2031	2016 - 2045
	MIROC	2026 – 2055	2059 - 2088	2019 – 2048	2034 - 2063
	MPI-LR	2006 – 2035	2029 - 2058	2004 – 2033	2021 - 2050
	NCCN	2027 – 2056	2062 - 2091	2019 – 2048	2034 - 2063
CCLM	CNRM	2021 – 2050	2042 - 2071	2015 – 2044	2029 - 2058
	ICHEC-r12	2010 – 2039	2031 - 2060	2005 – 2034	2021 - 2050
	HADGEM	2016 – 2045	2032 - 2061	2010 – 2039	2023 - 2052
	MPI-LR	2006 – 2035	2029 - 2058	2004 – 2033	2021 - 2050
ALADIN	CNRM	2021 – 2050	2042 - 2071	2015 – 2044	2029 - 2058
HIRHAM	ICHEC-r3	2009 – 2038	2030 - 2059	2006 – 2035	2023 - 2052
REMO	MPI-LR	2006 – 2035	2029 - 2058	2004 – 2033	2021 - 2050
RACMO-V1	ICHEC-r1	2006 – 2035	2028 - 2057	2003 – 2032	2021 - 2050
RACMO-V2	HADGEM	2016 – 2045	2032 - 2061	2010 – 2039	2023 - 2052
WRF	NCCN	2027 – 2056	2062 - 2091	2019 – 2048	2034 - 2063

3.2.5 The WRF Simulation and Data

WRF (version 3.8.1) was initialised with the Climate Forecast System Reanalysis (CFSR) 6-hourly data (Saha *et al.*, 2010, 2014), downloaded from the Research Data Archive at the National Centre for Atmospheric Research Computational and Information Systems Laboratory (available online at http://rda.ucar.edu/datasets). The pressure levels data have a horizontal resolution of 0.5° x 0.5°, whereas the SST and surface data have a horizontal grid resolution of 0.3° x 0.3°. Six convection schemes in the WRF model, namely, Kain-Fritch (KF), Modified Kain-Fritch, Modified Tiedtke, New Tiedtke, New Simplified Arakawa-Schubert, and the Betts-Miller-Janjic (BMJ) (Janjic, 1994) were selected for the first performance evaluation. The following physics parameterizations were used: the double-moment five class microphysics scheme (WSM5) (Lim and Hong, 2010), the Rapid Radiative Transfer Model for Global models (RRTMG) for both shortwave (SW) and longwave (LW) radiation (Iacono *et al.*, 2008), the Yonsei University planetary boundary layer (PBL) (Hong *et al.*, 2006), the Mellor-Yamada-Janjic TKE (Turbulence Kinetic Energy) PBL (MYJ) (Janjić, 1994) with Monin-Obukhov surface layer parameterization (Monin and Obukhov, 1954) for the BMJ CP scheme, and the four-layer Noah land surface model (Chen and Dudhia, 2001). In all model runs 38 vertical levels were used, more closely spaced in the PBL and in the tropopause region, were used with the model top at 30 hPa and the highest undamped layer at about 70 hPa. The timestep used was 1 min 40 sec (i.e., timestep=100) and the output was archived every 24 hrs (daily). The model domain on the Mercator projection covers latitude 10°S - 30°N and longitude 25°W-20°E, but the simulation evaluation for this thesis focussed on West Africa (Figure 3.2). A horizontal grid size of 25km (0.22° x 0.22°) was used, and the centre was at 10° N and longitude 0°.

3.3 METHODOLOGY

3.3.1 Definition of Rainfall Onset Date, Rainfall Cessation Date and Length of Rainy Season

In this study, rainfall onset dates and cessation dates (RODs and RCDs) are defined by following the ROD definition of Stern *et al*. (1981), and the ROD and the RCD definitions of Omotosho *et al*. (2000) (Table 3.2). These popular definitions have been shown to give reliable RODs and RCDs over West Africa (Dodd and Jolliffe, 2001; Laux *et al.*, 2008; Mounkaila *et al.*, 2014). Here, the definitions were applied to each dataset (observation and simulation) to obtain RODs and RCDs over each grid point in our study domain (West Africa; Figure 3.1), and the difference between the ROD and RCD (i.e., RCD minus ROD) is used as the LRS over the grid.

Table 3.2: Definition of ROD, RCD and LRS over West Africa

Parameter	**Definition**	**Reference**
Rainfall Onset Date (ROD) DEF1	The total of at least 20 mm of rainfall within 5 days. The starting day and at least two other days in this 5-day period must be wet (at least 0.1-mm rainfall recorded), followed by a no dry period of seven (7) or more consecutive days occurring in the following 30 days.	Stern *et al*. (1981)
Rainfall Onset Date (ROD) DEF2	The first two rains totalling 20 mm or more within 7 days, followed by 2 to 3 weeks each with at least 50 % of the weekly crop-water requirement and without a dry spell within 2 to 3 weeks.	Omotosho *et al*. (2000)
Rainfall Cessation Date (RCD)	Any day from 1st September after which there are 21 or more consecutive days of rainfall less than 50% of the crop-water requirement.	Omotosho *et al*. (2000)
Length of Rainy Season (LRS)	The period between rainfall onset and cessation dates (i.e. RCD minus ROD)	Omotosho *et al*. (2000) and Mugalavai *et al*. (2008)

3.3.2 Analysis of CMA S2S simulation data

To achieve the first objective, the six-hourly instantaneous and accumulated reforecasts data were de-accumulated into daily precipitation data before they were used in this study. The reforecasts datasets are analysed separately, from 10 to 60 days (i.e., up to two months). To evaluate the capability of the CMA model output data in predicting RODs, the reforecast data (10 - 60 days forecast) were compared with the observation.

3.3.3 Analysis of the Unified Model (MetUM) simulation

The definitions in Table 3.2 were applied to the MetUM data over each grid point in West Africa. The ability of the model to simulate ROD, RCD and the LRS was assessed by comparing the simulation results with the observations. This method was done to achieve the second objective of this study.

3.3.4 Analysis of the CORDEX RCM simulation

To evaluate the capability of the CORDEX simulations in reproducing the parameters (ROD, RCD and LRS), the simulated values were compared with the observed values. In the evaluation, the simulation mean (and median) was compared with the observations, and the spread among the simulations were compared with uncertainty in the observed values. To quantify the impacts of a warming level on the parameters, the differences between the projected future values (for the warming level) and the historical values (i.e., future minus historical) were calculated. The difference in the impacts of two GWLs (1.5°C and 2°C) was also quantified under the RCP4.5 and

RCP8.5 scenarios. For the present study, 30 years of data were analysed for past climate (1971–2000) and for the future climate at 1.5°C and 2°C GWLs above the pre-industrial levels for each of the RCP4.5 and RCP8.5 scenarios. The 30-year future climate data have different periods depending on the GWL, the model simulation, and the climate forcing scenario. This was the method used to achieve third objective of this research.

3.3.5 Performance evaluation of different convection schemes in WRF

Each performance test was run from 1 December 2009 to 31 December 2010, with the first month regarded as model spin-up. Six different simulations (1-year runs) were performed, using six convection schemes selected for this study, to evaluate how well the schemes simulate rainfall characteristics (i.e., monthly rainfall amount, ROD, RCD and LRS) over West Africa (Figure 3.2). This method was used to achieve the fourth objective. The performance of each convection scheme was evaluated by calculating the model bias and correlation with the observation (i.e., CHIRPS). The bias (Equation 3.1) is defined in this study as the difference between each scheme and the observation, while the correlation (Equation 3.2) is a measure of the linear agreement between the schemes and the observation. These statistical scores are widely used to evaluate the performance of models in meteorology and climate science research (Fonseca *et al.,* 2015). From these runs, the BMJ CP scheme was selected for further modification, because it had not undergone many modifications but had the potential to perform better in West Africa.

$$\text{Bias} = \frac{1}{n}\sum_{i=1}^{n}(M_i - O_i) \tag{3.1}$$

where M_i is the model data, O_i is the observation, and n is the number of data points.

$$\text{r} = \frac{1}{(n-1)}\sum_{i=1}^{n}\left(\frac{(M_i - \bar{M})}{\sigma_M}\right)\left(\frac{O_i - \bar{O}}{\sigma_O}\right) \tag{3.2}$$

where σ_M and σ_O are the standard deviations for the model and observation, respectively, $\bar{M}$ and $\bar{O}$ are the long-term means of the model and observation.

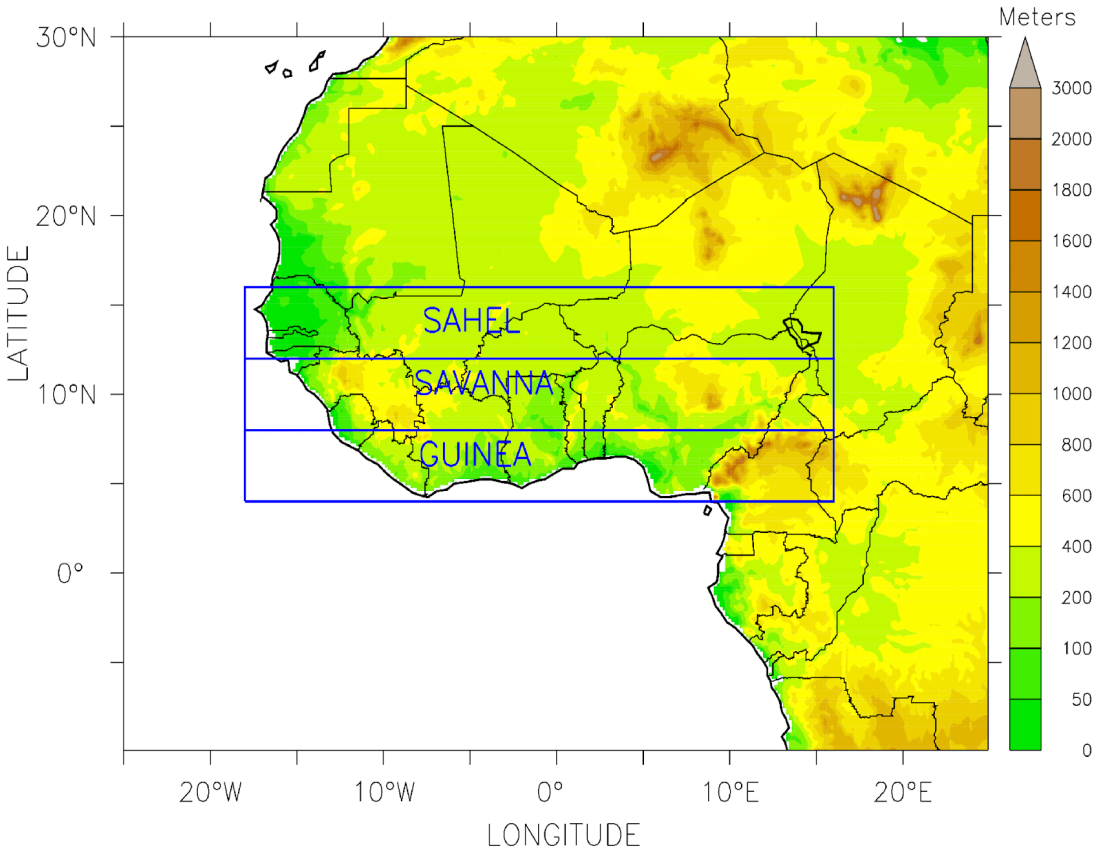

Figure 3.2: The WRF Model Domain showing Topography and West African Evaluation Area.

3.3.6 Sensitivity tests for the BMJ scheme in WRF

To achieve the fifth objective of this study, the WRF-BMJ (control run) and 19 other experiments were run to test the sensitivity of the rainfall characteristics to modifications in the parameters α (in the potential temperature reference profile) and F_S (in the humidity reference profile for deep convection). The equations presented in this section are the ones used in the WRF-BMJ scheme, as presented by earlier studies (Betts, 1986; Janjic, 1994; Fonseca *et al.*, 2015). The first-guess potential temperature reference profile (θ^f_{REF}) for deep convection, as defined in the BMJ scheme (Equation 3.3), includes a parameter α, that when increased will give a warmer (and hence moister) profile and therefore a reduction in the precipitation (Fonseca *et al.*, 2015), which is expressed as:

$$\begin{cases} P_M \leq P_L < P_B : \theta^f_{REF}(P_L) = \theta^f_{REF}(P_L - 1) + \alpha[\theta_{ES}(P_L) - \theta_{ES}(P_L - 1)] \\ P_T \leq P_L < P_M : \theta^f_{REF}(P_L) = \theta_{ES}(P_L) - \dfrac{P_L - P_T}{P_M - P_T}\{\theta_{ES}(P_M) - \theta^f_{REF}(P_M)\} \end{cases} \quad (3.3)$$

where P_M is the pressure at the freezing model level, P_L is the pressure at any model level in the cloudy air column (such that L increases upwards from P_B to P_T), P_B and P_T are cloud-base and cloud-top pressure levels.

The θ^f_{REF} is assumed to have a vertical gradient that is a fixed fraction α of the vertical gradient of the saturated equivalent potential temperature (θ_{ES}), following a moist virtual adiabat (i.e., an isopleth of virtual equivalent potential temperature) from the cloud base up to the freezing level. Above the freezing level, θ^f_{REF} slowly approaches and reaches the environmental θ_{ES} at the cloud top. Thus, θ^f_{REF} is defined as:

$$\theta^f_{REF} = \theta(p_o, T_o) \quad (3.4)$$

where p_o and T_o are the pressure and temperature at the level from which the air parcel is lifted (Fonseca *et al.*, 2015).

In the default BMJ scheme, the precipitation (ΔP) and the adjustments in temperature and humidity (ΔT and Δq) over one cumulus time step (Δt) are given by:

$$\begin{cases} \Delta P = \Delta P_{BM}\ F(E)\ \Delta t/\tau \\ \Delta T = \Delta T_{BM}\ F(E)\ \Delta t/\tau \\ \Delta q = \Delta q_{BM}\ F(E)\ \Delta t/\tau \end{cases} \quad (3.5)$$

where τ is the convective adjustment timescale, and F(E) is a linear function of the cloud efficiency defined by:

$$F(E) = \left(1 - \frac{\Delta S_{min}}{\Delta S}\right)\left[F_1 + (F_2 - F_1)\left(\frac{E' - E_1}{E_2 - E_1}\right)\right] \quad (3.6)$$

where ΔS is the entropy change per unit area for the cloudy air column multiplied by g, the acceleration of free fall, the constant F_1 = 0.7 is determined experimentally and F_2 = 1 for the chosen value of τ, while E_1 = 0.2 is determined empirically in Janjic (1994) and E_2 = 1 for the chosen value of c_1, a non-dimensional constant estimated experimentally and set to 5, and E' is constrained to be in the range [E_1E_2]:

$$E' = \begin{cases} E_1 & \text{if } E \leq E_1 \\ E & \text{if } E_1 \leq E \leq E_2 \\ E_2 & \text{if } E \geq E_2 \end{cases} \quad (3.7)$$

The humidity reference profile for deep convection (Equation 3.8 to 3.10), also includes a factor F_S; the smaller F_S is, the moister the humidity reference profile will be and, therefore, the smaller the amount of precipitation that is generated by the scheme. The first-guess reference specific humidity is said to be prescribed by the

lifting condensation level of an air parcel at pressure p_L (Fonseca *et al.*, 2015). The more negative $\wp(p_L)$ is, the drier the reference profile is at pressure level p_L, and $\wp(p_L)$ is piecewise linearly interpolated between the values at $\wp_M$, $\wp_B$ and $\wp_T$, which are in turn parameterized as a linear function of cloud efficiency E as follows:

$$\wp_M = (-5875Pa)\left[F_S + (F_R - F_S)\left(\frac{E' - E_1}{E_2 - E_1}\right)\right] \quad (3.8)$$

$$\wp_B = (-3875Pa)\left[F_S + (F_R - F_S)\left(\frac{E' - E_1}{E_2 - E_1}\right)\right] \quad (3.9)$$

$$\wp_T = (-1875Pa)\left[F_S + (F_R - F_S)\left(\frac{E' - E_1}{E_2 - E_1}\right)\right] \quad (3.10)$$

where $\wp_M$ is the pressure at the freezing level, $\wp_B$ is the pressure at the cloud bottom, and $\wp_T$ is the pressure at the cloud top. The parameter F_R is set to 1 while F_S is set to 0.85, an empirically determined value over the continental USA, as communicated by Z. Janjic (in 2013) and indicated in Fonseca *et al.* (2015).

According to Fonseca *et al.* (2015), the BMJ scheme's rainfall is very sensitive to changes in these two parameters, in particular to α, and asserts that when α is set to 1.5 the cumulus scheme produces almost no precipitation (i.e. the convection shuts down). In the present study, alpha (α) is modified 5 times (0.85, 0.9, 1.2, 1.4, and 1.6) and F_S is modified 4 times (0.3, 0.6, 0.85 and 0.9). The default values for α and F_S are 0.9 and 0.85 respectively.

The performance of the modifications is evaluated by calculating the model bias, correlation, and root mean square error (RMSE) with the observation. The RMSE (Equation 3.11) is defined in this study as a measure of how well the model (schemes)

performed (Willmott and Matsuura, 2005; Chai and Draxler, 2014) and is expressed as:

$$\text{RMSE} = \sqrt{\frac{1}{n}\sum_{i=1}^{n}(M_i - O_i)^2} \tag{3.11}$$

where M_i is the model data, O_i is the observation, and n is the number of data points.

A long run (31 years, i.e., 1980 - 2010) is performed on the selected combination for further analysis. In the climatological run, the first year (1980) was used as spin-up.

In this chapter, the datasets and the methodology that was used in this study have been presented. In addition, the definitions that were used in calculating the RODs, RCDs, and the LRS over West Africa have also been presented. This chapter has also discussed the methods used to quantify the impact of global warming on the rainfall parameters under review. Finally, the chapter has presented detailed analysis of the method used to improve the BMJ CP scheme in the WRF model to better simulate ROD, RCD, and the LRS over West Africa. The next chapter discusses the results that have been obtained on the evaluation of the CMA S2S model, the MetUM, the CORDEX RCMs, the WRF model development, and the projection of the impact of GWLs on ROD, RCD, and the LRS in West Africa.

CHAPTER FOUR

RESULTS AND DISCUSSION

4.1 INTRODUCTION

The results of this study are presented and discussed in this chapter, following the same order as the objectives, listed in Section 1.6. The differences and similarities in RODs with regard to different observation datasets and definitions used are initially assessed (Section 4.2) before the models are evaluated. In Section 4.3, the ability of other GCM dataset (e.g., the CMA S2S model data) in simulating RODs is examined. Thereafter, Section 4.4 presents the results of how a further development of the GCM (the UK Met Office Pre- vs Post - IMPALA model data) improved the simulation of seasonal rainfall prediction in West Africa. Section 4.5 assesses the capability of RCMs (from the CORDEX-Africa project) to simulate the parameters (ROD, RCD and LRS) over West Africa during the past climate (1971 - 2000). Section 4.6 then presents the results from the model development, during which sensitivity tests were conducted to modify the BMJ convection scheme in the WRF model. The influence of the modification on the rainfall parameters under review are discussed. Lastly, the final section of this chapter (Section 4.7) discusses the potential impacts of climate change at 1.5°C and 2°C GWLs on rainfall characteristics over West Africa.

4.2 THE UNCERTAINTIES IN THE OBSERVATION DATA

Before evaluating the performance of the dynamic models in simulating the rainfall characteristics, it is essential to quantify the uncertainties in the observations over West Africa. A comparison of model biases with the uncertainties will assist in putting

the model's performance in the right perspective. Here, the difference between the observations were quantified using one of the rainfall characteristics, viz., the ROD. This study focused on the uncertainties produced by differences in observation datasets (ARC2 and CHIRPS) and ROD definitions (DEF1 and DEF2). However, for easy comparison, the ROD obtained with ARC2 using DEF1 was used as the reference.

In general, the two observation datasets (CHIRPS and ARC2) produced similar ROD patterns over West Africa, regardless of the ROD definition used (Figure 4.1). The correlation between the two ROD patterns was high (r = 0.98 for DEF1). Both ROD patterns featured a zonal distribution of ROD with a northward increase from the coast inland. This northward increase in ROD has been linked to the transport of moisture from the Gulf of Guinea into the sub-continent by the WAM (Omotosho *et al.,* 2000; Sylla *et al.,* 2013a; Vellinga *et al.*, 2013). The datasets also showed a good agreement in inter-annual variability of ROD over each zone, especially over the Guinea and Sahel zones (Figure 4.2). Nevertheless, there were notable differences between the RODs from the two datasets. For example, with DEF1, the CHIRPS featured an earlier ROD (about 10 days; compared to ARC2) over parts of the coastal area, but a later ROD (again by about 10 days) inland (Figure 4.1b; contours); the maximum discrepancy between the two datasets (about 20 days) occurred over the south-west mountain range. With DEF2, the pattern of the discrepancy was the same as with DEF1, but the magnitude was higher (up to 30 days). This implied that, regardless of the method used, CHIRPS produced an earlier ROD than ARC2 over the coastal area, but a later ROD than ARC2 inland. Similar differences between datasets and ROD definitions have been reported in previous studies, which ascribed the differences to the resolution of the datasets (Sylla *et al.*, 2013, 2015; Mounkaila *et al.*, 2014;

Abiodun *et al.*, 2015, 2017). For example, Mounkaila *et al*. (2014) showed that TRMM gives a later ROD than GPCP over West Africa, regardless of the ROD definition used. However, the difference between CHIRPS and ARC2 obtained in the present study was larger than the one between TRMM and GPCP in Mounkaila *et al*. (2014), which could be as well ascribed to the differences in the resolution of these two datasets.

The correlation between each ROD pattern with respect to panel (a) in the two datasets for each definition are shown in panels (b) and (d). The results of panel (a) subtracted from the other panels are shown as contours on panels (b), (c) and (d).

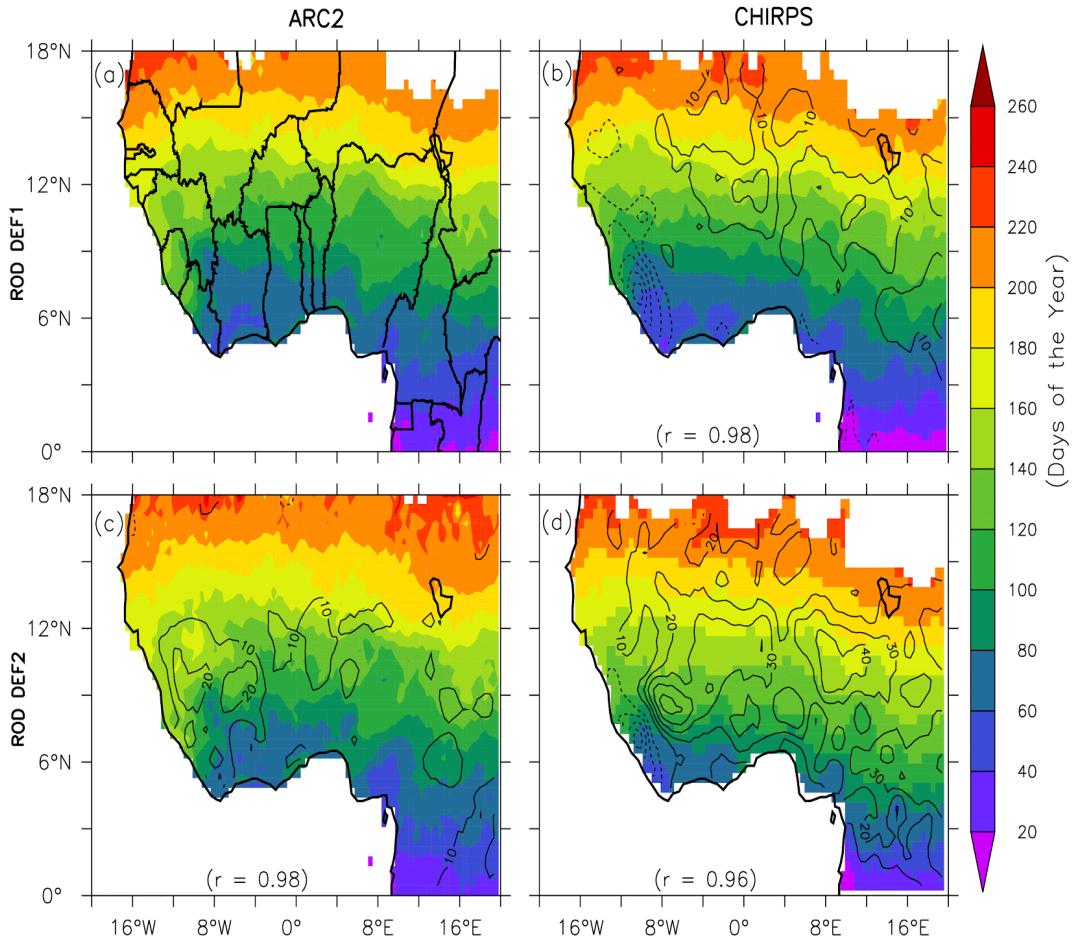

Figure 4.1: The Spatial Variation of RODs over West Africa as Depicted by ARC2 (Panels a and c) and CHIRPS (Panels b and d) using DEF1 and DEF2.

The RODs obtained with the two definitions are comparable, but DEF2 generally produces later ROD than the DEF1 (Figure 4.1, Table 4.1). The difference is up to 20 days over the Savanna zone in the ARC2 (Figure 4.1c; contours) and up to 30 days over the same area in the CHIRPS (not shown). However, the ROD uncertainty due to the differences in rainfall datasets and the ROD definitions were within ± 40 days in the ROD climatology over the region (Figure 4.1d). While the differences offset each other over parts of western Guinea Coast, they were additive over most parts of West Africa. The magnitude of the uncertainty varied from year to year over each zone. It ranged from 10 days (in 1997) to 25 days (in 1996) over the Guinea zone, from 20 days (in 2004) to 30 days (in 2009) over the Savanna, and from 10 days (in 2002) to 20 days (in 2003) over the Sahel (Figure 4.2). However, over each zone the coefficient of correlation between the two datasets (ARC2 and CHIRPS) was higher with DEF1 than with DEF2. Mounkaila *et al*. (2014) obtained similar results for the GPCP and TRMM datasets when they used the same ROD definitions over the same region. For the period 1994 - 2012, the mean RODs obtained by the two onsets definitions (DEF1 and DEF2) are shown in Table 4.1.

Table 4.1: The Mean RODs over West Africa using ARC2 and CHIRPS Datasets.

The difference between RODs from the two datasets (Δ in days) is Indicated for each Definition.

Methods	Guinea			Savanna			Sahel		
	ARC2	CHIRPS	Δ	ARC2	CHIRPS	Δ	ARC2	CHIRPS	Δ
DEF1	17 Mar	17 Mar	0	29 Apr	5 May	6	26 Jun	1 Jul	5
DEF2	24 Mar	4 Apr	11	9 May	25 May	16	1 Jul	9 Jul	8

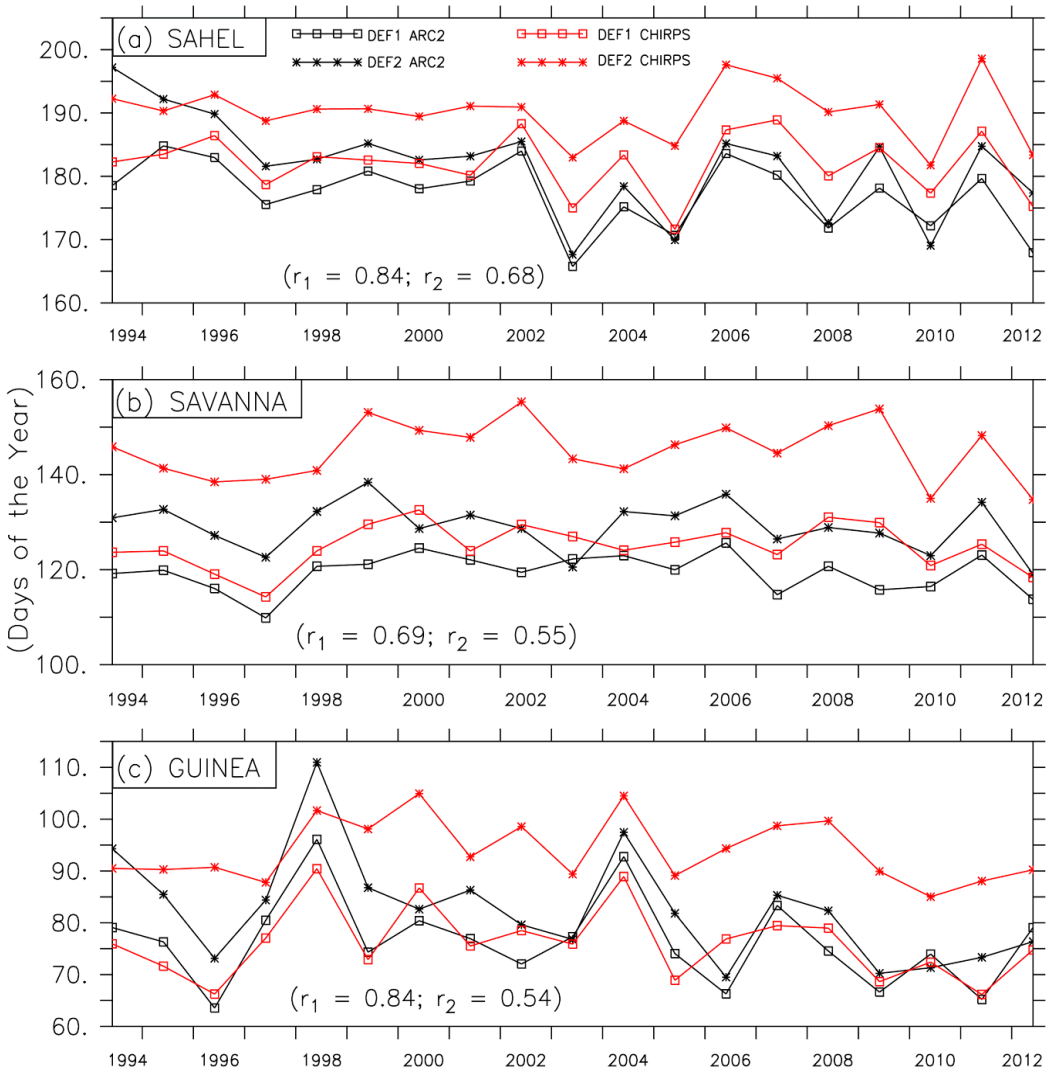

Figure 4.2: The Inter-annual Variability of RODs over Sahel (a), Savanna (b) and Guinea Coast, as Shown by ARC2 and CHIRPS using the DEF1 and DEF2

4.3 EVALUATION OF A GCM IN PREDICTING RAINFALL ONSET OVER WEST AFRICA

In this section, the capability of the China Meteorological Administration (CMA) S2S model to forecast rainfall onset and the characteristics of the WAM over West Africa at different lead-time is examined. Two ROD definitions were used in the evaluation, and the results of the evaluation are provided in Figures 4.3 - 4.7 and Table 4.2.

4.3.1 Spatial and temporal distribution of the CMA model

For both ROD definitions, the CMA model gave a realistic simulation of the spatial pattern of ROD over West Africa and reproduced all the essential features in the observed ROD pattern (Figure 4.3). For example, it reproduced the zonal distribution of the observed RODs and simulated the northward progression of RODs over West Africa well. This implied that the model captured well the northward movement of the WAM and the associated moisture transport from the Atlantic Ocean into the sub-continent. Nevertheless, the performance of the CMA model in simulating the RODs varied according to the definitions used. With DEF1, the correlation between the simulated and the observed ROD pattern (r) was more than 0.8 for all the forecasts. Among the forecasts (10- 20-, 30- 40- and 50- and 60-day lead-time), the 10-day forecast had the lowest correlation (r = 0.84) and the largest bias. The 10-day forecast showed a late ROD over most parts of West Africa and an early ROD over the eastern and the northern parts of West Africa. While the late bias was up 80 days over most parts of the Savanna and the Guinea zone (Figure 4.3a for DEF1), the early bias was about 20 days over the central Sahel and the Cameroon mountain range. The 20- to 60-day forecasts produced a much better forecast. Although they also featured a late ROD

over the south-western half of the sub-continent and an early ROD over the north-eastern half, the magnitude of their biases was about 40 days (half of that of 10-day forecast). The weaker performance of the 10-day forecast may be because, at 10 days, the model was still spinning and had not recovered from the imbalance in the initial condition. This suggested that the CMA model required more than 10 days of spin-up to reach an equilibrium state.

The contours (Figure 4.3) show the spatial distribution of the forecast bias (with reference to observation: mean of ARC2 and CHIRPS). The correlation between each forecast and the observation is indicated in the brackets.

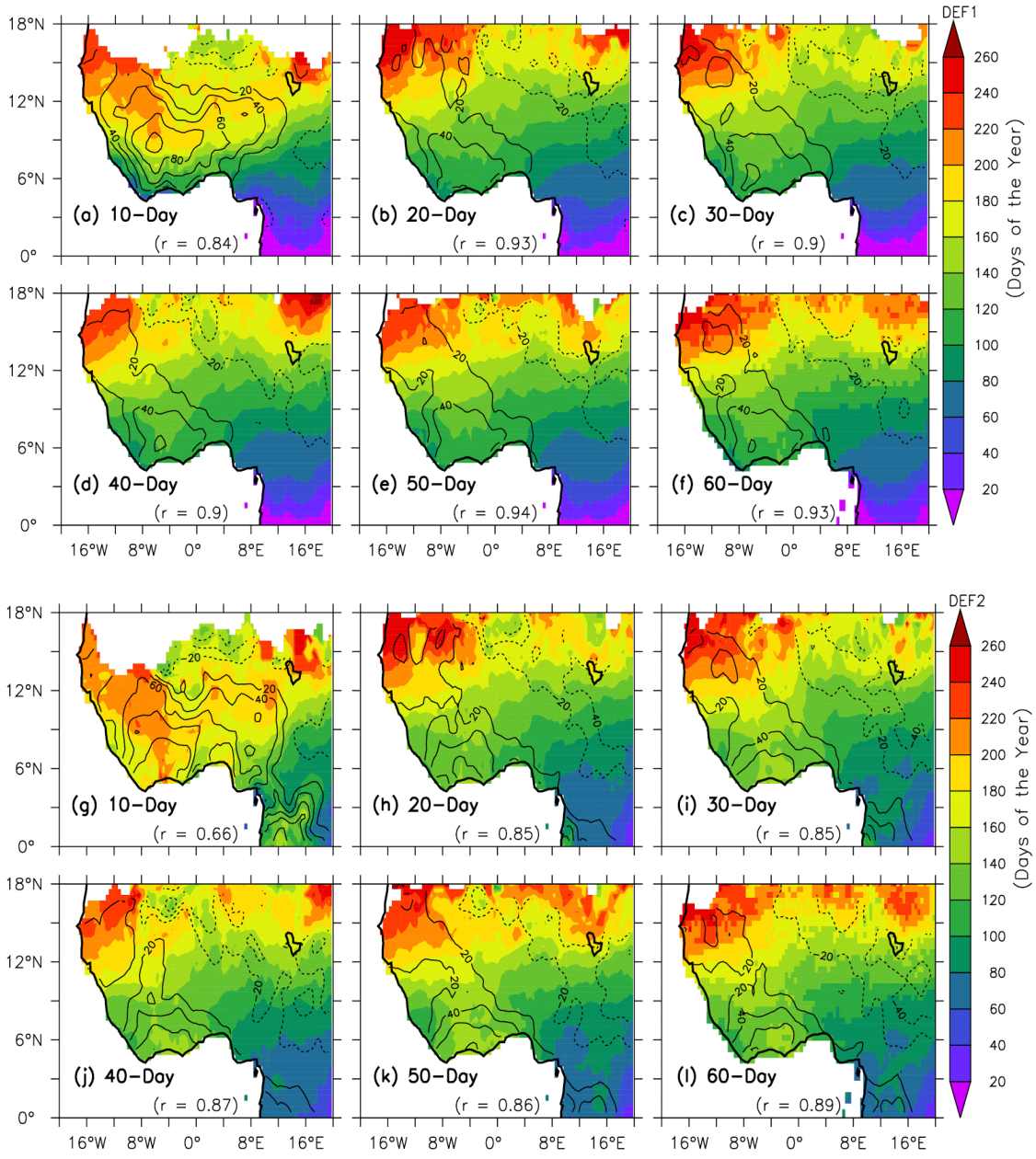

Figure 4.3: The Spatial Distribution of RODs over West Africa as Predicted by CMA in Different Lead Forecast Days (10 - 60 days) using DEF1 (panels a to f) and DEF2 (g to l).

The performance of the CMA forecast was weaker with DEF2 than with DEF1 (compare Figures 4.3 and 4.4; Table 4.2). For instance, the correlation between the forecast and the observations was lower with DEF2 ($0.6 \leq r \leq 0.87$) than with DEF1 ($0.84 \leq r \leq 0.94$). Although the patterns of the forecast biases with DEF1 and DEF2 were similar, the magnitude of the bias was higher with DEF2 (Table 4.2). For instance, with DEF2, the late ROD over the Guinea Coast was more than 40 days and the early ROD over the eastern Sahel was more 40 days (i.e. in 20 to 60 day forecasts; Figure 4.3). Nevertheless, the results of both ROD definitions (DEF1 and DEF2) agreed that the CMA forecast performed worst at the 10 day forecast, by comparing the biases and Root Mean Square Error values (Tables 4.2 and 4.3). Although the CMA model bias for the 20 to 60 day forecasts was high (±40 days), the magnitude was close to the uncertainty in the observation datasets (±30days).

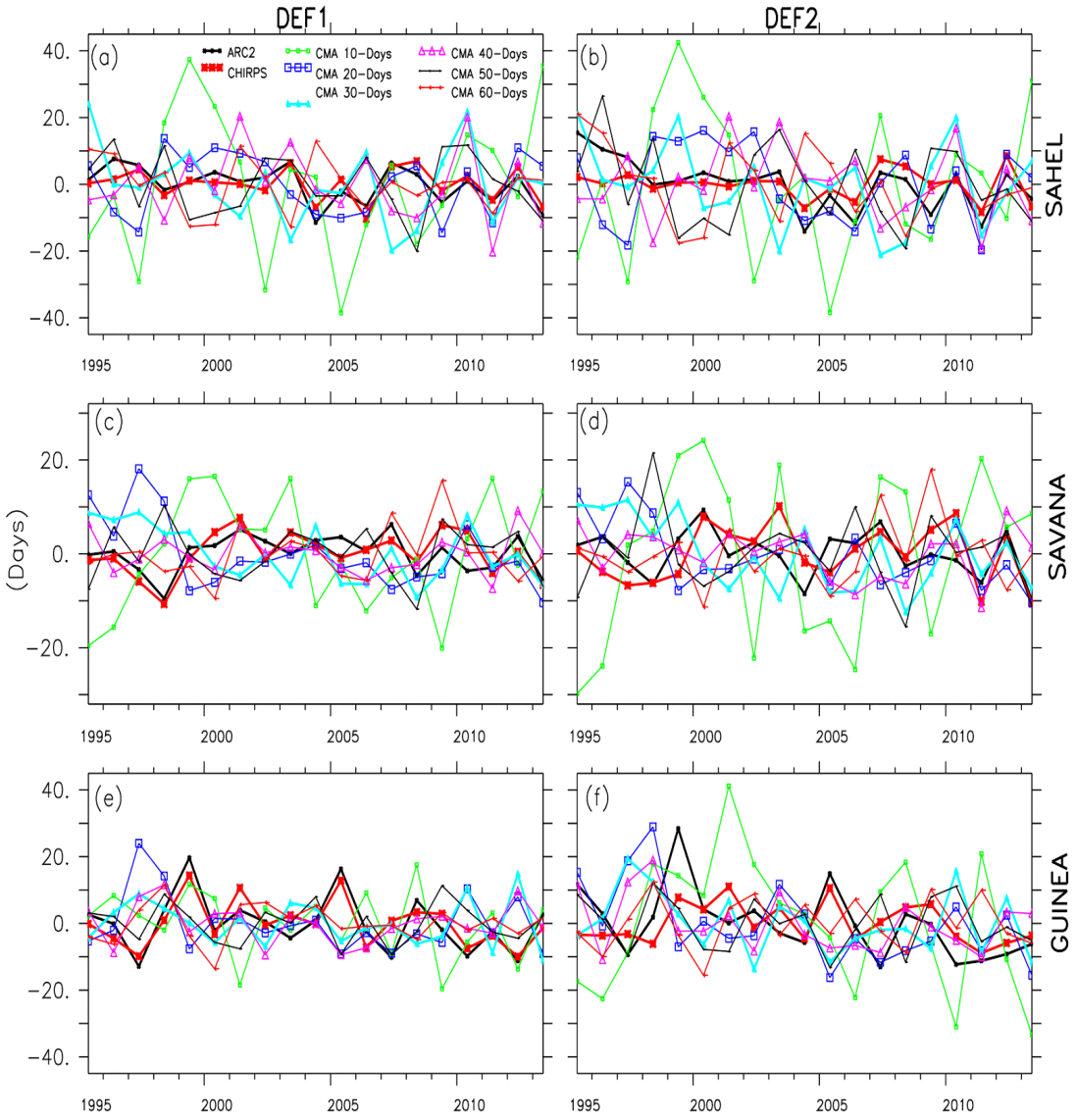

Figure 4.4: The Inter-annual Variability of RODs over the Climatic Zones as Simulated (CMA 10 - 60 days forecasts) and Observed (CHIRPS and ARC2) using DEF1 and DEF2.

Table 4.2: The Mean RODs over West Africa using the CMA Model Predictions for 10 - 60 Days and their Biases (Δ in days) from the Observed Mean.

DEF1	Guinea	Δ	Savanna	Δ	Sahel	Δ
Obs_Mean	17 Mar		2 May		28 Jun	
CMA-10	4 Apr	18	11 Jun	40	3 Jul	5
CMA-20	30 Mar	13	6 May	4	17 Jun	-11
CMA-30	3 Apr	17	7 May	5	15 Jun	-13
CMA-40	1 Apr	15	5 May	3	15 Jun	-13
CMA-50	1 Apr	15	5 May	3	22 Jun	-6
CMA-60	2 Apr	16	3 May	1	20 Jun	-8
DEF2						
Obs_Mean	29 Mar		17 May		5 Jul	
CMA-10	11 May	43	17 Jun	31	2 Jul	-3
CMA-20	15 Apr	17	13 May	-4	20 Jun	-15
CMA-30	16 Apr	18	15 May	-2	19 Jun	-16
CMA-40	14 Apr	16	13 May	-4	17 Jun	-18
CMA-50	16 Apr	18	13 May	-4	26 Jun	-9
CMA-60	14 Apr	16	11 May	-6	21 Jun	-14

Table 4.3: The Root Mean Square Error of RODs over West Africa as Obtained with DEF1 and DEF2 using the CMA Model Prediction for 10 - 60 Days.

Methods	CMA-10	CMA-20	CMA-30	CMA-40	CMA-50	CMA-60
DEF1	18.6	0.6	0.2	1.9	2.4	1.5
DEF2	32.7	0.6	1.4	1.3	3.3	0.3

The model performed well in capturing the magnitude of the inter-annual variability of ROD (Figures 4.4 and 4.5). Regardless of the definition, the normalised standard deviations of all the forecasts (except 10-day forecast) clustered around 0.8 over the Guinean zone, around 1.0 over the Savanna zone, and around 2.0 over the Sahel zone (Figure 4.5). This implied that the model slightly underestimated the magnitude of the inter-annual variability over the Guinea zone, slightly overestimated it over the Sahel zone and captured it well over the Savanna. Nevertheless, the correlation between the simulated and the observed ROD was poor ($r < 0.4$) over all the zones. In general, the results showed that the CMA forecasts performed better with DEF1 than with DEF2, and that they performed best over the Savannah zone.

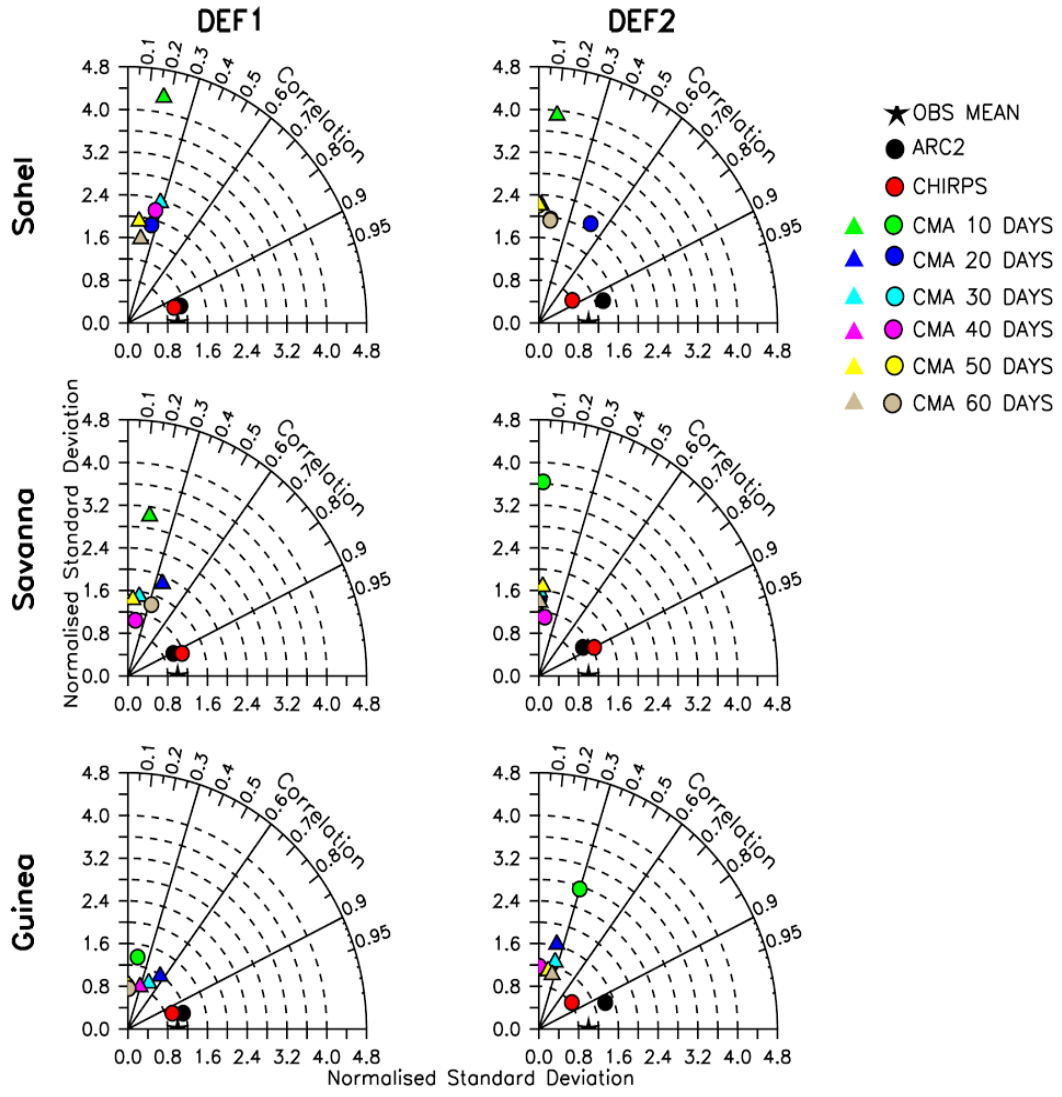

Figure 4.5: Taylor Diagram of RODs Showing the Correlation and Normalized Standardized Deviation between Observations and the CMA Forecasts using DEF1 and DEF2. The triangles (Δ) represent Negative Correlation.

4.3.2 The West African Monsoon and RODs

The CMA forecasts gave realistic simulations of the seasonal movement of the WAM and its associated rainfall patterns (Figures 4.6 and 4.7). The WAM system featured the Inter-Tropical Discontinuity (ITD) and the African Easterly Jet (AEJ). The forecasts captured the inland movement of the ITD from 8°N in January to its northernmost position (20°N) in August and its retreat to 8°N in December. Following the ITD, the monsoon rains started in March over the Guinea zone and moved inland to their northernmost position in the Sahel around August (Figures 4.6 a and b), before retreating southward and reaching the Guinea zone in September. The forecasts (except for the 10-day forecast) reproduced the three main phases of the WAM rainfall pattern, namely: the onset, the peak and the southward retreat. Over the Guinea zone, they captured the periods of the major and minor rainy seasons (Mar-Apr and Sept-Oct, respectively) and featured the break of the monsoon rain period (the so-called "little dry season") (Omotosho and Abiodun, 2007) in August. They also reproduced the "monsoon jump", which is an important feature in the northward movement of the WAM (e.g., Le Barbe *et al.,* 2002; Mounkaila *et al.,* 2014), between 8°N and 10°N in June - July.

The rainfall in millimeters per day (shaded), RODs (green thick and red dashed lines) and the model prediction is 10 to 60 days are shown in Figure 4.6. The contours represent the corresponding surface meridional winds and ITD (thick continuous lines).

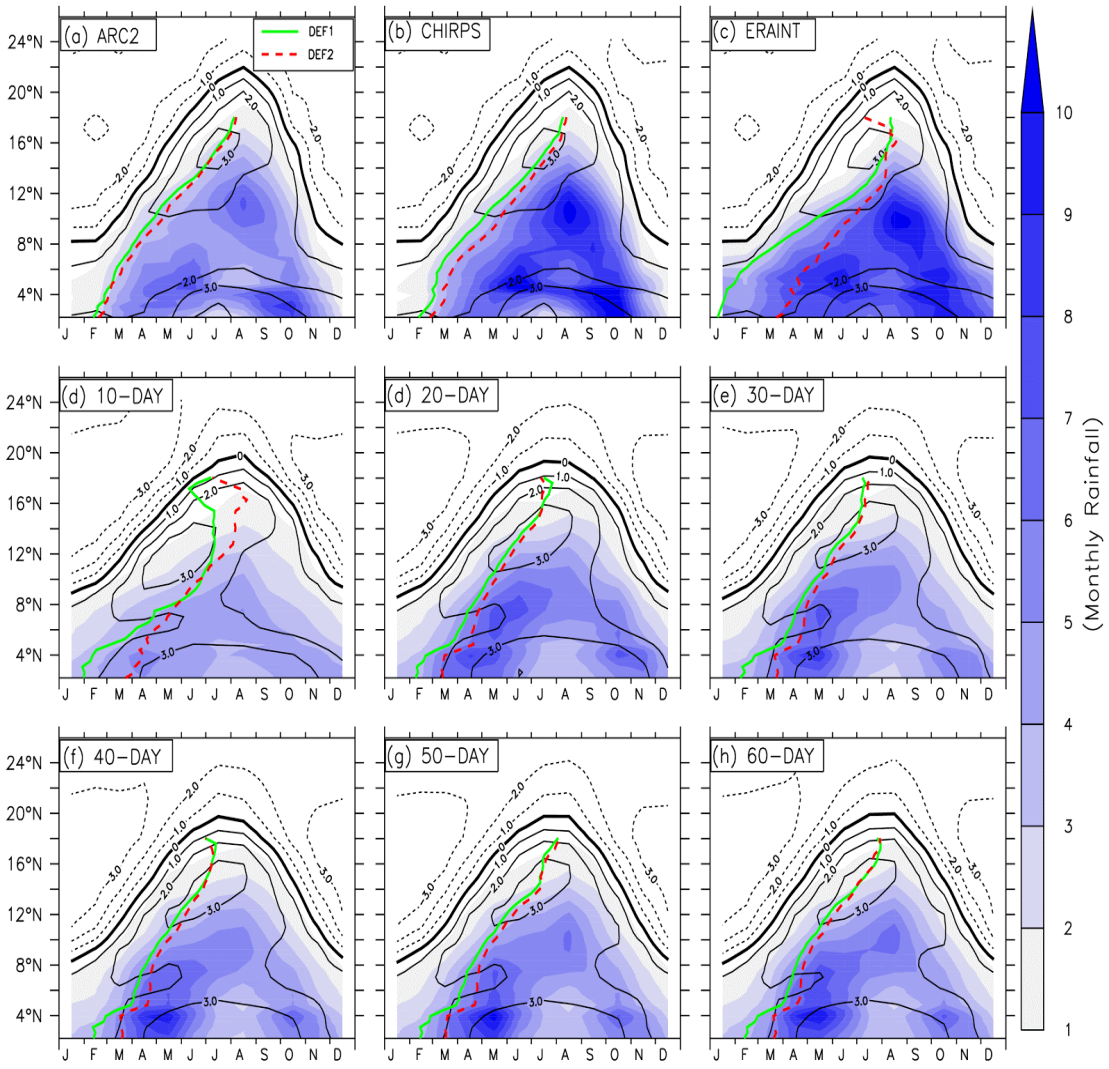

Figure 4.6: Time–latitude Cross-section of Monthly Rainfall and RODs Averaged over 15°W–15°E for ARC2 and CHIRPS, ERA_INT and the CMA Model Prediction of 10 to 60 Days over West Africa.

Nevertheless, the CMA struggled to reproduce the magnitude of the monsoon rainfall and to effectively link the northward progression of the ROD with that of WAM features. For instance, all the forecasts underestimated the Sahelian rainfall during the peak of the monsoon season (August). Furthermore, in both ARC2 and CHIRPS, the RODs (DEF1 and DEF2) over each latitude occurred about two months after the passage of the ITD, but it was more than 2 months in some forecasts, especially in the 10-day forecast. Nonetheless, the ROD lines were better simulated in the CMA forecasts (10- 60-day forecasts) than in the ERA-Interim (Figure 4.6c). Given that the model captured the dynamics and moisture distribution of the WAM well, the biases of the CMA model in simulating the rainfall and the ROD may be attributed to the rainfall parameterization schemes in the model. The parameterizations scheme may not sufficiently couple the monsoon dynamics with the boundary layer moisture in producing rainfall over the region.

Figure 4.7 shows that the moisture at 850hpa follows the characteristics of the WAM (the onset, the peak and the southward retreat), and the African Easterly Jet (AEJ; 700hpa zonal winds) is stronger between April-October.

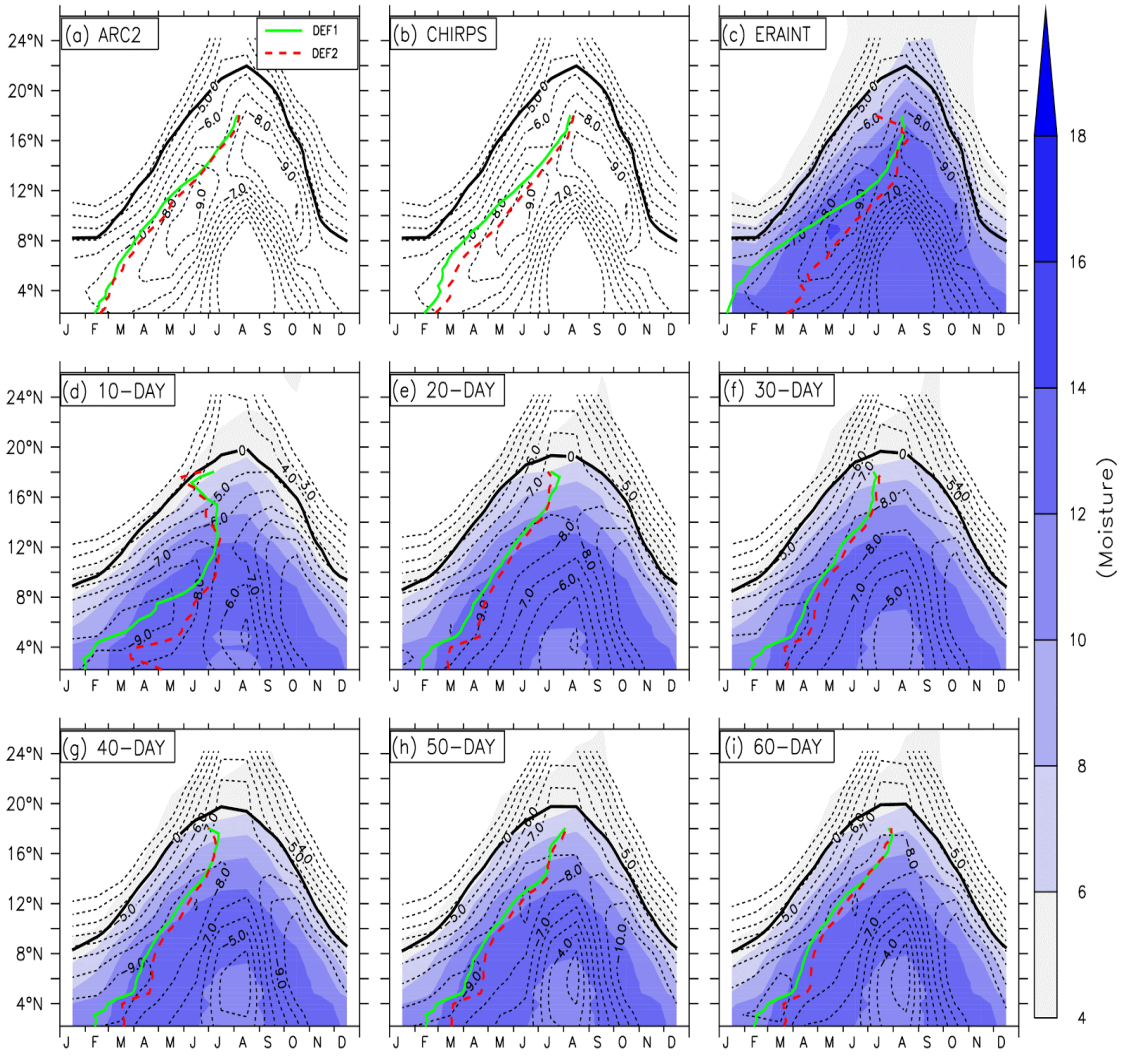

Figure 4.7: Time–latitude Cross-section of Monthly Specific Humidity at 850hPa (kg/kg; shaded) and RODs Averaged over 15°W–15°E for ARC2 and CHIRPS, ERA_INT and the CMA Model Prediction of 10 to 60 Days over West Africa.

4.4 PERFORMANCE EVALUATION OF THE MetUM IN PREDICTING SEASONAL RAINFALL CHARACTERISTICS OVER WEST AFRICA

This section discusses how well the old and new versions of the MetUM (pre- versus post - IMPALA version) to simulate the spatial and temporal features of RODs, RCDs and LRS over West Africa. The purpose here is to ascertain how a further development of the MetUM influenced the simulation of the rainfall parameters that are being considered in this study. The evaluation utilises two hierarchies of the GCM: the atmosphere-only model and the coupled model.

4.4.1 Spatial and temporal distribution of ROD by the MetUM data

The models reproduced the observed spatial ROD characteristics well, although there were some biases (Figure 4.8, biases are contours). The models, both the old and the new version (for both the atmosphere-only model and the coupled model), realistically reproduced the zonal distribution of the observed RODs and realistically simulated their northward progression over West Africa. This could be seen from the high values of the spatial correlation (r = 0.77 to 0.93) with respect to the observed data of ARC2 (Figure 4.8a). The model's ability to simulate the inland movement of RODs meant that it captured the dynamics of the WAM and the associated moisture flow over the sub-continent. Nonetheless, there were some discrepancies between the old and the new version of the model for both the coupled and the atmosphere-only models, with regard to the simulated RODs. For instance, the old versions simulated a late RODs over some areas in the Guinea zone (especially the southern part; Figure 4.8c and e). This bias in the model might suggests that the old version transported less moisture for rainfall over those areas (leading to a late onset). The late onset bias found in this

study agreed with the findings of Williams et al. (2015) and James et al. (2018), who reported that the MetUM HadGEM3-GC2 had a dry bias over West Africa. Moreover, the atmosphere-only version of the old model simulated very early onset dates (between 10 to 20 days) over most parts of the Savanna and the northern Sahel (Figure 4.8c). This could suggest that the rainfall parameterization schemes might have been tuned to transport more moisture inland (leading to an early onset of the rainy season). A major improvement in the new version (especially in the atmosphere-only model) was seen over the Sahel, where the model was able to simulate the observed late RODs in many areas (Figure 4.8d). The simulation of late RODs over the southern Guinea zone and the eastern parts of Nigeria had also been resolved in the new model (shown by the high spatial correlation; r = 0.93). However, there seemed to be more moisture transport by rainfall parameterization schemes in the improved version, which was causing the simulation of early RODs over the Guinea and Savanna zones. This early ROD bias in the new model version was up to about 20 days over the Guinea and Savanna zones, while there was a late ROD bias of about 10 days over the Sahel (Figure 4.8d and f).

The correlation between each ROD pattern with respect to panel (a) are shown in panels (b) to (d). The results of panel (a) subtracted from the other panels are shown as contours.

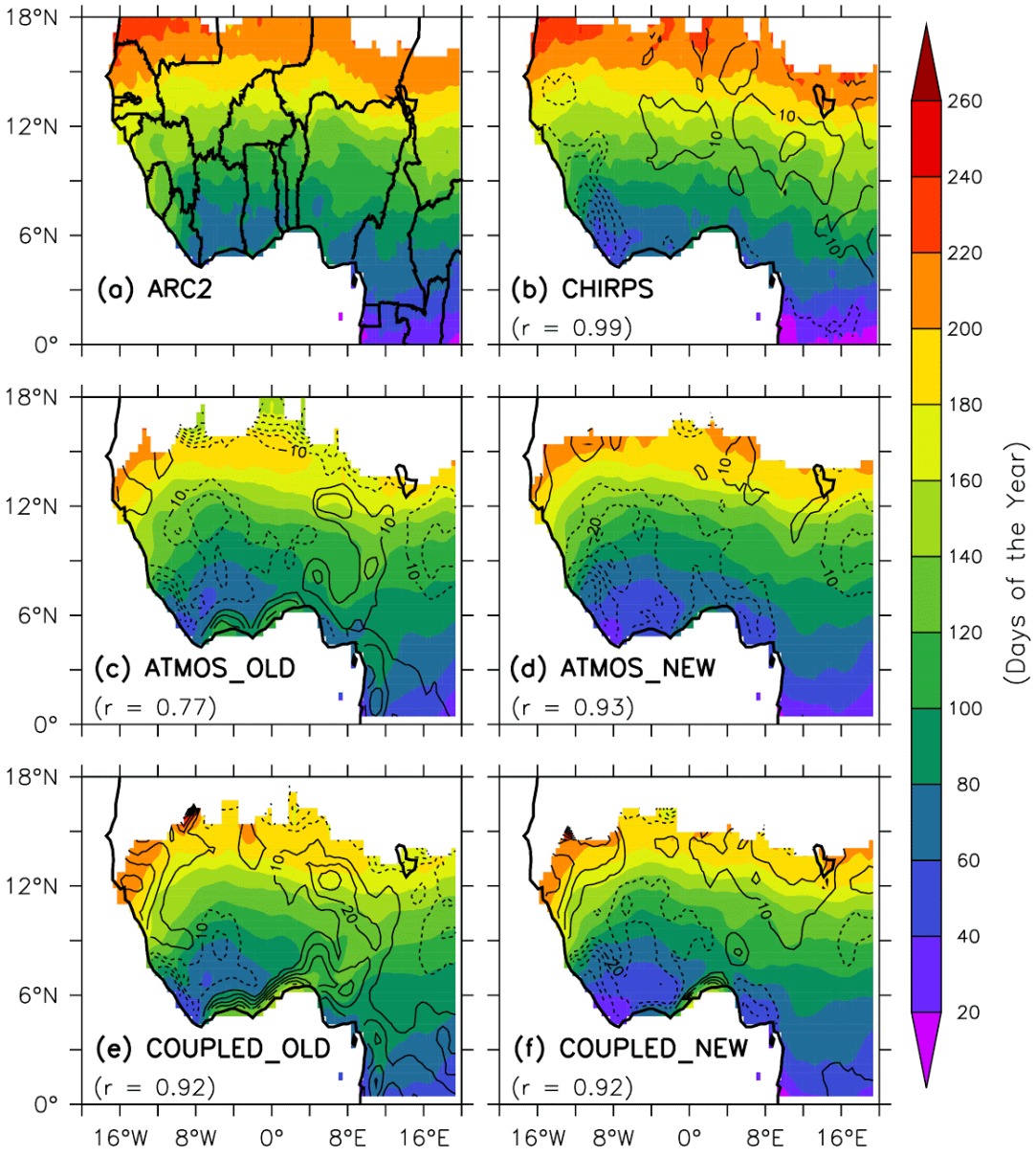

Figure 4.8: Spatial Distribution of RODs over West Africa as depicted by ARC2 (a), CHIRPS (b) and the MetUM data (c to f) using DEF1.

Since the coupled model versions do not have the same calendar as the observations (due to the ocean component), they were (i.e. the coupled model versions) not considered in the evaluation of the model's interannual variability (Figure 4.9). Thus, only the atmosphere-only version was considered. In general, however, the old model (atmosphere-only) was unable to replicate the observed interannual variability for the period of study (1989 - 2008). This was confirmed by the very low temporal correlation values over all the zones except the Sahel ($r_om = 0.13$). However, the new version produced a comparably higher temporal correlation than the old version over the Savanna and Guinea zones (Figure 4.9b and c; $r_nm = 0.12$ and 0.16 respectively). This agreed with Sheen *et al*. (2017) that recent analysis had demonstrated reasonable skill in the inter-annual variability and multi-year forecasting using the MetUM. There was an improvement in the new version of the atmosphere-only model, but more work needs to be done to ensure a better simulation of ROD and inter-annual variability over West Africa.

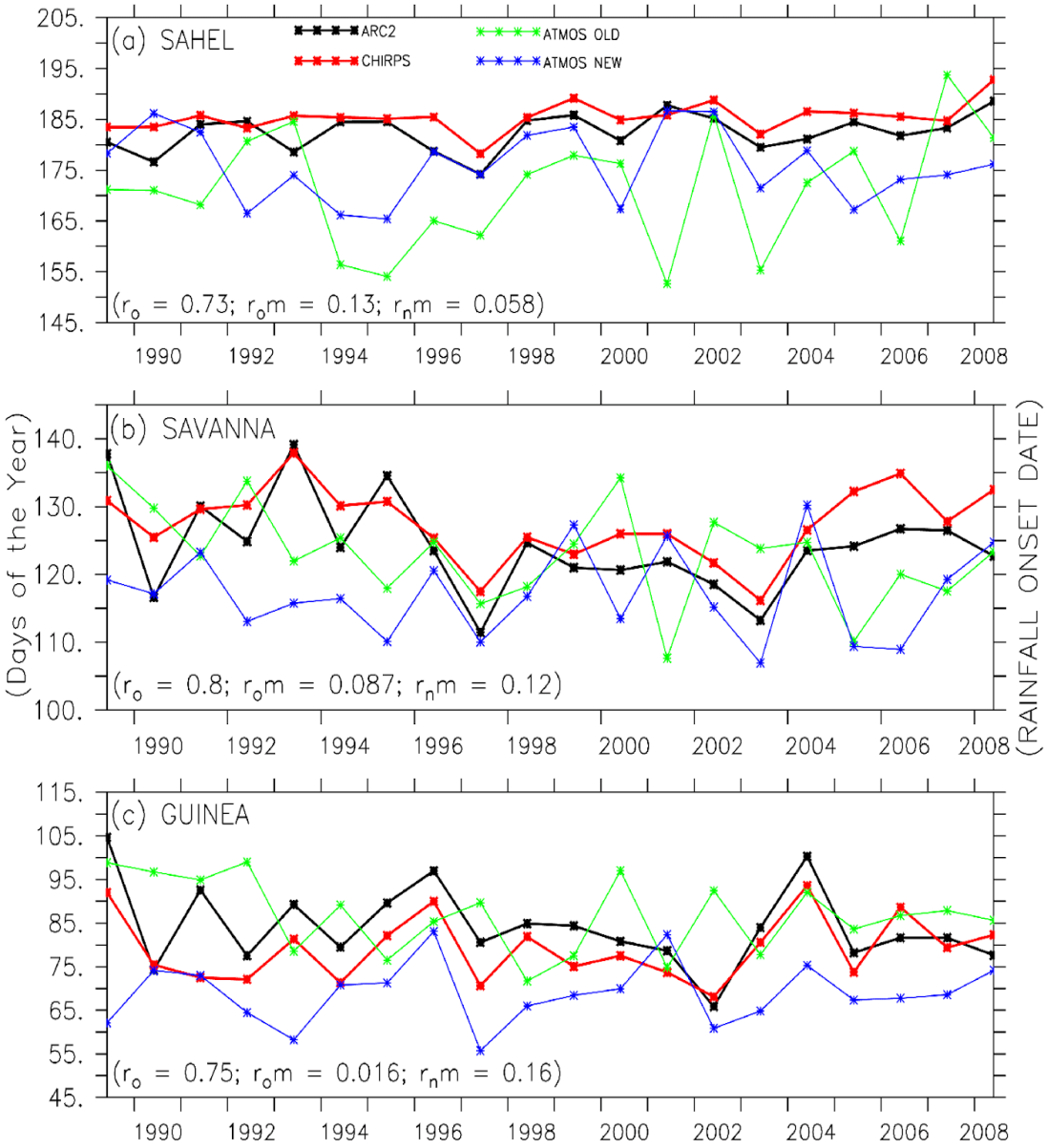

Figure 4.9: The Inter-annual variability of RODs over Sahel (a), Savanna (b) and Guinea Coast (c) as Depicted by Observations and the "Atmosphere only" (old and new) Version of the MetUM using DEF1.

4.4.2 Spatial and temporal distribution of RCD by the MetUM data

The models also produced a reliable simulation of RCDs over West Africa, although the simulated RCD spatial pattern did not show strong correlation (r = 0.56 to 0.67; Figure 4.10) with the observed patterns, as was the case with the RODs. The simulations also agreed with the observations on the zonal distribution and southward increase of the RCDs. The models performed better over the central Savanna (i.e., less bias; contours), irrespective of the version used. In general, the atmosphere-only versions gave a higher spatial correlation with the observation than did the coupled version (Figure 4.10c and d). However, there were some notable biases in the simulated RCDs. For example, all the versions (new and old versions of both coupled and atmosphere-only) simulated very early rainfall cessation over most parts of the sub-region. Also, except for the old version of the atmosphere-only model (Figure 4.10c), the other versions simulated late RCDs over the central Guinea Coast region, which was more pronounced in the new versions. Even with the improved versions, the MetUM reproduced a bias of about 30 days early in simulating RCDs over West Africa. The weaknesses in the model to simulate the end of the monsoon season confirmed the assertion by earlier studies that "none of the current generation of general circula-tion models (GCMs) was built in Africa (Watterson et al. 2014), and the relevant processes operating there have not always been the first priority for model de-velopment" (James *et al*. 2018: page 313).

The correlation between each ROD pattern with respect to panel (a) are shown in panels (b) to (f) of Figure 4.10. The results of panel (a) subtracted from the other panels are shown as contours.

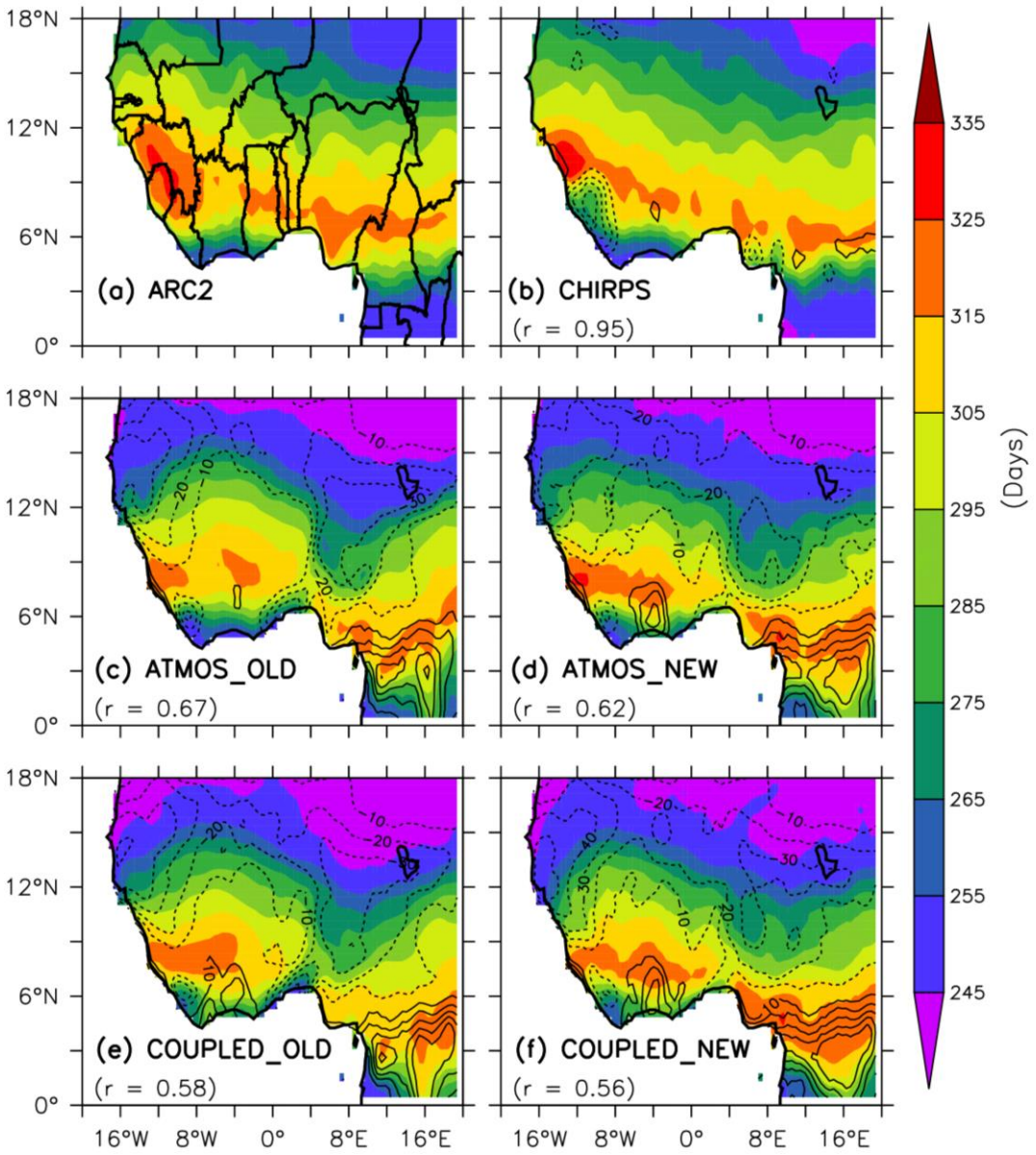

Figure 4.10: Spatial Distribution of RCDs over West Africa as Depicted by ARC2 (a), CHIRPS (b) and the MetUM Data (c to f) using DEF1.

Like the RODs, the atmosphere-only version of the model was compared with the observations in the inter-annual variability simulation. Again, the models struggled to capture the observed inter-annual variability (Figure 4.11). This was seen in the poor temporal correlation values (mostly out of phase; negative) across all three zones, but especially over the Guinea Coast. Moreover, the models simulated very early RCDs over the Sahel (Figure 4.11a) in comparison with the other zones. This agreed with James *et al*. (2018) that the model underestimates precipitation in the Sahel. Over the Savanna zone, the old version of the model even captured the inter-annual variation of RCDs better (in terms of phase agreement), albeit with low correlation values. The new version of the model thus still needs continuous modification over West Africa, as it generally failed to simulate the inter-annual variation of the end of the rains.

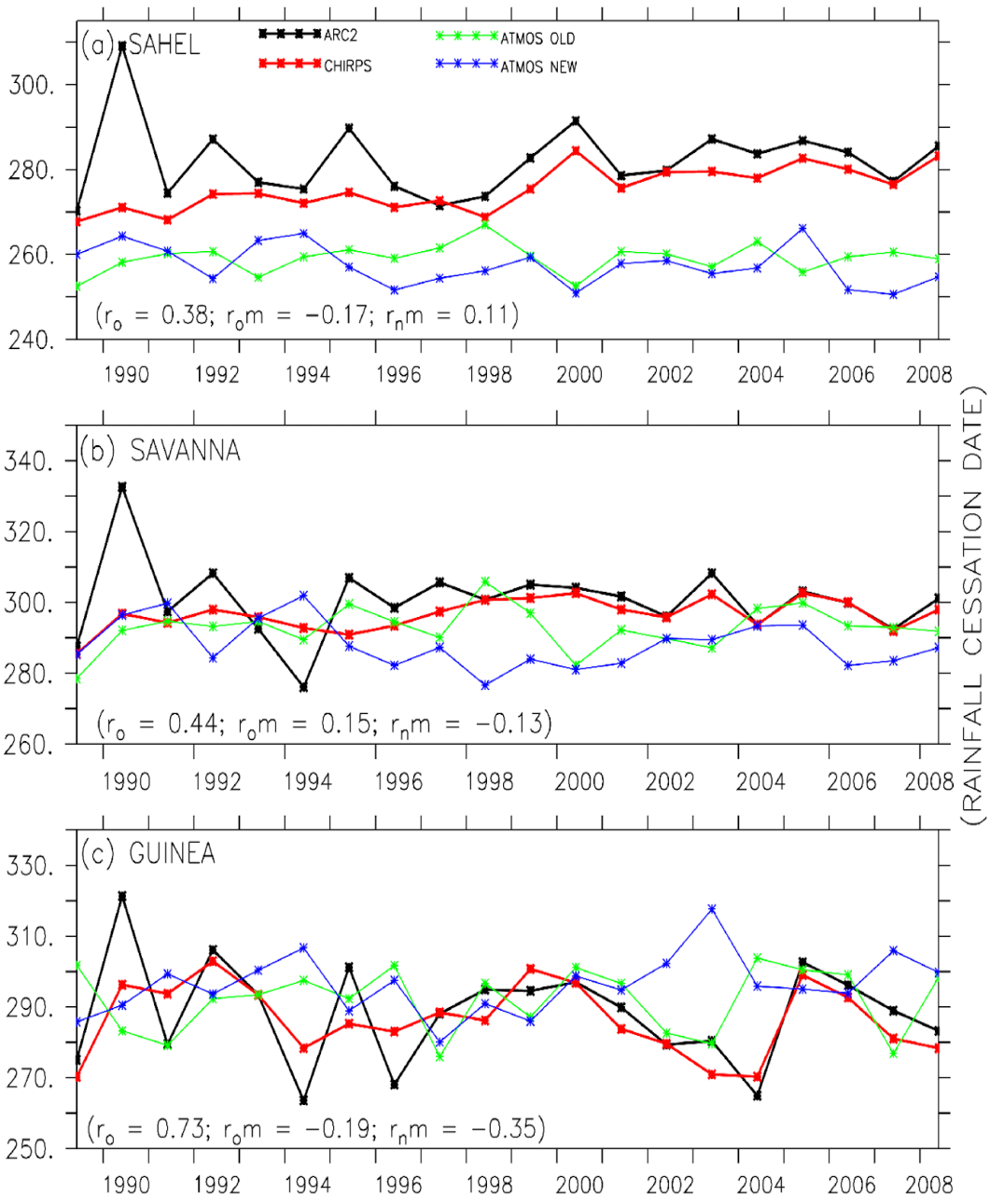

Figure 4.11: The Inter-annual Variability of RCDs over Sahel (a), Savanna (b) and Guinea Coast (c) as Depicted by Observations and the "Atmosphere only" (old and new) Version of the MetUM using DEF1.

4.4.3 Spatial and temporal distribution of LRS by the MetUM data

The models' ability to simulate the essential characteristics of the observed ROD and RCD was shown in the simulation of the LRS (Figure 4.12). This was reflected in the high values of the spatial correlation (r = 0.79 to 0.92; Figure 4.12c to f). As was the case with the RCD, the simulations agreed with regard to the observations on the zonal distribution and southward increase of the LRS. In other words, the rainy season was shorter in the north, and longer towards the south, which could be attributed to the bimodal rainfall regime in the south. The shorter LRS over the southern Guinea zone in the old versions had been resolved in the new versions, which now even overestimate the LRS over the same areas. Again, the magnitude of the early bias over the entire region had been reduced in the new versions (especially in the atmosphere-only version). Conversely, there were some biases in the simulations. All the versions over-estimated the LRS in most parts of the Guinea zone, while they under-estimated the LRS over the Sahel and the eastern part of West Africa. The old version of the atmosphere-only (Figure 4.12c), did not show a strong spatial correlation with the observations, when compared to the coupled model. It was again found that the new versions of the model (both the coupled and the atmosphere-only) over-estimated the LRS over the central Guinea Coast region. This might be because of the models' early RODs and late RCDs simulation over those areas. The model bias in this study supports the call for the explicit inclusion of African experts in model development, as this will help to advance a region-specific evaluation of these models, and lead to a better understanding of how the models behave, in order to help determine how to improve them (James *et al.,* 2015; Rowell *et al.,* 2015; Baumberger *et al.,* 2017; James *et al.,* 2018).

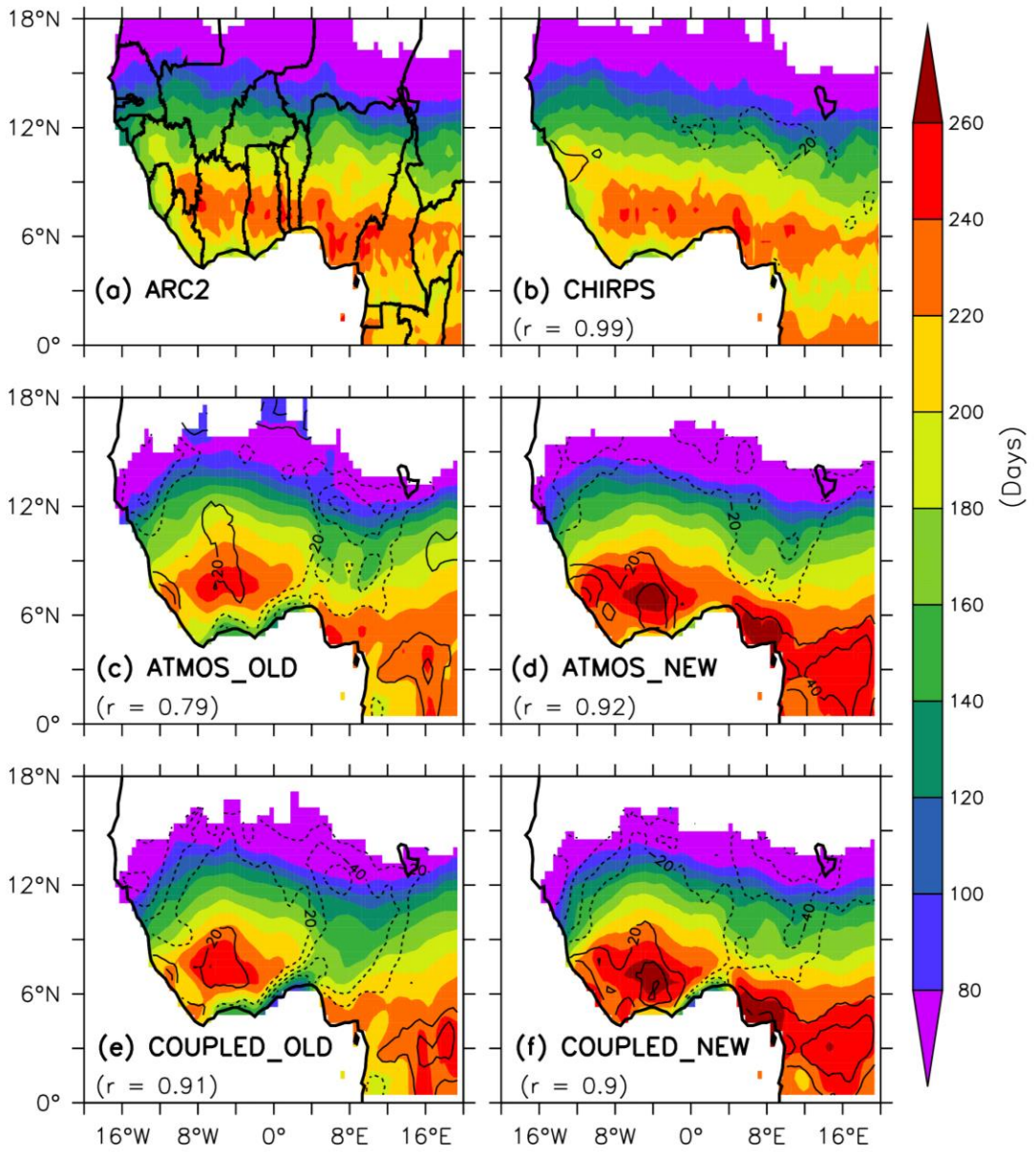

Figure 4.12: Spatial Distribution of the LRSover West Africa as Depicted by ARC2

(a), CHIRPS (b) and the MetUM Data (c to f) using DEF1.

The correlation between each ROD pattern with respect to panel (a) are shown in panels (b) to (f). The results of panel (a) subtracted from the other panels are shown as contours (Figure 4.12).

The poor performance of the model in simulating the inter-annual variability in the earlier discussions was replicated in the LRS (Figure 4.13). Generally, there was weak agreement (less correlation) between the model and the observations in terms of temporal variation. However, the old version of the model could simulate the inter-annual variability of LRS closer to the observation than the new version over the Sahel and Savanna (i.e., in terms of the range and correlation values). Finally, both the old and the new versions of the model were unable to simulate the observed temporal variation of the LRS in the Guinea zone (i.e. ., they showed a negative correlation).

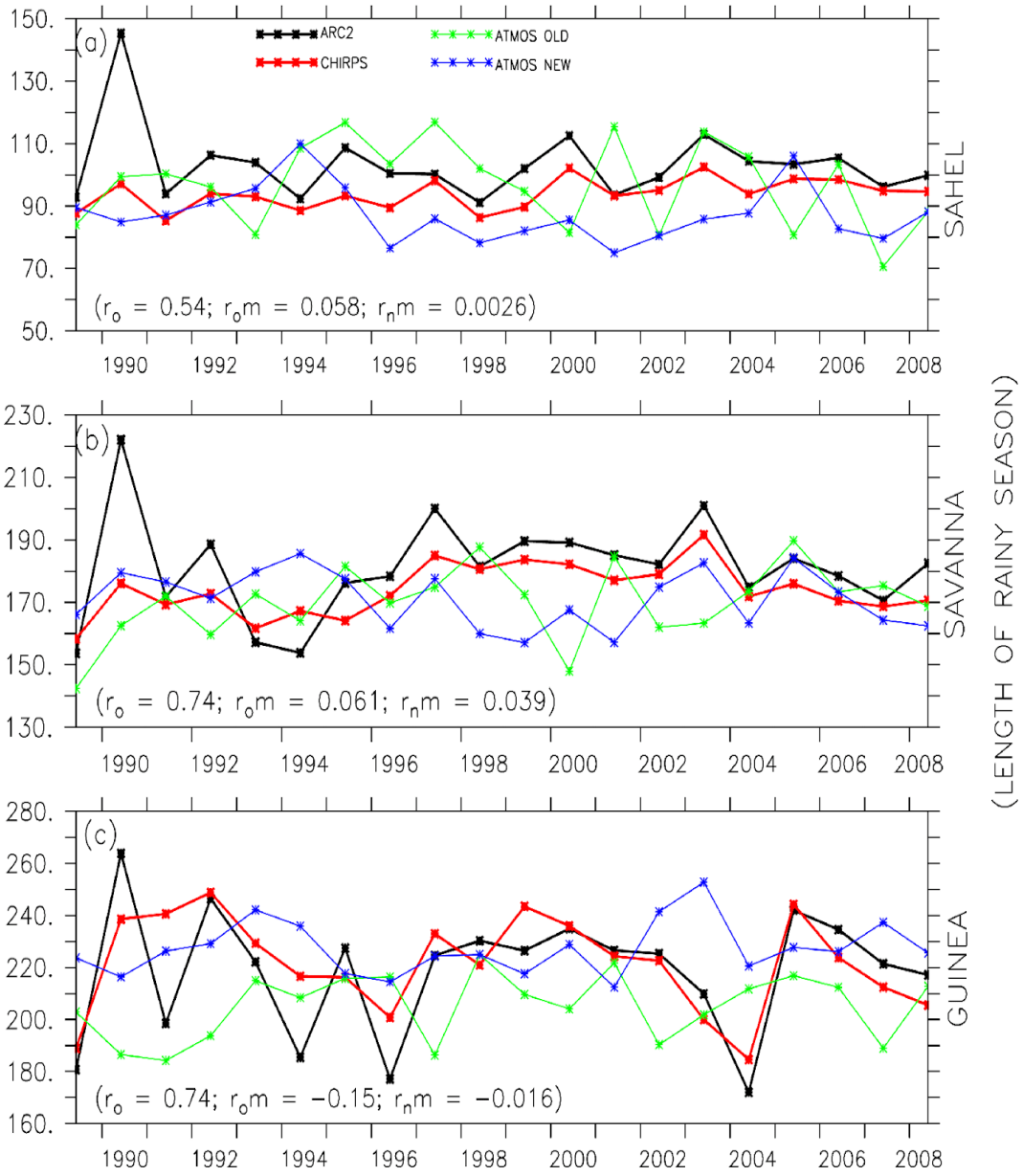

Figure 4.13: The Inter-annual Variability of LRS over Sahel (a), Savanna (b) and Guinea Coast (c) as Depicted by Observations and the "Atmosphere-only" (old and new) Version of the MetUM using DEF1.

4.5 CAPABILITY OF RCMs IN SIMULATING SEASONAL RAINFALL CHARACTERISTICS OVER WEST AFRICA

This section discusses how RCMs from the CORDEX-Africa project perform in simulating ROD, RCD and LRS for past the climate (1971 - 2000) over West Africa.

4.5.1 Evaluation of ROD by the CORDEX RCMs

The RCM ensemble realistically reproduced the spatial distribution of RODs over West Africa (Figure 4.14). The correlation between the simulated and the observed values was high (r_o = 0.97), and all the essential features in the observed pattern were well reproduced by the models (Figure 4.14a and b). As observed, the RCMs simulated a northward progression of RODs, from 1March (i.e., day 60 of the year) along the coast to about 15June (i.e., day 200 of the year) around 18°N. This progression corresponds to the northward transport of moisture (from the Gulf of Guinea into the sub-continent) by the WAM (Omotosho *et al.*, 2000; Sylla *et al.*, 2013). However, the simulated ROD was too early (about 30 days early) over the western part of the Guinea zone and too late (about 20 days late) over the central and eastern parts of the zone (Figure 4.14d). This bias could be because the RCMs overestimated the influence of the south-west mountain range (i.e., orographic lifting between Sierra Leone, Liberia, and Cote d'Ivoire). That is, the RCMs might have produced too much rainfall west of the mountain (causing a too early onset) and transported less moisture for rainfall east of the mountain (leading to a late onset). Nonetheless, more than 50% of the simulations overestimated the average ROD over the Guinea zone. In contrast, more than 75% of the models underestimated the average ROD over the Sahel zone, where the model ensemble produced too early onset dates

(about 20 days early). The opposite sign in the simulation bias over the Guinea and Sahel suggested that the mechanism for producing rainfall during the early stage of the rainy season in the models was too weak over the Guinea, but too strong over the Sahel zone. Conversely, the RCMs featured their best performance over the Savanna zone, where the model bias was less than 10 days and the observed RODs were between the 2nd and 3rd quartile of the model spread.

Each box plot indicates the minimum, 25th percentile, median, 75th percentile and maximum values of the RCMs ensemble (Figure 4.14).

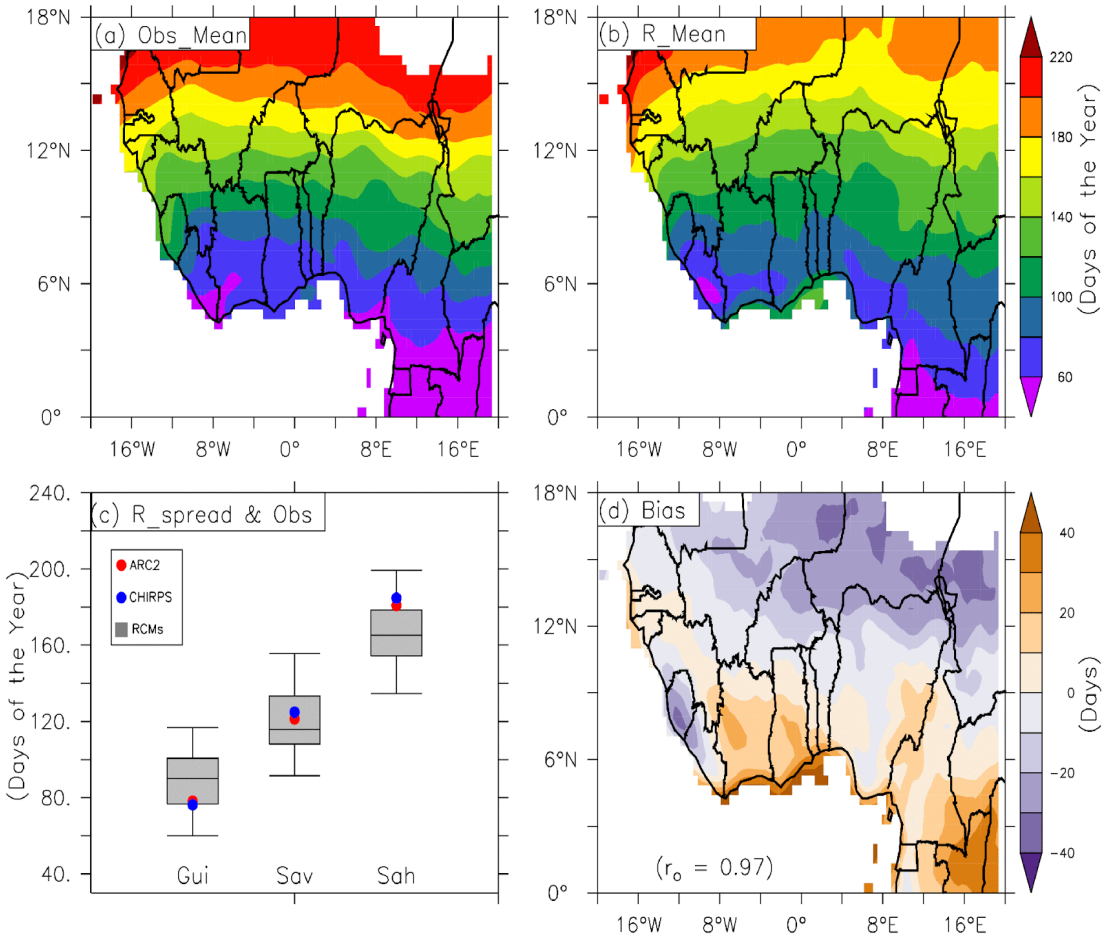

Figure 4.14: The Climatology of RODs over West Africa, as Observed (panel a; Average of ARC2 and CHIRPS) and Simulated (panel b; RCMs Ensemble Mean). Panels (c and d) show the Box Plot and the Bias and the Correlation between the Observed and Simulated Values (r_o).

4.5.2 Evaluation of RCD by the CORDEX RCMs

The models also gave a credible simulation of RCDs over West Africa, where the simulated RCD pattern strongly correlated with the observed pattern (r_c = 0.94; Figure 4.15). The simulations agreed with the observations on the zonal distribution and southward increase of the RCDs. The southward increase depicted the southward retreat of the WAM with its moisture-laden air over the region (e.g., Nicholson, 2013; Vellinga *et al.*, 2013). The simulated RCDs ranged from 7September (day 250 of the year) over the Sahel to 16November (day 320 of the year) over the Guinea zone. These dates were almost the same as the observed dates over the Sahel and Savanna, although they were too early over the Guinea zone. Over each zone, the observed mean RCD fell within the 1st and 3rd quartile of the model simulation (Figure 4.15c). The simulated RCD bias was generally smaller than that of the simulated ROD. It was less than 5 days in the Sahel and Savanna zone, but up to 10 days in the Guinea zone (especially over the south-west mountain range). This bias suggested that the RCMs also struggled to reproduce the mechanisms that induced rainfall during the late-rainy season (September to November) over the Guinea zone. This could be attributed to a too shallow moisture depth or a too weak convection triggering mechanism in the models.

Each box plot indicates the minimum, 25th percentile, median, 75th percentile and maximum values of the RCMs ensemble (Figure 4.15).

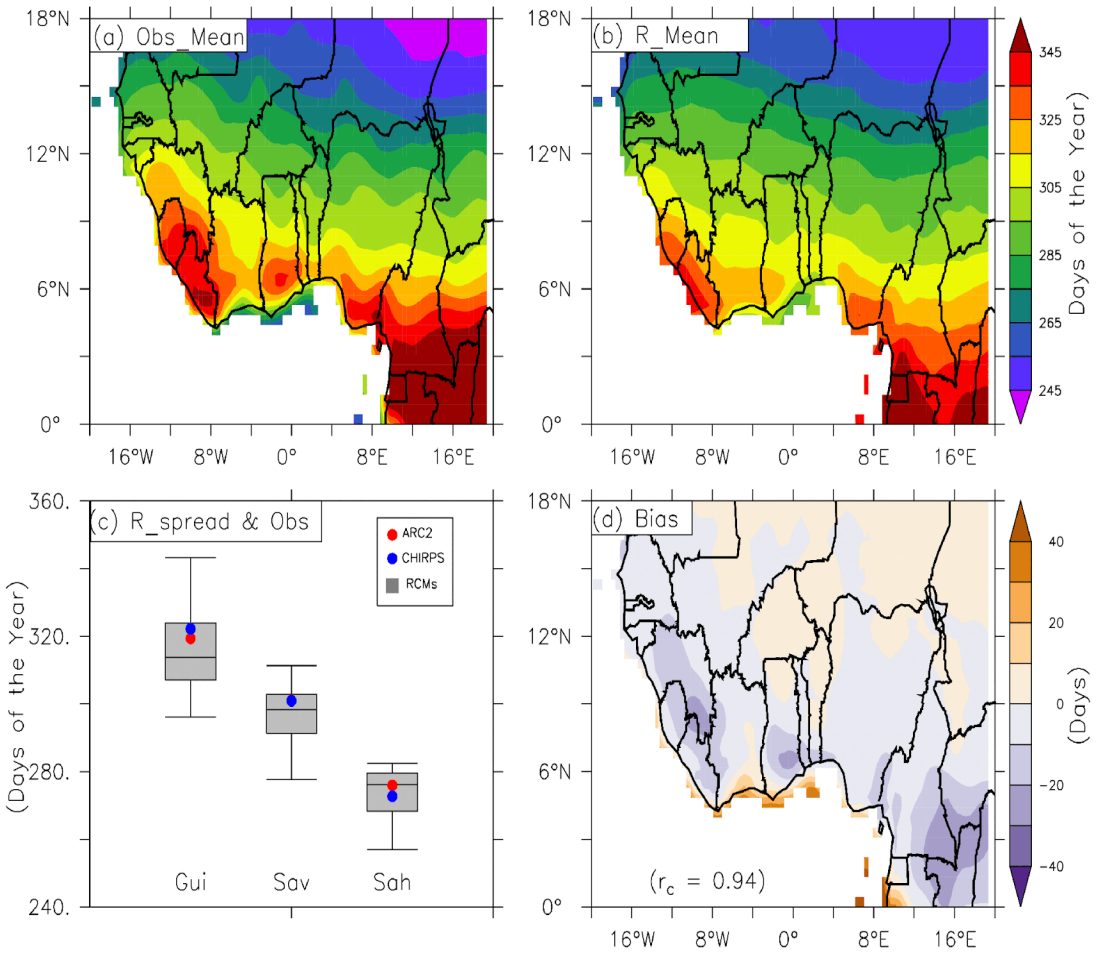

Figure 4.15: The Climatology of RCDs over West Africa, as Observed (panel a; Average of ARC2 and CHIRPS) and Simulated (panel b; RCMs Ensemble Mean). Panels (c and d) show the Box Plot and the Bias and the Correlation between the Observed and Simulated Values (r_o).

4.5.3 Evaluation of LRS by the CORDEX RCMs

The good performance of the models in reproducing ROD and RCD was reflected in the simulated LRS (Figure 4.16). The level of agreement between the observed and the simulated LRS was also high (r_L= 0.97). In both the observations and the simulation, the LRS was longest (about 240 days) over the Guinea zone (where the ROD was earliest, and the RCD was latest) and shortest (about 60 days) over the Sahel zone (where the ROD was latest, and the RCD was earliest). However, the pattern of the simulated LRS bias was a mirror image of that of the ROD, because of the larger simulation bias in the ROD than in the RCD. Hence, the models overestimated the LRS (by up to 25 days) over the central and eastern parts of the Guinea zone but underestimated it (by up to 25 days) over the western part of the same zone and the western part of the Sahel. However, the level of agreement between the observed and simulated ROD showed that the model generally captured the dynamics of the monsoon system that drives the onset and cessation of rainfall over West Africa. The results further corroborated the findings of previous studies on the reliability of the CORDEX simulation datasets for studying West African climate (e.g., Nikulin *et al.*, 2012; Mounkaila *et al.*, 2014; Klutse *et al.*, 2016; Sylla *et al.*, 2016; Diasso and Abiodun, 2017).

Each box plot depicts the minimum, 25th percentile, median, 75th percentile and maximum values of the RCMs ensemble (Figure 4.16).

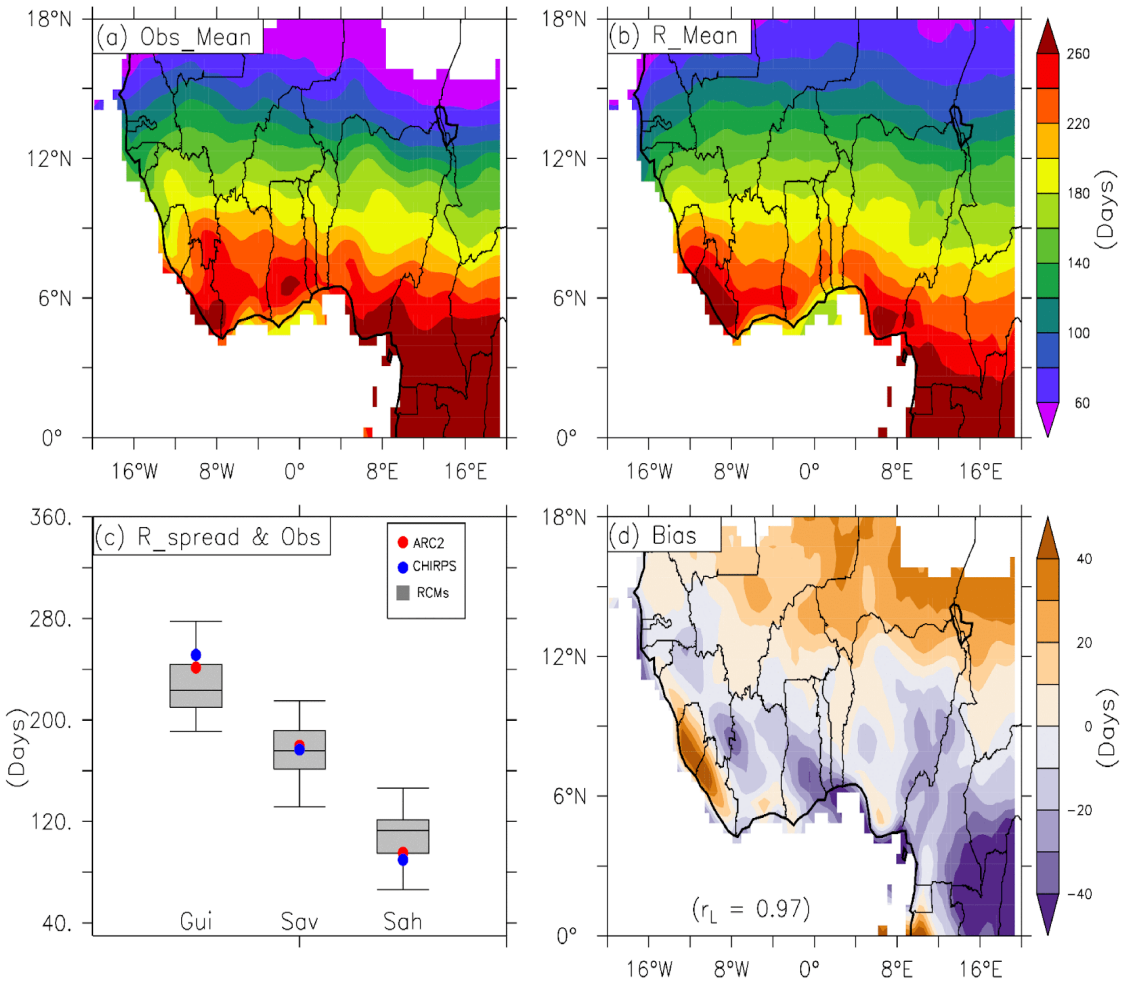

Figure 4.16: The Climatology of LRS over West Africa, as Observed (panel a; Average of ARC2 and CHIRPS) and Simulated (panel b; RCMs Ensemble Mean). Panels (c and d) show the Box Plot and the Bias and the Correlation between the Observed and Simulated Values (r_o).

4.6 EVALUATION AND SENSITIVITY OF CONVECTION SCHEMES IN THE WRF MODEL TO SIMULATE SEASONAL RAINFALL CHARACTERISTICS OVER WEST AFRICA

This section examines the sensitivity of rainfall characteristics among different convection schemes in the WRF model and looks at how an alteration in a convection scheme affects the simulation of these rainfall characteristics.

4.6.1 Evaluation of the simulated rainfall characteristics

4.6.1.1 Monthly Rainfall

The results showed that all the convection schemes overestimated the average monthly rainfall over the different zones and over the whole of West Africa, except for the modified Tiedtke which underestimated the average monthly rainfall in the Sahel (Figure 4.17). This overestimation had been reported by other researchers too (e.g., Fonseca *et al.*, 2015; Mugume *et al.*, 2017). Nevertheless, the schemes were reasonably able to simulate the characteristics of the WAM; the start the monsoon, the peak (in August) and the retreat southwards (in September) over the Savanna and the Sahel (Figure 4.17a and b). Over the Guinea Coast region, the schemes were also able to reproduce the break in rainfall (the little dry season) in July - August (Figure 4.17c).

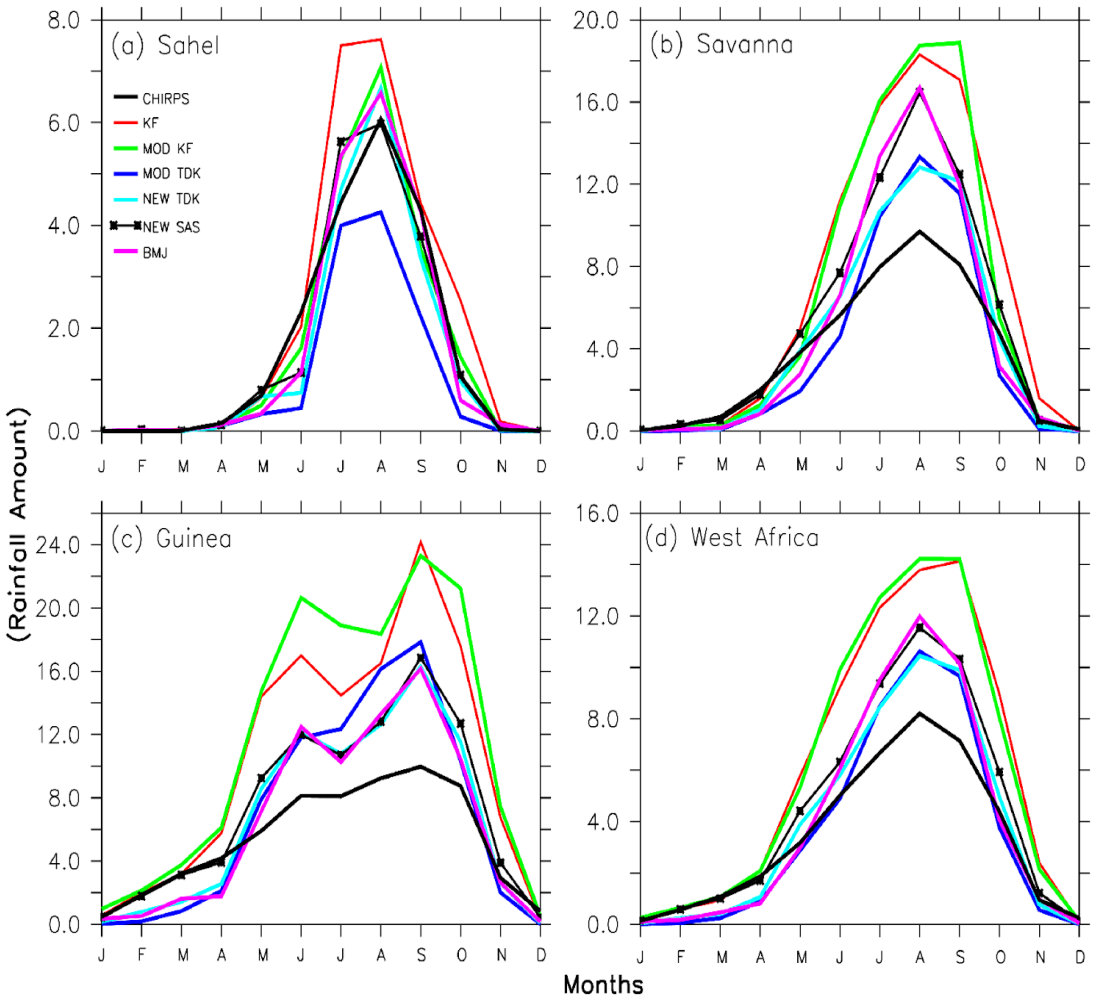

Figure 4.17: Mean Monthly Rainfall (mm/day) as represented by CHIRPS and Six Different Convection Schemes in the WRF Model over the Three Zones in West Africa.

4.6.1.2 Rainfall Onset, Cessation and Length of Rainy Season

The CP schemes practically replicated the spatial distribution of RODs over the study area, albeit with some biases (Figure 4.18). There was a high spatial correlation between each scheme and the observation (r = 0.9 to 0.95), and all the important features of the observed pattern were well reproduced by the schemes. For instance, almost all the schemes simulated a northward movement of RODs from the coastal region (south) as was the case in the observation. However, most of the schemes simulated ROD too early (about 20 days early) over some parts of the Guinea zone and too late (about 40 days late) over most areas of the sub-continent. This simulation bias could suggest that the mechanism for producing rainfall during the early stage of the rainy season in the model was too weak over the Guinea, but too strong inland (Kumi and Abiodun, 2018). Nonetheless, the CP schemes performed best in simulating the ROD characteristics over West Africa, which echoed the need to modify them for more robust simulation results.

The correlation between the observed and each convection scheme are shown in brackets. The results of panel (a) subtracted from each scheme are shown as contours (Figure 4.18).

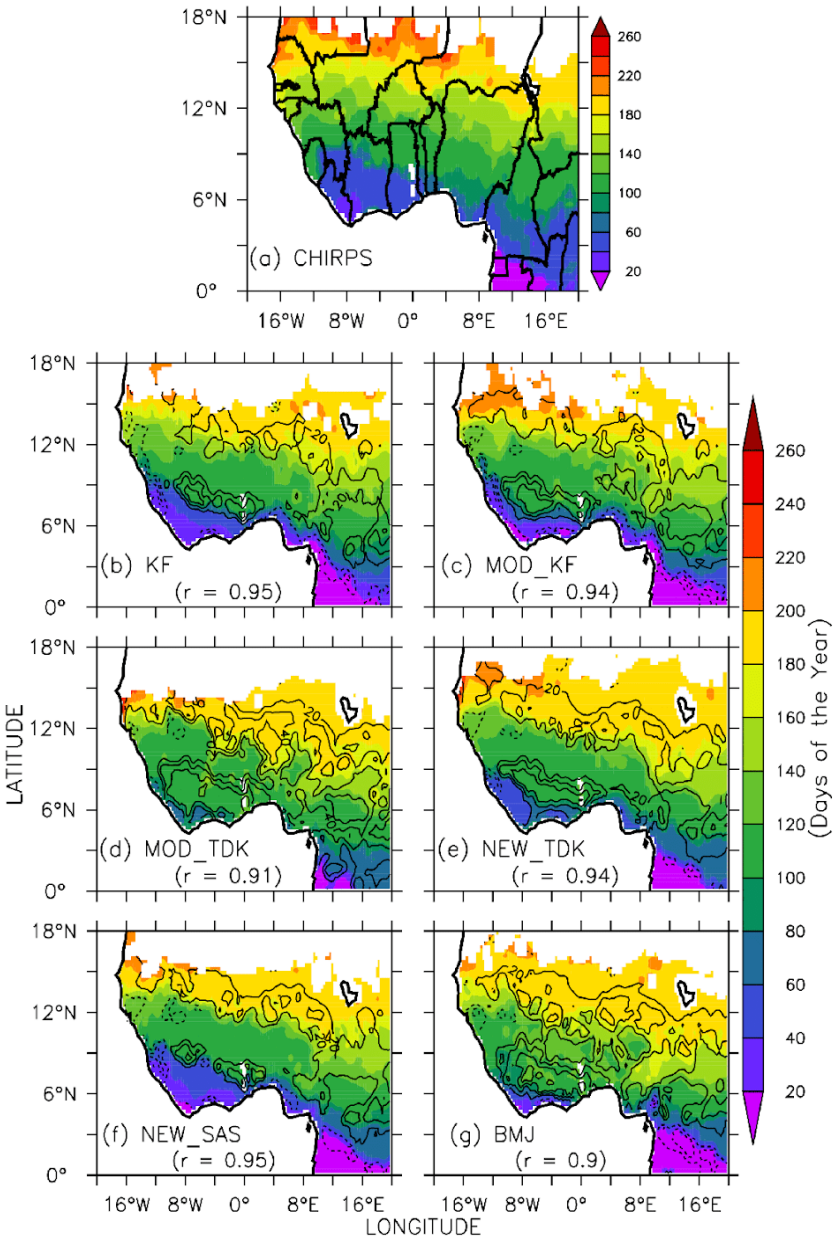

Figure 4.18: The Spatial Distribution of RODs over West Africa as Shown by CHIRPS (panel a) and Simulated by Different Convection Schemes in the WRF Model (panels b to g).

The schemes also realistically simulated the RCDs and showed the major features as in the observation (Figure 4.19). As for the ROD, there was good agreement between the schemes and the observation on the spatial distribution pattern, where the RCD decreased northward from the coastal areas. Although there were some biases in the simulation, all the schemes simulated early RCD over the Sahel and late RCD over the southern Guinea zone. The bias could be as a result of the inability of the schemes to strongly trigger convection (i.e., too shallow moisture depths) over the Sahel, while the opposite might have occurred in the Guinea zone. The spatial correlation of the RCD between the schemes and the observation (r = 0.43 to 0.67) was not as high as that of the ROD, although it was not too weak. However, the best performance of all the schemes was over the Savanna, where the simulations were almost the same as the observed spatial pattern.

The correlation between the observed and each convection scheme are shown in brackets. The results of panel (a) subtracted from each scheme are shown as contours (Figure 4.19).

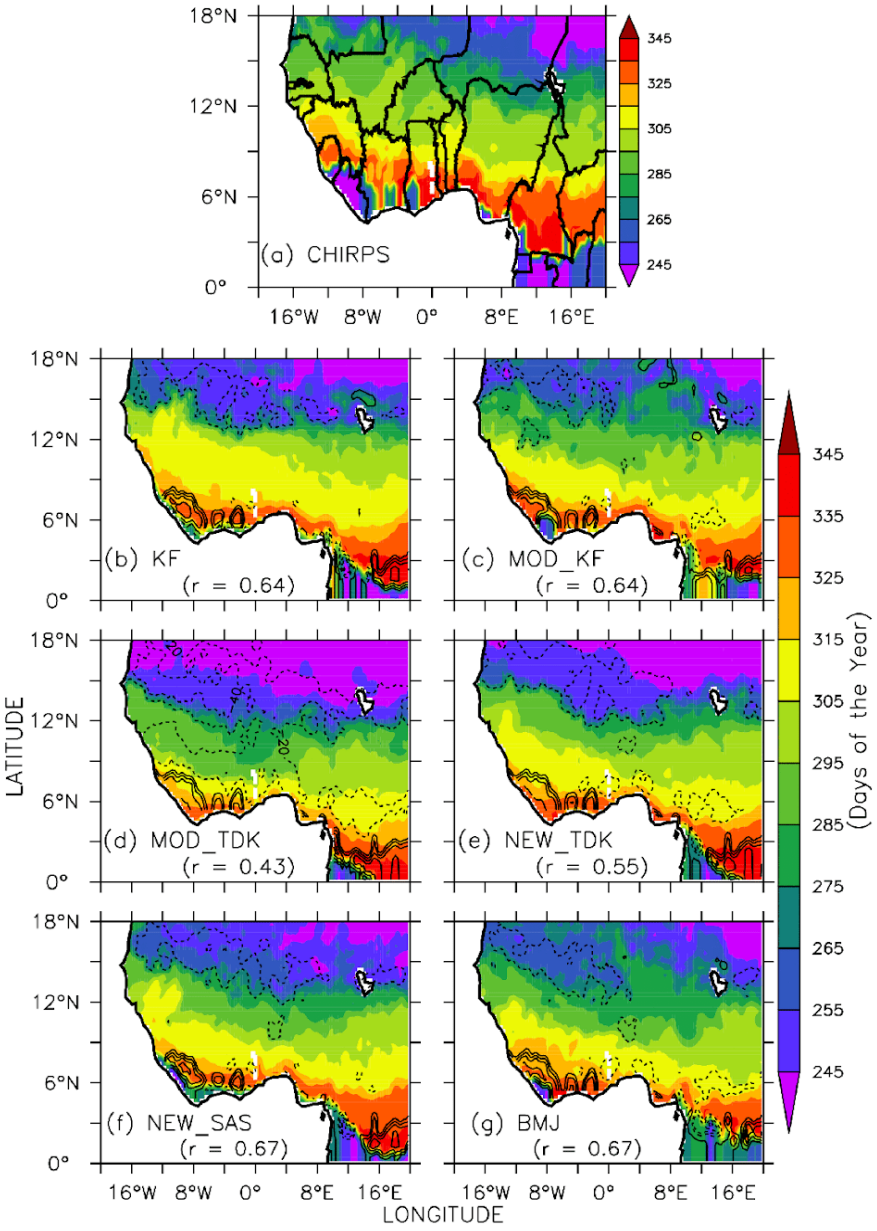

Figure 4.19: The Spatial Distribution of RCDs over West Africa as Shown by CHIRPS (panel a) and Simulated by Different Convection Schemes in the WRF Model (panels b to g).

As in the case of ROD and RCD, the schemes performed well in simulating the LRS over West Africa (Figure 4.20). The spatial correlation between the schemes and the observation was quite higher (r = 0.84 to 0.91) than that of the RCD. All the schemes realistically simulated the pattern and features of the observed LRS, with the longest season in the south and shortest in the north. The performance of the convection schemes in simulating ROD and RCD over the three zones was deeply reflected in the simulation of the LRS. That is, the early ROD and the late RCD in the Guinea zone had contributed to the late LRS over the same zone, just as the late ROD and early RCD in the Sahel had resulted to the early LRS over this zone. However, the magnitude of the bias in simulating the LRS over the sub-region (i.e., the underestimate of the LRS) was higher than that of the RCD and mirrored that of the ROD. Despite these discrepancies, the results showed that all the schemes were capable of simulating the features of the West African rainfall characteristics.

The correlation between the observed and each convection scheme are shown in brackets. The results of panel (a) subtracted from each scheme are shown as contours (Figure 4.20).

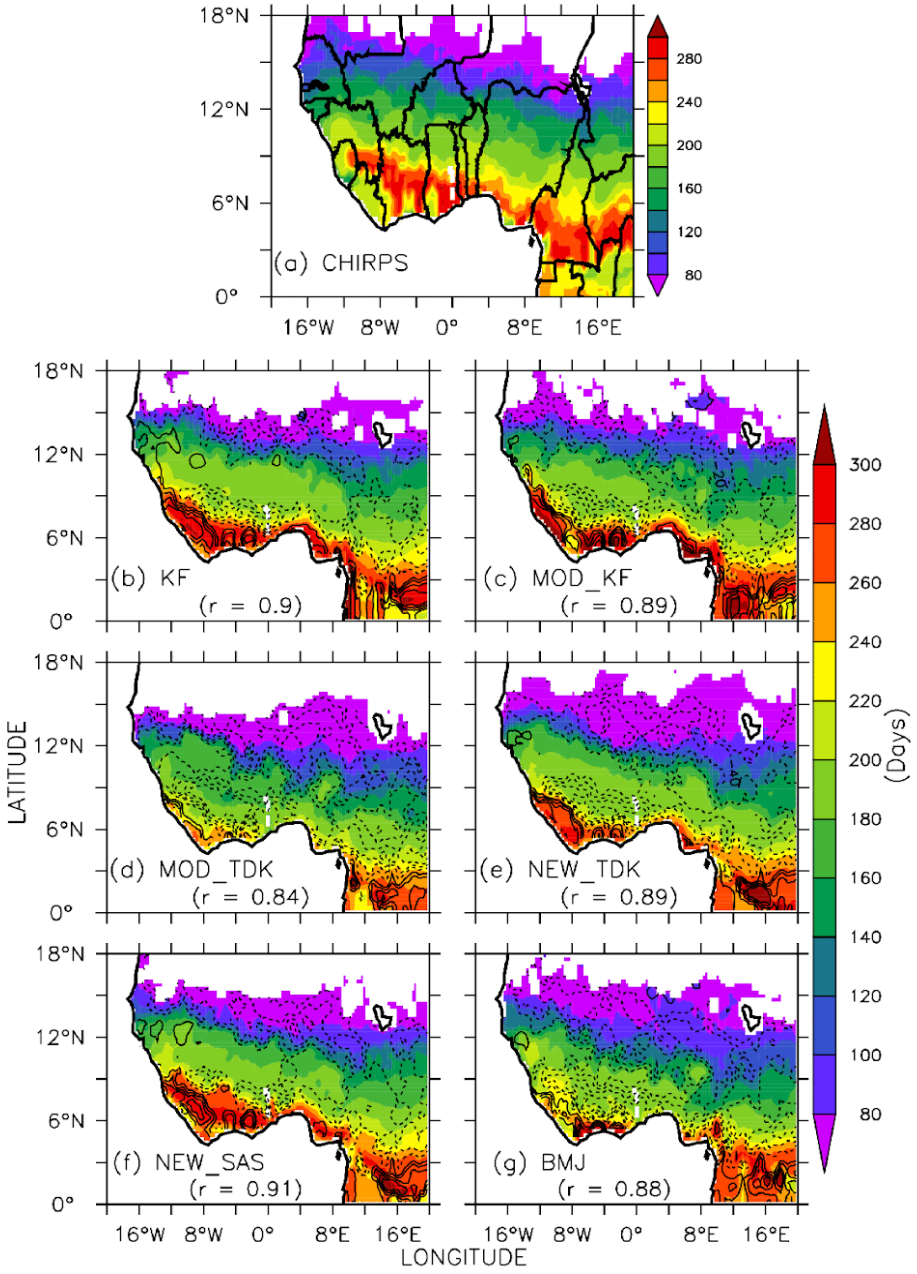

Figure 4.20: The Spatial Distribution of the LRS over West Africa as Shown by Observation (CHIRPS; panel a) and Simulated by Different Convection Schemes in the WRF Model (panels b to g).

4.6.2 Sensitivity Tests

4.6.2.1 Monthly Rainfall Amount

In these sensitivity tests, 20 experiments were performed to evaluate changes in simulated rainfall characteristics due to modifications in the parameters α (in the temperature reference profile) and F_S (in the humidity reference profile). In all the experiments, the temperature reference profile was made warmer: α was set to 0.85 (as suggested by Betts 1986), 0.9 (the default value), 1.2, 1.4 and 1.6, while F_S was set to be moister: F_S was set to 0.3, 0.6, 0.85 (the default value) and 0.9 (a slight increase from the default value). The mean monthly rainfall produced by modifications in α and F_S were sensitive to the zones (Sahel, Savanna and Guinea; Figure 4.21). However, this study sought to look for the best combination of these parameters over the whole of West Africa, hence Figure 4.21 (d) is discussed. The results showed that a smaller α (i.e., a less warm or 'cooler' temperature reference profile) and a larger F_S (i.e., a less moist or 'drier' humidity reference profile) led to the scheme producing excessive rainfall over the study area (e.g., $\alpha = 0.85$ and $F_S = 0.85$; $\alpha = 0.85$ and $F_S = 0.9$; $\alpha = 0.9$ and $F_S = 0.9$). The opposite, i.e., a larger α (a warmer temperature reference profile) and a smaller F_S (a moister humidity reference profile) led to the scheme producing less rainfall over the study area (e.g., $\alpha = 1.4$ to 1.6, and $F_S = 0.3$ to 0.6). The modification experiments on the mean monthly rainfall amount suggested that, when α was set to 1.2 and F_S was set to 0.6, the simulation agreed more with the observation (CHIRPS), albeit with small bias. Setting $F_S = 0.6$, agreed with the recommendation by Janjic (1994) and Fonseca *et al*. (2015). However, setting $\alpha = 1.2$ did not produce very little rainfall, as found by Fonseca *et al*. (2015); the discrepancy between the results obtained in this study and those of Fonseca *et al*. (2015) may be

due to the different geographical locations and durations of the simulations. For the simulation of rainfall amount in West Africa, $\alpha = 1.2$ and $F_S = 0.6$ was thus recommended by this study and was tested for a period of a 30-year run (climatology).

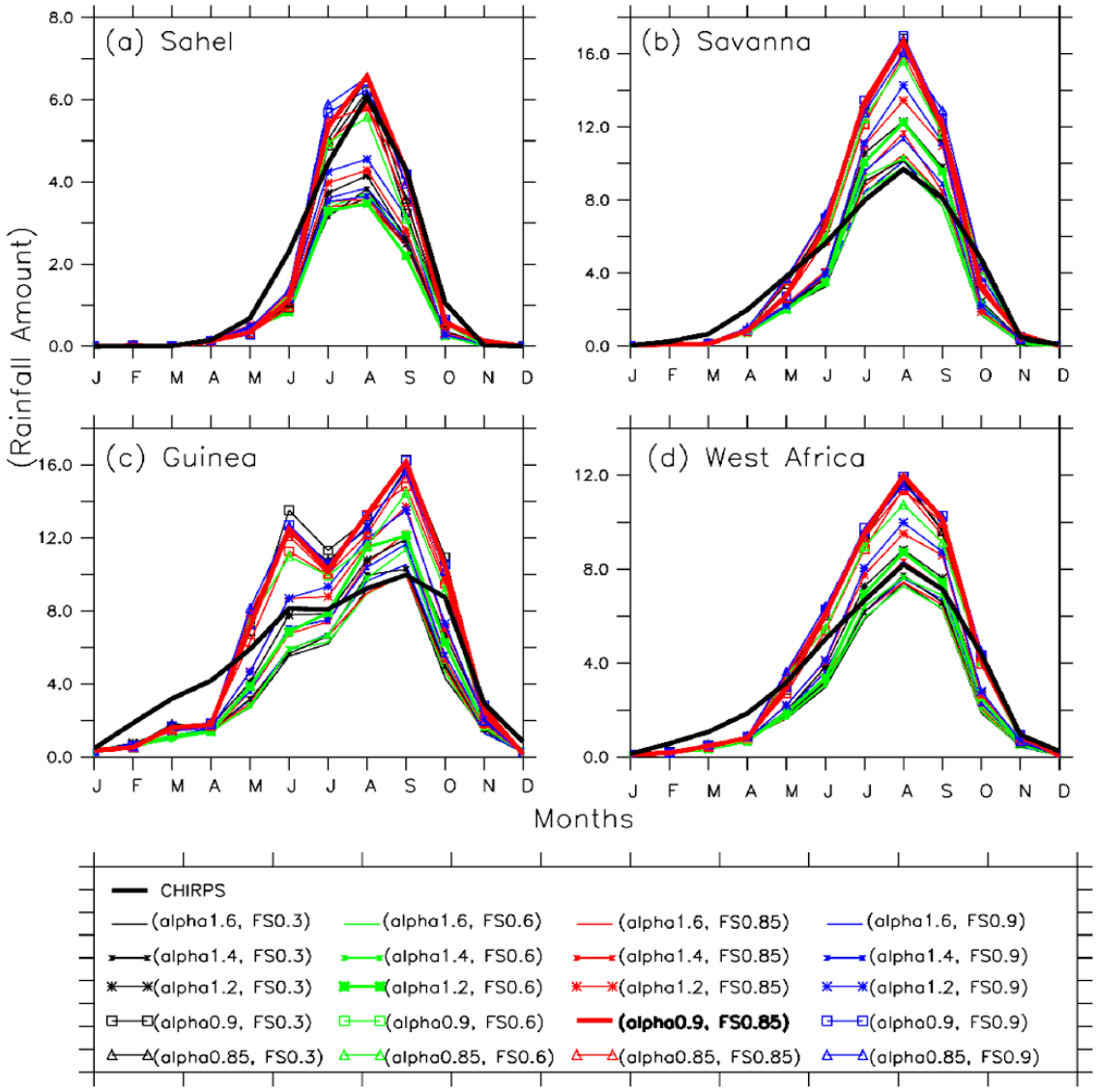

Figure 4.21: Monthly Rainfall as Represented by CHIRPS, Default WRF-BMJ (alpha0.9, Fs0.85) and Modifications to the BMJ Scheme over the Three Zones in West Africa.

4.6.2.2 Onset, Cessation and Length of the Rainy Season

Figure 4.22 shows the ROD bias to sensitivity in modifications of α and F_S over West Africa. The figure shows a 4x5 matrix run, where F_S increased horizontally and α increased vertically. Generally, the magnitude of the positive bias (late ROD) increased with increasing α, except for Figure 4.22(p) (in red box), which is the default BMJ scheme. The reverse occurred in the simulation of RCD (Figure 4.23) and the LRS (Figure 4.24); the magnitude of the negative bias (early RCD and LRS) increased with increasing α. Considering the three statistical measures used, Figure 4.22(u) (α = 0.85 and F_S = 0.9; in blue box) was suggested as the best fit for this study, since it had the lowest bias (and RMSE) and high correlation for ROD, RCD and LRS (e.g., Smith *et al.,* 1996). The meaning of this combination is that a smaller α, as suggested by Betts (1986), and a larger Fs (a small increase in the default value), produced excessive rainfall (Figure 4.21) but simulated ROD, RCD, and LRS closer to the observed pattern in the study area.

The Root Mean Square Error (rmse) and Correlation (r) between the parameters and observation (CHIRPS) are in brackets. Panel (u; in blue box) is the suggested modification (Figure 4.22 to 4.24).

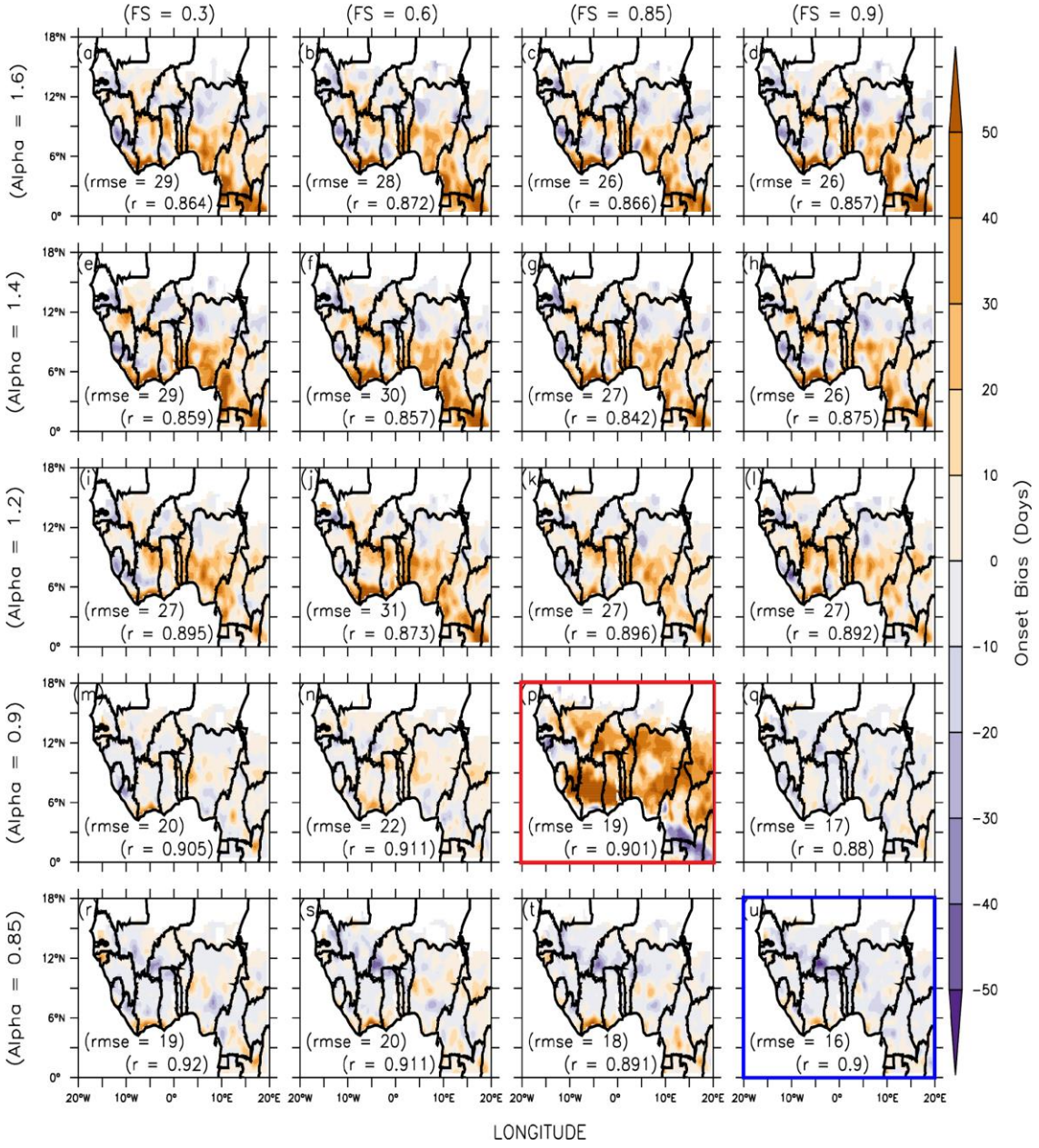

Figure 4.22: ROD Bias with Respect to the Default WRF-BMJ (panel p; in red box) and Modification to the BMJ Scheme (panels a to n, q to u) over West Africa.

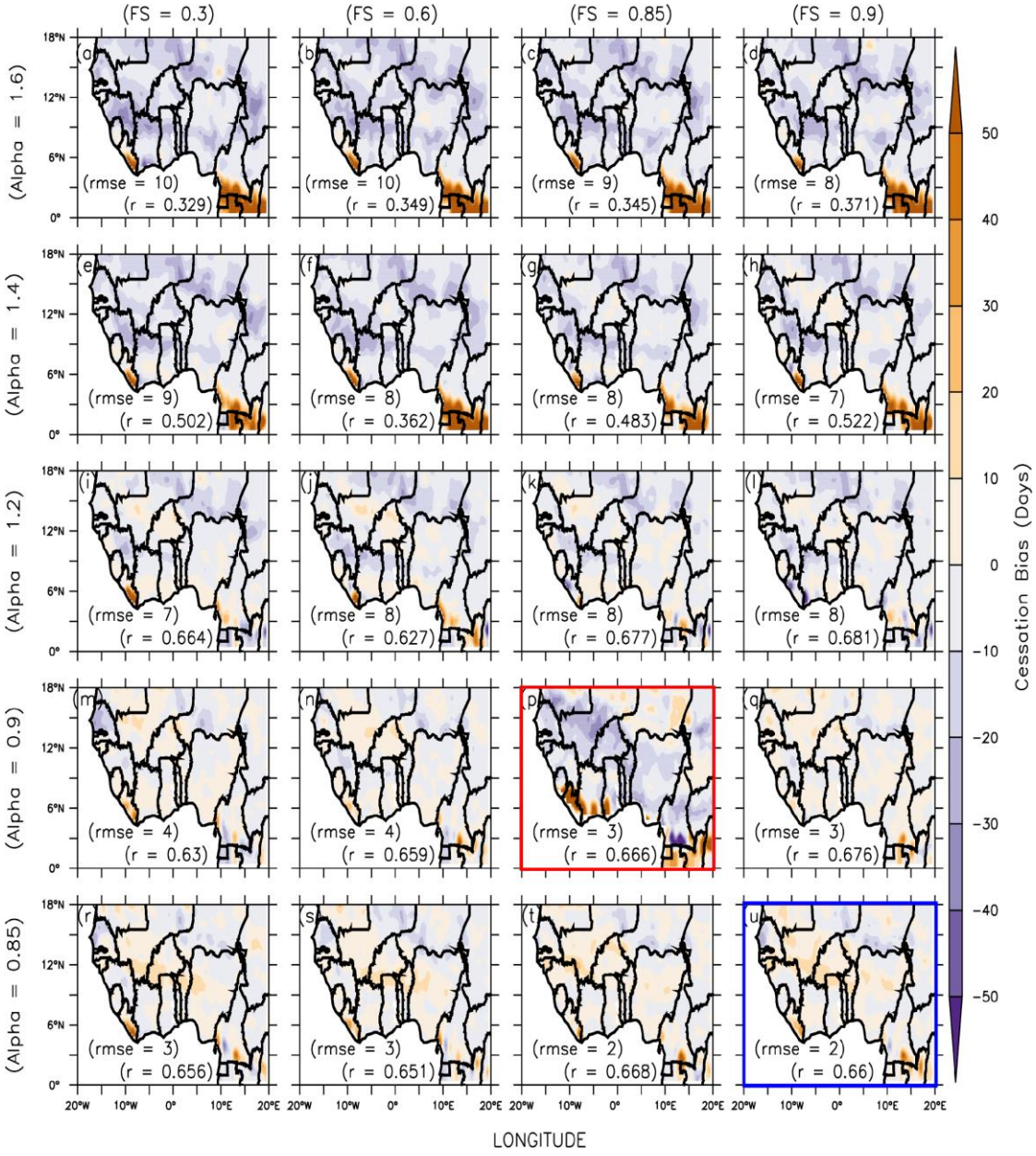

Figure 4.23: RCD Bias with Respect to the Default WRF-BMJ (panel p; in red box) and Modification to the BMJ Scheme (panels a to n, q to u) over West Africa.

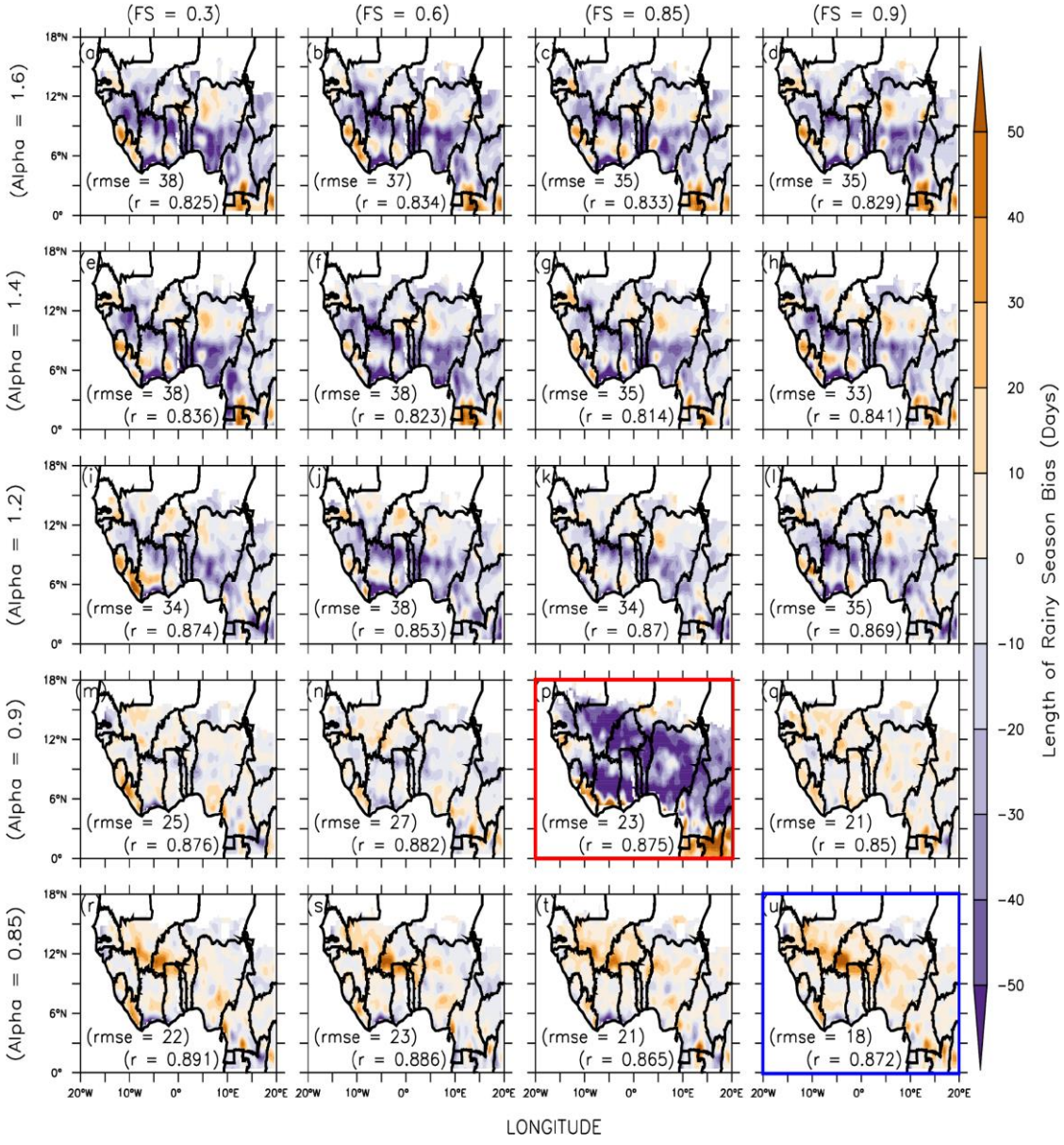

Figure 4.24: LRS Bias with Respect to the Default WRF-BMJ (panel p; in red box) and Modification to the BMJ Scheme (panels a to n, q to u) over West Africa.

4.6.3 Evaluation of 30-year simulation from the Modified BMJ Scheme

4.6.3.1 Monthly Rainfall Climatology

The results showed that the modified BMJ scheme gave a more realistic simulation of the observed mean monthly rainfall than the default WRF (Figure 4.25). For instance, over the Savanna and the whole of West Africa, the modified scheme gave a better estimate of the observed mean rainfall amount than the control WRF (Figure 4.25b and d). This showed that there is a much more significant improvement in the simulation of the observed mean monthly rainfall by the modified scheme than in the default WRF-BMJ scheme. Although the modified scheme overestimated the JAS (July - September) rainfall amount over the Guinea zone, it still gave a better simulation than the default scheme (Figure 4.25c). However, the modified scheme failed to give a realistic simulation over the Sahel (Figure 4.25a); it underestimated the peak of the monsoon in August (Omotosho and Abiodun, 2007; Vellinga *et al.,* 2012; Akinseye *et al.,* 2016) as well as the total amount. Such failures in the modified scheme may require further modifications such as interior (analysis) nudging, as suggested by Fonseca *et al*. (2015) who also modified the BMJ over the tropics.

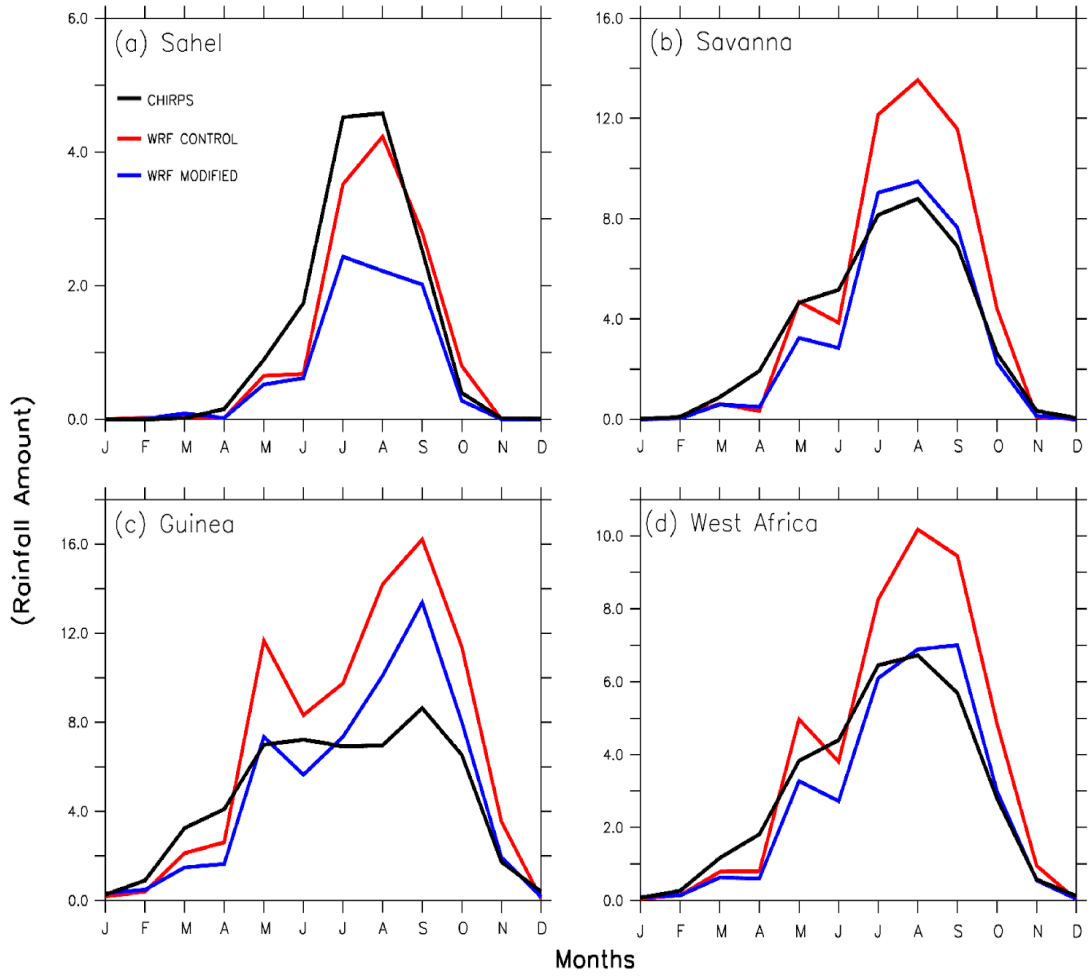

Figure 4.25: Monthly Rainfall as Represented by CHIRPS, Default WRF-BMJ (alpha0.9, Fs0.85) and the Modification (alpha1.2, Fs0.6) to BMJ Scheme for 30 Year Period (1981-2010).

4.6.3.2 Climatology of Rainfall Onset Dates

The modified BMJ scheme gave a better representation of the observed spatial ROD distribution than the default BMJ scheme (Figure 4.26), although there were some discrepancies. That is, the new scheme was able to represent the northward progression of RODs (Omotosho *et al.,* 2000; Sylla *et al.,* 2013; Diaconescu *et al.,* 2015) more accurately than the default scheme. This better simulation was more pronounced over the Sahel, where the new scheme was able to simulate the late ROD over most areas more accurately than the default scheme. The high spatial correlation value between the modified scheme and observation (r = 0.9, Figure 4.26c), and the low RMSE value (rmse = 39, Figure 4.26f) compared to the default scheme (r = 0.88, rmse = 50, Figure 4.26b and e), was a clear evidence of improvement in the new scheme. However, the modified scheme could not rectify the early ROD over the south-west mountain range in the Guinea Coast region. This could suggest that the new scheme overestimated the influence of orographic lifting, especially between Sierra Leone, Liberia, and Cote d'Ivoire, and hence a further improvement of the scheme is needed in the tropics (Fonseca *et al.,* 2015).

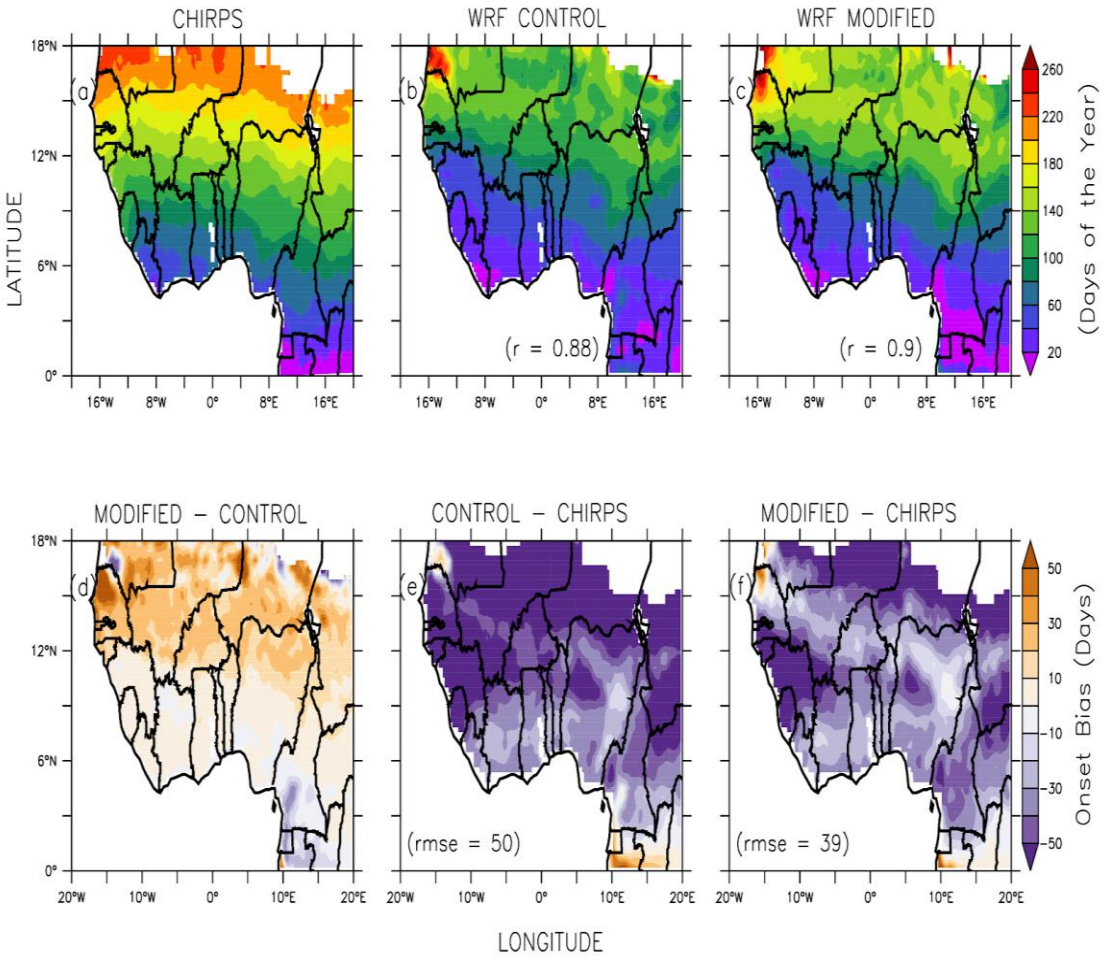

Figure 4.26: Spatial Distribution of ROD as Represented by CHIRPS, Default WRF-BMJ (alpha0.9, Fs0.85) and the Modification (alpha0.85, Fs0.9) to BMJ Scheme for 30 Year Period (1981-2010).

4.6.3.3 Climatology of Rainfall Cessation Dates

Although the RMSE showed that the modified scheme (rmse = 9) gave a better simulation of RCD than the default scheme (rmse = 13), the spatial correlation was very poor (r = 0.27, Figure 4.27). The new and default BMJ schemes both struggled to simulate the spatial distribution of the RCDs over West Africa, as represented in the observation. The southward increase of RCDs as shown by the observation was poorly replicated by the convection schemes. This southward increase has been documented as being associated with the retreat of the WAM, which transports moisture into the sub-region from the Atlantic Ocean (Redelsperger *et al.,* 2002). The inability of the CP schemes to simulate this distinct feature suggested that more work needs to be done regarding the schemes' ability to simulate the three main features of the WAM (Omotosho and Abiodun, 2007; Klein *et al.,* 2015) over a long period.

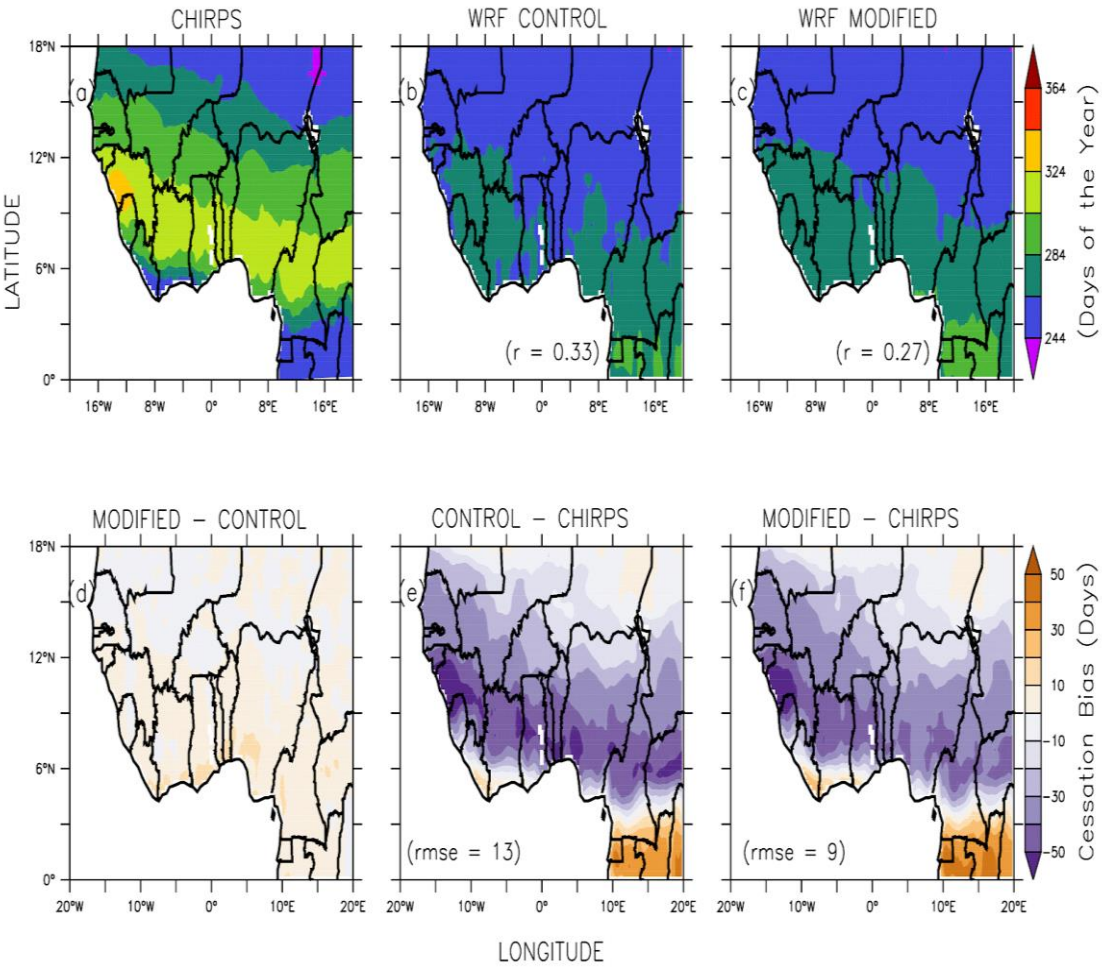

Figure 4.27: Spatial Distribution of RCD as Represented by CHIRPS, Default WRF-BMJ (alpha0.9, Fs0.85) and the Modification (alpha0.85, Fs0.9) to BMJ Scheme for 30 Year Period (1981-2010).

4.6.3.4 Climatology of Length of Rainy Season

The modified BMJ scheme was better able to simulate the observed features of the LRS than the default scheme, although there were some biases (Figure 4.28). It was able to simulate the observed spatial distribution of the LRS, in that there was a shorter season in the north that increased towards the south of the sub-region. This could be seen especially over the Sahel, and also with the RMSE value (rmse = 17, Figure 4.28c and f). However, the modified scheme overestimated the LRS over the southern Guinea Coast and the north of the Sahel (Figure 4.28c). The reason could be because the new scheme simulated early RODs over these areas and failed to properly simulate the end of the rains over the same areas (especially in the Guinea zone), thus resulting in an extension of the LRS. Over the Sahel, the minor late bias could be due to the scheme's inability to distinctively simulate the cessation of the rains over those areas. However, results from the modified BMJ scheme in this study have shown that a further improvement in the convection schemes of RCMs may improve their performance in specific areas at the regional level (Ma and Tan, 2009; Flaounas *et al.*, 2011; Fonseca *et al.*, 2015).

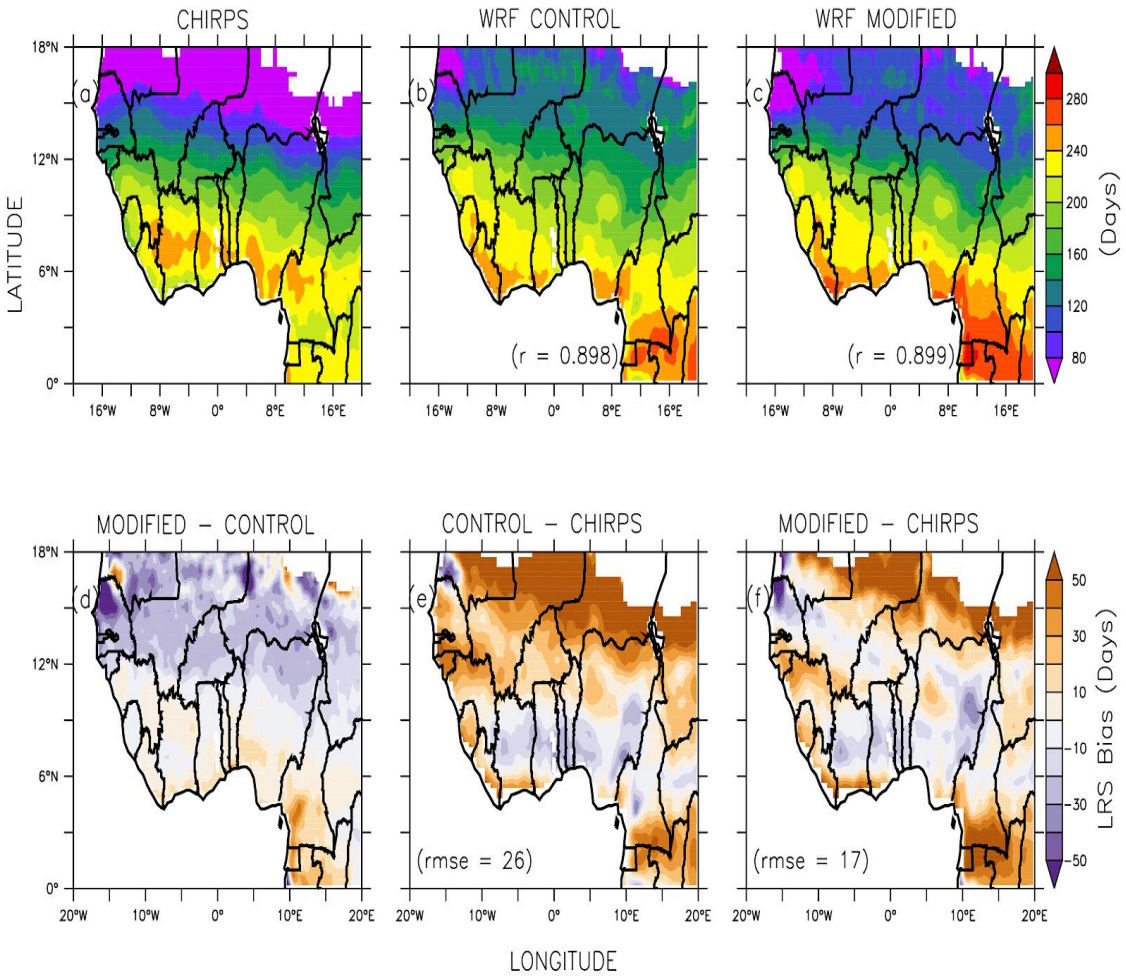

Figure 4.28: Spatial Distribution of LRS as Represented by CHIRPS, Default WRF-BMJ (alpha0.9, Fs0.85) and the Modification (alpha0.85, Fs0.9) to BMJ Scheme for 30 Year Period (1981-2010).

4.7 POTENTIAL IMPACTS OF 1.5°C AND 2°C GLOBAL WARMING ON ROD, RCD AND LRS IN WEST AFRICA

This section assesses the impacts of climate change on the characteristics of seasonal rainfall over West Africa under 1.5°C and 2°C GWLs. The future projections are also assessed under RCP4.5 and RCP8.5 scenarios.

4.7.1 Future projections of ROD, RDC and LRS under RCP4.5

The RCM ensemble mean projected a delay in future RODs (Figure 4.29). Although the horizontal distribution of the projected delay was similar under both GWLs (GWL15 and GWL20), the period of the delay was generally higher under GWL20 than GWL15 (Figure 4.29a and d). Under both GWLs, the maximum delays (about 4 days in GWL15 and 6 days in GWL20) were located over the eastern and western parts of the Sahel zone, as well as over the western mountain range in the Guinea zone. The major differences between the ROD delays under GWL15 and GWL20 also occurred over these locations. Hence, these locations were suggested as hotspots of global-induced delay in ROD. Nevertheless, there was a discrepancy among the simulations with regard to the sign of the mean ROD changes over each zone. While some simulations suggested an increase (up to 10 days delayed) in the ROD, others suggested no change or a decrease (up to 3 days early). The level of uncertainty was higher with GWL20 than with GW15, especially over the Guinea and Savanna zones. This notwithstanding, more than 75% of the models did agree on delayed RODs over the zones for both GWL15 and GWL20 (Figure 4.29g).

The impact of global warming on RCDs was weaker than it was with regard to RODs (Figure 4.29). In comparison with RODs, the magnitude of the RCD change was low,

and the maximum change was confined over the western part of the Guinea zone, where the RCM ensemble projects up to 6 days' delay in RCD. However, the magnitude and area of the RCD delay increased with the warming level. For instance, over the central part of the Guinea and Savanna zones, the delay was 2 days longer under GWL20 than GWL15. This suggested that, with moist soil conditions over West Africa during the later southward retreat of WAM, a warmer boundary (induced by the global warming) could enhance evaporation and make the boundary layer moister for more convection, thereby extending the RCD. Nevertheless, the mean RCD projection over each zone was associated with a large uncertainty, because there was a weak agreement among the models on the projected mean RCD over the zones (Figure 4.29h). Over each zone, irrespective of the warming level, almost half of the simulations disagreed that there will be an increase in RCD following global warming. The degree of the uncertainty was higher with GWL20 than GWL15. This disagreement may be attributed to differences in the sensitivity of CP to the boundary layer in the RCMs. However, the uncertainty associated with the projected changes in RCD was higher than that of the RODs.

As projected changes in the ROD were stronger than those in the RCD, the pattern of changes in the LRS mirrored that of the ROD (Figure 4.29). So, a decrease in LRS was projected over most areas of West Africa. The maximum decrease (about 6 days) was located over the western and eastern parts of the Sahel zone. The delay in rainfall onset over the western Sahel agreed with some previous studies that used CORDEX models (e.g., Mariotti *et al.*, 2014; Diallo *et al.*, 2016). These studies did not only suggest a projected delay in the onset of the rains over the said area, but also projected a shortening of the rainy season over this part of the Sahel. While Mariotti *et al.* (2014) associated the precipitation decrease with a weakening of the 6-9 day regime of

the activity of the African Easterly Waves (AEWs), Diallo *et al*. (2016) attributed the cause to large warming, probably a result of lower evaporative cooling and cloudiness found in that region. Despite the delay in ROD over the western part of the Guinea zone, an increase in the LRS was projected over this area because of the delay in RCD. This suggested a forward shift in the rainy season of this area. Nevertheless, the response of LRS changes to the increase in warming level varied over the region. For instance, Figure 4.29 shows that, while the additional warming (i.e., from GWL15 to GW20) intensified the LRS decreases over the Sahel zone (by up 3 days) and strengthened the LRS increases over the western part of the Guinea and Savanna zones (by about 2 days), it reduced the magnitude of the LRS decreases over the eastern part the of Guinea and Savanna zones. There was uncertainty in the projected changes in average LRS over the zones because of the disagreement among the simulations regarding the direction of the LRS changes (±6 days over the Guinea and Savanna zones and ±8 days over the Sahel zone). The level of this uncertainty increased with the warming level (Figure 4.29i). Nonetheless, for both GWL15 and GW20, more than 50% of the simulations agreed on a decrease in mean LRS over each of the zones. Hence the level of uncertainty in the LRS projection was lower than that of the RCD but higher than that of the ROD.

The future projections over each climatic zone over West Africa (i.e. Guinea, Savanna, and Sahel) are shown in panels (g, h, and i, respectively). Each box plot indicates the minimum, 25th percentile, median, 75th percentile and maximum values of the RCMs ensemble. The contours represent the difference between GWL15 (1.5°C) and GWL20 (2°C). The significant areas are indicated with dots, showing where at least 15 (79%) of the models agree on the sign of change (Figure 4.29).

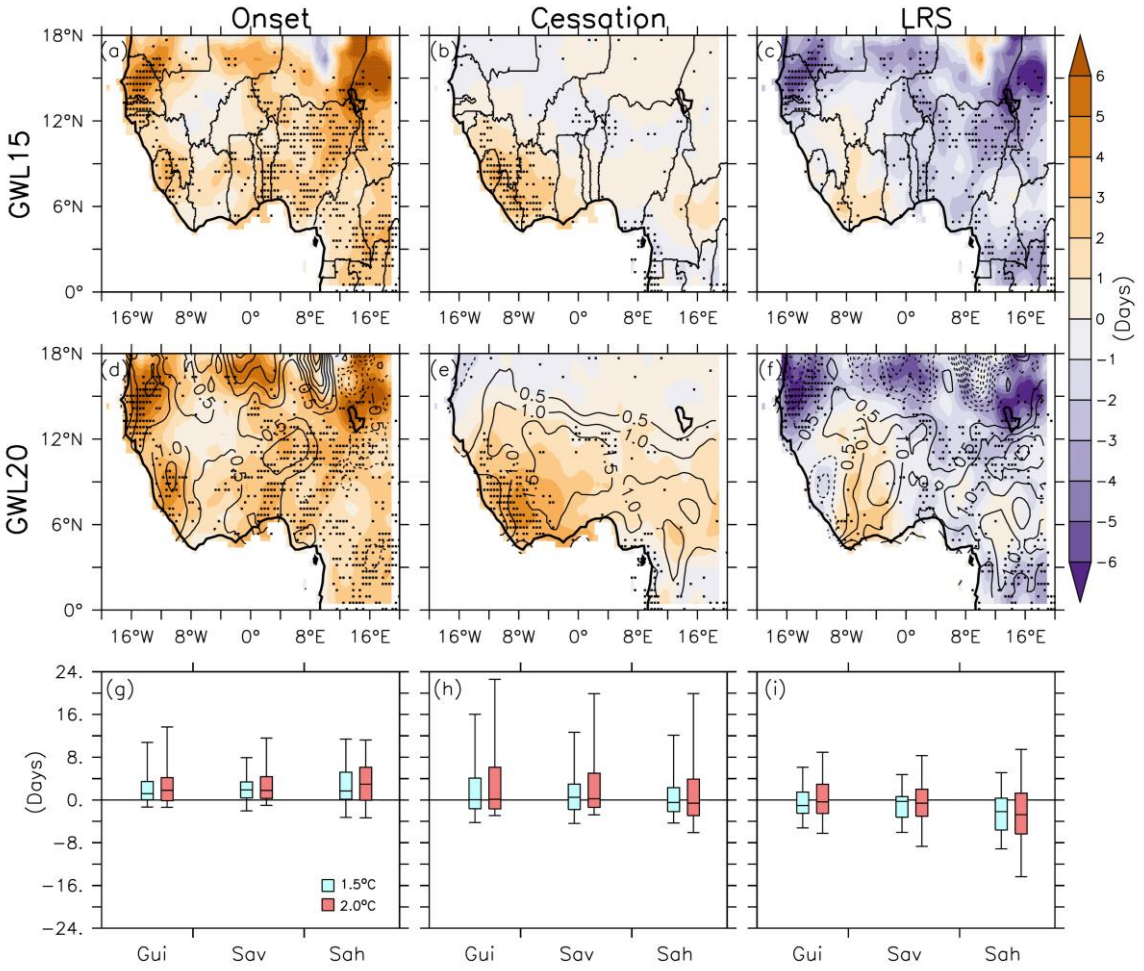

Figure 4.29: The Future Projection of RODs (panel a, d) RCDs (panel b, e) and LRS (panel c, f) over West Africa (shaded) for GWL15 and GWL20 (top and middle panels) under RCP4.5 Scenario. Panels (g, h, and i) show the Box Plots.

4.7.2 Future projections of ROD, RDC and LRS under RCP8.5 Projection

There were some notable differences between the RCP8.5 and RCP4.5 projections (compare Figures 4.29 and 4.30). For example, in contrast to the RCP4.5 projection, the RCP8.5 projection featured early RODs (up to 2 days) over the central Savanna and Sahel zones, and indicated that further warming may make this even earlier. This suggested that the increased greenhouse gas (GHG) forcing (i.e., RCP8.5) may encourage an early start of rains over these areas. Furthermore, over most parts of West Africa (except for the western part), the period of delay in the RCD was shorter in the RCP8.5 scenario than in RCP4.5. Also, with GWL15, the magnitude of the decrease in LRS over most part of West Africa was smaller in the RCP8.5 projection. The strongest disagreement among the models occurred in the projection of LRS over the Savanna (under GWL15) and the Sahel (under GWL20) under the RCP8.5 scenario. While the level of uncertainties in the projected changes in RCD and LRS under the RCP8.5 scenario was the same with that of RCP4.5, the level of uncertainties in the ROD projection was lower under RCP4.5 than RCP8.5.

The differences between the impacts of GWL15 and GWL20 also differed (in magnitude and direction) under RCP8.5 and RCP4.5 scenarios. For example, the RCP4.5 projection indicated that the increase in GWL (from GWL15 to GWL20) enhanced the ROD delay (by up to 2 days) over the whole of West Africa, but the RCP8.5 projection suggested that the increase enhanced the delay (by about 1 day) only over the Guinea zone, while fostering early ROD over the Sahel zone. In addition, while RCP4.5 projected a further delay in RCD (up to 2 days) over most parts of West Africa under the warmer climate, RCP8.5 limited the delay (about 1 day) in the south-western part of the Guinea zone. Hence, with RCP8.5, the additional warming (i.e., from GWL15 to GWL20) generally encouraged a decrease in the LRS

over the Guinea zone and an increase in the LRS over the Sahel zone, but, with RCP4.5, the reverse was true. The discrepancy between the RCP8.5 and RCP4.5 projections may be attributed to a number of factors. First, it may be that feedback mechanisms in the climate system enhanced the different perturbations in the parameters in different directions. A delay in RCD in one year may trigger an early ROD in the following year, if the soil was still moist before the ROD, and vice-versa. Secondly, it could also be that the different warming rate in the two scenarios induced different magnitudes of inter-annual variability of the parameters. Lastly, it may be due to varied differences in the simulations, especially given the magnitudes of the changes and the uncertainty in the projections.

However, both RCP4.5 and RCP8.5 scenarios featured a delay in RODs over the western and eastern Sahel and, a delay in RCD over the western part of the Guinea Coast, and a shorter LRS over the western and eastern Sahel also featured in the RCP8.5 scenario. And, in most cases, the level of uncertainty associated with the projected changes over each zone for both scenarios was comparable. Some of the outcomes from this study agreed with some previous studies in West Africa (e.g., Diffenbaugh and Giorgi, 2012; Ibrahim *et al.*, 2014; Sylla *et al.*, 2016). For instance, Ibrahim *et al*. (2014) and Sylla *et al*. (2016) had reported a shortening of the rainy season over the Sahel zone. Unlike these studies, however, the present study quantified the uncertainty with regard to the projections and focused on the impacts of GWLs. The results further showed that, in addition to the impacts on rainfall amounts over West Africa (Sarr, 2012), climate change may alter the ROD and the LRS over West Africa. The above results suggested that farmers may need to modify their crop management and planting practices to accommodate the projected changes in the ROD

and LRS to reduce crop failures and mitigate the climate risks associated with such projections.

The future projections over each climatic zone over West Africa (i.e. Guinea, Savanna, and Sahel) are shown in panels (g, h, and i, respectively). Each box plot indicates the minimum, 25th percentile, median, 75th percentile and maximum values of the RCMs ensemble. The contours represent the difference between GWL15 (1.5°C global warming level) and GWL20 (2°C global warming level). The significant areas are indicated with dots, showing where at least 15 (79%) of the models agree on the sign of change (Figure 4.30).

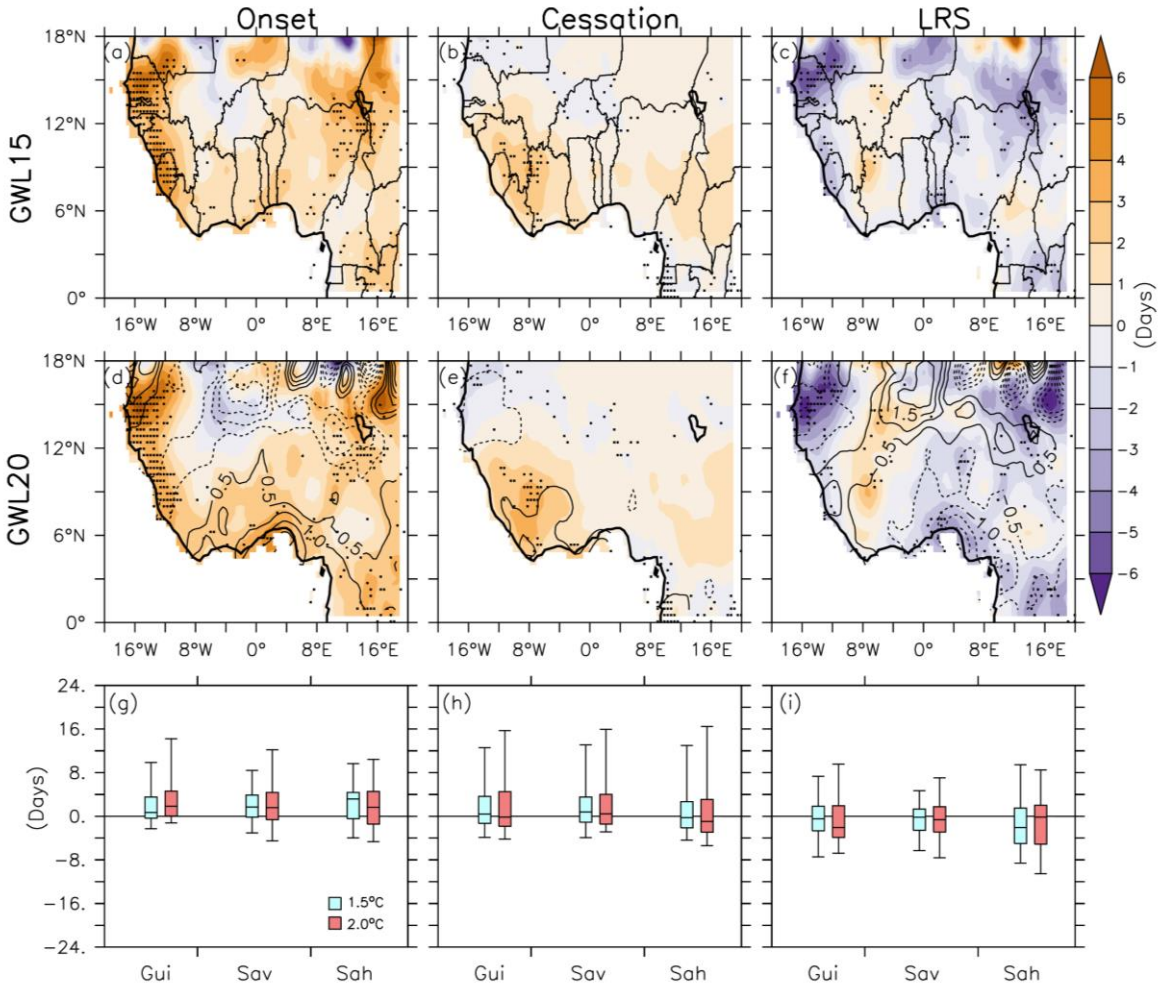

Figure 4.30: The Future Projection of RODs (panel a, d) RCDs (panel b, e) and LRS (panel c, f) over West Africa (shaded) for GWL15 and GWL20 (top and middle panels) under RCP8.5 Scenario. Panels (g, h, and i) show the Box Plots.

This chapter has discussed the results of this study, as outlined in the objectives in Section 1.6. The ability of GCMs and RCMs to simulate the WAM rainfall, RODs, RCDs and the LRS over West Africa was discussed. Moreover, the performance of different CP schemes in the WRF model, as well as the effect of modifications to the BMJ CP scheme in simulating rainfall characteristics over West Africa, were also discussed in this chapter. Lastly, this chapter also discussed the potential impacts of climate change at 1.5°C and 2°C GWLs on rainfall characteristics over West Africa. The next chapter, which is the final chapter of this thesis, enumerates some of the key findings from this study in the form of conclusion. It also presents some limitations to this study, and finally make recommendations for future work to be done.

CHAPTER FIVE

CONCLUSION AND RECOMMENDATIONS

5.1 CONCLUSION

As part of efforts to improve seasonal rainfall prediction over West Africa, this study has evaluated the capability of a GCM in simulating seasonal rainfall characteristics over West Africa. It then examined how a further development of GCM improves the simulation of seasonal rainfall prediction in that region. Furthermore, this study assessed how well the contemporary RCMs from the CORDEX-Africa project simulate the characteristics of seasonal rainfall over the study domain. This led to a further analysis of the sensitivity of seasonal rainfall characteristics under different convective schemes in the WRF model. The study was then extended to examine how a further modification of a convective scheme (the Betts-Miller Janjic or BMJ) could improve the seasonal rainfall prediction by the WRF model over West Africa. Finally, this study assessed the impact of climate change on the characteristics of seasonal rainfall over West Africa for policy and decision-making purposes. Two rainfall observation datasets (ARC2 and CHIRPS), model simulation outputs from both GCMs and RCMs, and reanalysis data have been used to describe some of the characteristics of rainfall in the past, present and future climate over the study domain.

Results from the study can be summarised as follows:

- The CMA model gave a realistic simulation of the spatial patterns and the inter-annual variability of ROD with the two definitions used in this study. The model was also able to simulate the observed seasonal movement of the WAM and its associated rainfall patterns, although it struggled to reproduce the

magnitude of the monsoon rainfall and to effectively link the northward progression of the ROD with the WAM features.

- The MetUM (both old and new versions of the atmosphere-only and coupled models) was able to credibly reproduce the zonal distribution of observed RODs, RCDs and LRS, and correctly simulate their progression over West Africa (albeit with some biases) but it performed poorly in simulating their inter-annual variability. However, the new versions in the simulation of these parameters have resulted in some improvements in this regard.
- The CORDEX RCM ensemble provided a representative simulation of RODs, RCDs and LRS in the historical climate and captured all the essential features in the observed field. Over each climatic zone, the RCM spread enclosed the observed values.
- Almost all of the selected convection schemes in the WRF model overestimated average monthly rainfall over the different zones and over the whole of West Africa but did practically replicate the observed spatial distribution of RODs, RCDs, and LRS over the study area, albeit with some biases.
- This study suggested that, for the simulation of the rainfall amount, the parameters α (in the temperature reference profile) and F_S (in the humidity reference profile) in the BMJ scheme should be set to 1.2 and 0.6 respectively, and for the simulation of ROD, RCD, and LRS, setting up $\alpha = 0.85$ and $F_S = 0.9$ simulated with the lowest bias over West Africa.
- For both 1.5°C and 2°C GWLs under the two scenarios (RCP4.5 and RCP8.5), the RCM ensemble projected a delayed ROD and a shorter LRS over the

western and eastern Sahel, and a shorter LRS over the western part of the Guinea Coast.

- In some cases, the increase in global warming from 1.5°C to 2.0°C produced different impacts under the two scenarios. While it enhanced a late ROD over the whole of West Africa under the RCP4.5, it fostered an early ROD over the Sahel zone under the RCP8.5. The increase also encouraged a decrease in the LRS over the Sahel zone and an increase in the LRS over the Guinea zone but produced opposite results under RCP8.5.

This study is expected to help improve the prediction of ROD, RCD and LRS over the study area using dynamic climate models. The outcome has shown the strengths and weaknesses of some of the dynamic models selected for this study. This study has also demonstrated the need to adopt other datasets and tools as part of efforts to provide reliable seasonal forecasts over West Africa. The outcome of the study has also suggested a version of the WRF model with an improved convection scheme for the seasonal prediction of rainfall over West Africa. The outcomes of this thesis will serve as a guide to model developers, policy makers and the general public in decision-making processes before and during the rainy season.

5.2 CONTRIBUTION TO KNOWLEDGE

The outcome of this study has produced a version of WRF with an improved convection scheme for seasonal prediction of rainfall onset date, rainfall cessation date and the length of rainy season over West Africa. Also, the results of this study has contributed in creating awareness on the use of other observation and model datasets by researchers and forecasters in the sub-continent. This will serve as a guide to model

developers, policy makers and the general public in decision-making on agricultural and water resources planning, before and during the rainy season in West Africa.

5.3 LIMITATIONS OF THE STUDY

To improve the robustness of these results and make them more relevant for policymakers, the study can be improved in several ways. Firstly, the S2S datasets have some limitations. Their resolution (1.5° x 1.5°) is too low to capture some of the mesoscale convective systems that trigger the convection of rainfall, which makes the model unable to accurately simulate some features of the WAM. Increasing the resolution of the S2S model may account for some of the biases. Again, this study was able to use only one out of the 11 S2S datasets because of the dynamics and complexity of the models. For instance, some of the datasets are generated "on the fly" while others are "fixed". The reforecast days are also different from one dataset to another. Nevertheless, the present study has shown that the CMA S2S model has the capability to simulate RODs over West Africa in lead-times before the actual start of the monsoon rains. Information from this study may be beneficial to forecasters and researchers within the sub-region, in their efforts to provide reliable forecasts of the onset of the rainy season.

Likewise, the MetUM has some biases in simulating ROD, RCD and LRS over West Africa, which may be due to the rainfall parameterization schemes in both the old and new versions of the model. This was seen in their respective simulations; for example, while the old version seemed to transport less moisture for rainfall over the sub-continent, the new version seemed to transport more, thus leading to the early onset of

rainfall. Despite these biases, the MetUM could realistically simulate the spatial pattern of the observed characteristics of the rainfall parameters over the sub-region.

Additionally, the magnitudes of the projected changes in mean ROD, RCD and LRS by the CORDEX models were small. This may be because of the long-term averaging; the magnitude of the projected inter-annual variability could be larger. Furthermore, this study only had access to 19 simulations. A lack of relevant upper level data for all the simulations used in the study hindered the analysis of dynamic changes associated with the results. However, the present study has shown that ROD, RCD and the LRS in West Africa are indeed sensitive to the ongoing global warming. The study also identified the hot-spot of future changes in these parameters under the 1.5°C and 2°C warming levels but cautioned that these changes may not be linear to the warming levels nor to the climate forcing scenarios. Nonetheless, the results may help to minimise the climate risk for agriculture and food security in West Africa.

Finally, due to time constraints, many other analyses could not be carried out during the model development section of this study, which could affect the final results that are presented. Limited access to a high speed computing system at the Centre for High Performance Computing (CHPC) delayed the outcomes of the model analyses due to long queues on the cluster (in most cases) before submitted jobs were run.

5.4 RECOMMENDATIONS FOR FUTURE WORK

To address the limitations of the S2S models, developers of the model (the global centres) could make the dynamics and even the download of the datasets less complex for researchers to improve access. To achieve the best performance of the MetUM over West Africa in simulating ROD, RCD and LRS, the rainfall parameterization

schemes need to be re-examined in both old and new versions of the model. Furthermore, information on the impacts of global warming on the inter-annual variability of ROD, RCD and LRS by the CORDEX would be particularly useful to farmers and stakeholders who need to make decisions based on year-to-year variations in these parameters. Also, increasing the number of the simulations (this study only had access to 19 simulations) will improve the spread of the model results and the level of uncertainty associated with the results. Again, it is recommended that CORDEX Phase 2 should archive upper-level variables for all the participating RCMs for future studies. Finally, it is recommended by this study that African experts should be encouraged to participate in model development for better representation of these models in the region.

REFERENCES

Abeberese, A. B., Ackah, C., and Asuming, P. (2017). *Productivity losses and firm responses to electricity shortages: Evidence from Ghana*. Working paper.

Abiodun, B. J., Adeyewa, Z. D., Oguntunde, P. G., Salami, A. T., and Ajayi, V. O. (2012). Modeling the impacts of reforestation on future climate in West Africa. *Theoretical and Applied Climatology*, *110*(1-2), 77-96.

Abiodun, B. J., Gutowski, W. J., Abatan, A. A., and Prusa, J. M. (2011). CAM-EULAG: A non-hydrostatic atmospheric climate model with grid stretching. *Acta Geophysica*, *59*(6), 1158.

Abiodun, B. J., Pal, J. S., Afiesimama, E. A., Gutowski, W. J., and Adedoyin, A. (2008). Simulation of West African monsoon using RegCM3 Part II: impacts of deforestation and desertification. *Theoretical and Applied Climatology*, *93*(3-4), 245-261.

Adedoyin, J. A. (2000). SST-induced climate change in tropical North Africa: the intermediary role of lower tropospheric oscillations. *Meteorology and Atmospheric Physics*, *75*(3-4), 135-147.

Adejuwon, J. O., and Odekunle, T. O. (2004). Skill assessment of the existing capacity for extended-range weather forecasting in Nigeria. *International Journal of Climatology: A Journal of the Royal Meteorological Society*, *24*(10), 1249-1265.

Afiesimama, E. A. (2007). Annual cycle of the mid-tropospheric easterly jet over West Africa. *Theoretical and Applied Climatology*, *90*(1-2), 103-111.

Afiesimama, E. A., Pal, J. S., Abiodun, B. J., Gutowski, W. J., and Adedoyin, A. (2006). Simulation of West African monsoon using the RegCM3. Part I: model

validation and interannual variability. *Theoretical and Applied Climatology*, *86*(1-4), 23-37.

Akinseye, F. M., Agele, S. O., Traore, P. C. S., Adam, M., and Whitbread, A. M. (2016). Evaluation of the onset and length of growing season to define planting date - 'a case study for Mali (West Africa)'. *Theoretical and applied climatology*, *124*(3-4), 973-983. DOI 10.1007/s00704-015-1460-8

Ali, A., Amani, A., Diedhiou, A., and Lebel, T. (2005). Rainfall estimation in the Sahel. Part II: Evaluation of rain gauge networks in the CILSS countries and objective intercomparison of rainfall products. *Journal of Applied Meteorology*, *44*(11), 1707-1722.

Amekudzi, L. K., Yamba, E. I., Preko, K., Asare, E. O., Aryee, J., Baidu, M., and Codjoe, S. N. (2015). Variabilities in rainfall onset, cessation and length of rainy season for the various agro-ecological zones of Ghana. Climate, 3(2), 416-434. doi:10.3390/cli3020416

Ati, O. F., Stigter, C. J., and Oladipo, E. O. (2002). A comparison of methods to determine the onset of the growing season in northern Nigeria. International journal of climatology, 22(6), 731-742.

Barnston, A. G., He, Y., and Unger, D. A. (2000). A forecast product that maximizes utility for state-of-the-art seasonal climate prediction. Bulletin of the American Meteorological Society, 81(6), 1271-1280.

Barnston, A. G., Van den Dool, H. M., Zebiak, S. E., Barnett, T. P., Ji, M., Rodenhuis, D. R., Cane, M. A., Leetmaa, A., Graham, N. E., Ropelewski, C. R., O'Lenic, E. A., Livezey, R. E., and Kousky, V. E. (1994). Long-lead seasonal forecasts -

where do we stand?. Bulletin of the American Meteorological Society, 75(11), 2097-2114.

Baumberger, C., Knutti, R., and Hirsch Hadorn, G. (2017). Building confidence in climate model projections: an analysis of inferences from fit. Wiley Interdisciplinary Reviews: Climate Change, 8(3), e454.

Blench, R. (1999). Seasonal climatic forecasting: who can use it and how should it be disseminated. Natural Resource Perspectives, 47(001).

Camberlin, P., Janicot, S., and Poccard, I. (2001). Seasonality and atmospheric dynamics of the teleconnection between African rainfall and tropical sea-surface temperature: Atlantic vs. ENSO. International Journal of Climatology, 21(8), 973-1005.

Chai, T., and Draxler, R. R. (2014). Root mean square error (RMSE) or mean absolute error (MAE)?–Arguments against avoiding RMSE in the literature. *Geoscientific model development*, *7*(3), 1247-1250.

Chiang, J. C., Kushnir, Y., and Giannini, A. (2002). Deconstructing Atlantic Intertropical Convergence Zone variability: Influence of the local cross-equatorial sea surface temperature gradient and remote forcing from the eastern equatorial Pacific. Journal of Geophysical Research: Atmospheres, 107(D1), ACL-3.

Cook, K. H. (1999). Generation of the African easterly jet and its role in determining West African precipitation. Journal of climate, 12(5), 1165-1184.

Cook, K. H., and Vizy, E. K. (2006). Coupled model simulations of the West African monsoon system: Twentieth-and twenty-first-century simulations. Journal of climate, 19(15), 3681-3703.

Daron, J. D. (2014). Regional climate messages: East Africa. Scientific report from the CARIAA adaptation at scale in Semi-Arid Regions (ASSAR) Project.

Dee, D. P., Uppala, S. M., Simmons, A. J., Berrisford, P., Poli, P., Kobayashi, S., Andrae, U., Balmaseda, M.A., Balsamo, G., Bauer, P., Bechtold, P., Beljaars, A.C.M., van de Berg, L., Bidlot, J., Bormann, N., Delsol, C., Dragani, R., Fuentes, M., Geer, A.J., Haimberger, L., Healy, S.B., Hersbach, H., Hólm, E.V., Isaksen, L., Kållberg, P., Köhler, M., Matricardi, M., McNally, A.P., Monge-Sanz, B.M., Morcrette, J.J., Park, B.K., Peubey, C., de Rosnay, P., Tavolato, C., Thépaut, J.N., and Vitard, F,. (2011). The ERA-Interim reanalysis: Configuration and performance of the data assimilation system. Quarterly Journal of the royal meteorological society, 137(656), 553-597.

Déqué, Michel and Calmanti, Sandro and Christensen, Ole Bøssing and Aquila, Alessandro Dell and Maule, Cathrine Fox and Haensler, Andreas and Nikulin, Grigory and Teichmann, C. (2017). A multi-model climate response over tropical Africa at +2 °C. Climate Services, 7, 87–95. http://doi.org/10.1016/J.CLISER.2016.06.002.

Diaconescu, E. P., Gachon, P., Scinocca, J., and Laprise, R. (2015). Evaluation of daily precipitation statistics and monsoon onset/retreat over western Sahel in multiple data sets. Climate Dynamics, 45(5-6), 1325-1354.

Diallo, I., Giorgi, F., Deme, A., Tall, M., Mariotti, L., and Gaye, A. T. (2016). Projected changes of summer monsoon extremes and hydroclimatic regimes over West Africa for the twenty-first century. Climate dynamics, 47(12), 3931-3954. DOI 10.1007/s00382-016-3052-4

Diallo, I., Sylla, M. B., Giorgi, F., Gaye, A. T., and Camara, M. (2012). Multimodel GCM-RCM ensemble-based projections of temperature and precipitation over West Africa for the early 21st century. International Journal of Geophysics, 2012. Volume 2012 (2012), Article ID 972896. doi:10.1155/2012/972896

Diasso, U., and Abiodun, B. J. (2017). Drought modes in West Africa and how well CORDEX RCMs simulate them. Theoretical and Applied Climatology, 128(1-2), 223-240. DOI 10.1007/s00704-015-1705-6

Diffenbaugh, N. S., and Giorgi, F. (2012). Climate change hotspots in the CMIP5 global climate model ensemble. Climatic change, 114(3-4), 813-822. DOI 10.1007/s10584-012-0570-x

Dodd, D. E., and Jolliffe, I. T. (2001). Early detection of the start of the wet season in semiarid tropical climates of western Africa. International journal of climatology, 21(10), 1251-1262. DOI: 10.1002/joc.640

Doherty, O. M., Riemer, N., and Hameed, S. (2014). Role of the convergence zone over West Africa in controlling Saharan mineral dust load and transport in the boreal summer. Tellus B: Chemical and Physical Meteorology, 66(1), 23191.

Donnelly, C., Greuell, W., Andersson, J., Gerten, D., Pisacane, G., Roudier, P., and Ludwig, F. (2017). Impacts of climate change on European hydrology at 1.5, 2 and 3 degrees mean global warming above preindustrial level. Climatic Change, 143(1-2), 13-26. DOI 10.1007/s10584-017-1971-7

Dosio, A., and Panitz, H. J. (2016). Climate change projections for CORDEX-Africa with COSMO-CLM regional climate model and differences with the driving

global climate models. Climate Dynamics, 46(5-6), 1599-1625. DOI 10.1007/s00382-015-2664-4

Eltahir, E. A., and Gong, C. (1996). Dynamics of wet and dry years in West Africa. Journal of Climate, 9(5), 1030-1042.

Fitzpatrick, R. G., Bain, C. L., Knippertz, P., Marsham, J. H., and Parker, D. J. (2015). The West African monsoon onset: A concise comparison of definitions. Journal of Climate, 28(22), 8673-8694. DOI: 10.1175/JCLI-D-15-0265.1

Folland, C., Owen, J., Ward, M. N., and Colman, A. (1991). Prediction of seasonal rainfall in the Sahel region using empirical and dynamical methods. Journal of Forecasting, 10(1-2), 21-56.

Fontaine, B., and Janicot, S. (1996). Sea surface temperature fields associated with West African rainfall anomaly types. Journal of climate, 9(11), 2935-2940.

Fontaine, B., Roucou, P., Gaetani, M., and Marteau, R. (2011). Recent changes in precipitation, ITCZ convection and northern tropical circulation over North Africa (1979–2007). International Journal of Climatology, 31(5), 633-648.

Fontaine, B., Trzaska, S., and Janicot, S. (1998). Evolution of the relationship between near global and Atlantic SST modes and the rainy season in West Africa: statistical analyses and sensitivity experiments. Climate Dynamics, 14(5), 353-368.

Funk, C. C., Peterson, P. J., Landsfeld, M. F., Pedreros, D. H., Verdin, J. P., Rowland, J. D., Romero, B.E., Husak, G.J., Michaelsen, J.C., and Verdin, A. P. (2014). A quasi-global precipitation time series for drought monitoring (No. 832). US Geological Survey. Reston, VA. https://doi.org/10.3133/ds832.

Funk, C., Peterson, P., Landsfeld, M., Pedreros, D., Verdin, J., Shukla, S., Husak, G., Rowland, J., Harrison, L., Hoell, A., and Michaelsen, J. (2015). The climate hazards infrared precipitation with stations - a new environmental record for monitoring extremes. Scientific data, 2, 150066.

Gilliland, E. K., and Rowe, C. M. (2007, January). A comparison of cumulus parameterization schemes in the WRF model. In Proceedings of the 87th AMS Annual Meeting and 21th Conference on Hydrology (Vol. 2).

Giorgi, F. (2010). Uncertainties in climate change projections, from the global to the regional scale. In EPJ Web of conferences (Vol. 9, pp. 115-129). EDP Sciences.

Giorgi, F., Jones, C., and Asrar, G. R. (2009). Addressing climate information needs at the regional level: the CORDEX framework. World Meteorological Organization (WMO) Bulletin, 58(3), 175.

Grist, J. P., and Nicholson, S. E. (2001). A study of the dynamic factors influencing the rainfall variability in the West African Sahel. Journal of climate, 14(7), 1337-1359.

Gu, G., and Adler, R. F. (2004). Seasonal evolution and variability associated with the West African monsoon system. Journal of climate, 17(17), 3364-3377.

Hagos, S. M., and Cook, K. H. (2007). Dynamics of the West African monsoon jump. Journal of Climate, 20(21), 5264-5284.

Hastenrath, S. (2000). Interannual and longer term variability of upper-air circulation over the tropical Atlantic and West Africa in boreal summer. International Journal of Climatology, 20(12), 1415-1430.

Hewitt, H. T., Roberts, M. J., Hyder, P., Graham, T., Rae, J., Belcher, S. E., Bourdallé-Badie, R., Harris, C., Copsey, D., Coward, A., Guiavarch, C., Hill, R., Hirschi, J.J.-M., Madec, G., Mizielinski, M.S., Neininger, E., New, A.L., Rioual, J.-C., Sinha, B., Storkey, D., Shelly, A., Thorpe, L., and Wood, R.A. (2016). The impact of resolving the Rossby radius at mid-latitudes in the ocean: Results from a high-resolution version of the Met Office GC2 coupled model. Geoscientific Model Development, 9(10), 3655-3670.

Hulme, M., and Tosdevin, N. (1989). The tropical easterly jet and Sudan rainfall: a review. Theoretical and applied climatology, 39(4), 179-187.

Ibrahim, B., Karambiri, H., Polcher, J., Yacouba, H., and Ribstein, P. (2014). Changes in rainfall regime over Burkina Faso under the climate change conditions simulated by 5 regional climate models. Climate dynamics, 42(5-6), 1363-1381. DOI 10.1007/s00382-013-1837-2

Ilesanmi, O. O. (1971). An empirical formulation of an ITD rainfall model for the Tropics: A case study of Nigeria. Journal of Applied Meteorology, 10(5), 882-891.

Ingram, K. T., Roncoli, M. C., and Kirshen, P. H. (2002). Opportunities and constraints for farmers of West Africa to use seasonal precipitation forecasts with Burkina Faso as a case study. Agricultural systems, 74(3), 331-349.

Ingram, K. T., Roncoli, M. C., and Kirshen, P. H. (2002). Opportunities and constraints for farmers of West Africa to use seasonal precipitation forecasts with Burkina Faso as a case study. Agricultural systems, 74(3), 331-349.

Issa Lélé, M., and Lamb, P. J. (2010). Variability of the intertropical front (ITF) and rainfall over the West African Sudan–Sahel zone. Journal of Climate, 23(14), 3984-4004.

James, R., Washington, R., and Jones, R. (2015). Process-based assessment of an ensemble of climate projections for West Africa. Journal of Geophysical Research: Atmospheres, 120(4), 1221-1238.

James, R., Washington, R., Abiodun, B., Kay, G., Mutemi, J., Pokam, W., Hart, N., Artan, G., and Senior, C. (2018). Evaluating climate models with an African lens. Bulletin of the American Meteorological Society, 99(2), 313-336.

James, R., Washington, R., Schleussner, C. F., Rogelj, J., and Conway, D. (2017). Characterizing half-a-degree difference: a review of methods for identifying regional climate responses to global warming targets. Wiley Interdisciplinary Reviews: Climate Change, 8(2), 2-17. 8:e457. doi: 10.1002/wcc.457

Janicot, S., Harzallah, A., Fontaine, B., and Moron, V. (1998). West African monsoon dynamics and eastern equatorial Atlantic and Pacific SST anomalies (1970–88). Journal of Climate, 11(8), 1874-1882.

Jenkins, G. S., Gaye, A. T., and Sylla, B. (2005). Late 20th century attribution of drying trends in the Sahel from the Regional Climate Model (RegCM3). Geophysical Research Letters, 32(22).

Karmalkar, A. V., and Bradley, R. S. (2017). Consequences of Global Warming of 1.5 C and 2 C for Regional Temperature and Precipitation Changes in the Contiguous United States. PloS one, 12(1), e0168697. doi:10.1371/journal. pone.0168697.

Kim, K. M., Lau, W. K. M., Sud, Y. C., and Walker, G. K. (2010). Influence of aerosol-radiative forcings on the diurnal and seasonal cycles of rainfall over West Africa and Eastern Atlantic Ocean using GCM simulations. Climate dynamics, 35(1), 115-126.

Klein, C., Heinzeller, D., Bliefernicht, J., and Kunstmann, H. (2015). Variability of West African monsoon patterns generated by a WRF multi-physics ensemble. Climate Dynamics, 45(9-10), 2733-2755.

Klutse, N. A. B., Sylla, M. B., Diallo, I., Sarr, A., Dosio, A., Diedhiou, A., Owusu, K., Sarr, A., Kamga, A., Lamptey, B., Ali, A., Gbobaniyi, E.O., Lennard, C., Hewitson, B., Nikulin, G., Panitz, H.-J., and Büchner, M. (2016). Daily characteristics of West African summer monsoon precipitation in CORDEX simulations. Theoretical and applied climatology, 123(1-2), 369-386. DOI 10.1007/s00704-014-1352-3

Kumi, N., and Abiodun, B. J. (2018). Potential impacts of 1.5° C and 2° C global warming on rainfall onset, cessation and length of rainy season in West Africa. Environmental Research Letters. https://doi.org/10.1088/1748-9326/aab89e

Kuusaana, E. D., and Bukari, K. N. (2015). Land conflicts between smallholders and Fulani pastoralists in Ghana: Evidence from the Asante Akim North District (AAND). Journal of rural studies, 42, 52-62.

Laux, P., Kunstmann, H., and Bárdossy, A. (2008). Predicting the regional onset of the rainy season in West Africa. International Journal of Climatology, 28(3), 329-342. DOI: 10.1002/joc.1542

Le Barbé, L., Lebel, T., and Tapsoba, D. (2002). Rainfall variability in West Africa during the years 1950–90. Journal of climate, 15(2), 187-202.

Leduc-Leballeur, M., De Coëtlogon, G., and Eymard, L. (2013). Air-sea interaction in the Gulf of Guinea at intraseasonal time-scales: wind bursts and coastal precipitation in boreal spring. Quarterly Journal of the Royal Meteorological Society, 139(671), 387-400.

Lemburg, A., Bader, J., and Claussen, M. (2017, April). Is there a clear relationship between the Tropical Easterly Jet and Sahel rainfall?. In EGU General Assembly Conference Abstracts (Vol. 19, p. 8181).

Manabe, S., Smagorinsky, J., and Strickler, R. F. (1965). Simulated climatology of a general circulation model with a hydrologic cycle. Mon. Wea. Rev, 93(12), 769-798.

Marchant, R., Mumbi, C., Behera, S., and Yamagata, T. (2007). The Indian Ocean dipole–the unsung driver of climatic variability in East Africa. African Journal of Ecology, 45(1), 4-16.

Mariotti, L., Diallo, I., Coppola, E., and Giorgi, F. (2014). Seasonal and intraseasonal changes of African monsoon climates in 21st century CORDEX projections. Climatic change, 125(1), 53-65. DOI 10.1007/s10584-014-1097-0

Marteau, R., Sultan, B., Moron, V., Alhassane, A., Baron, C., and Traoré, S. B. (2011). The onset of the rainy season and farmers' sowing strategy for pearl millet cultivation in Southwest Niger. Agricultural and forest meteorology, 151(10), 1356-1369. www.elsevier.com/locate/agrformet

Mason, S. J., Goddard, L., Graham, N. E., Yulaeva, E., Sun, L., and Arkin, P. A. (1999). The IRI seasonal climate prediction system and the 1997/98 El Niño event. Bulletin of the American Meteorological Society, 80(9), 1853-1874.

MEINKE, I., Roads, J., and Kanamitsu, M. (2007). Evaluation of RSM-simulated precipitation during CEOP. Journal of the Meteorological Society of Japan. Ser. II, 85, 145-166.

Mera, R., Laing, A. G., and Semazzi, F. (2014). Moisture variability and multiscale interactions during spring in West Africa. Monthly Weather Review, 142(9), 3178-3198.

Mounkaila, M. S., Abiodun, B. J., and Omotosho, J. B. (2014). Assessing the capability of CORDEX models in simulating onset of rainfall in West Africa.Theoretical and Applied Climatology, 119(1-2), 255-272. DOI 10.1007/s00704-014-1104-4

Mugalavai, E. M., Kipkorir, E. C., Raes, D., and Rao, M. S. (2008). Analysis of rainfall onset, cessation and length of growing season for western Kenya. Agricultural and forest meteorology, 148(6), 1123-1135. www.elsevier.com/locate/agrformet

Mugume I, Waiswa D, Mesquita MDS, Reuder J, Basalirwa C, et al. (2017) Assessing the Performance of WRF Model in Simulating Rainfall over Western Uganda. J Climatol Weather Forecasting 5: 197. doi:10.4172/2332-2594.1000197

Nicholson, S. E. (2009). A revised picture of the structure of the “monsoon” and land ITCZ over West Africa. Climate Dynamics, 32(7-8), 1155-1171.

Nicholson, S. E. (2013). The West African Sahel: A review of recent studies on the rainfall regime and its interannual variability. ISRN Meteorology, 2013. Volume 2013 (2013), Article ID 453521, 2-7. http://dx.doi.org/10.1155/2013/453521

Nicholson, S. E., and Grist, J. P. (2001). A conceptual model for understanding rainfall variability in the West African Sahel on interannual and interdecadal timescales. International Journal of Climatology: A Journal of the Royal Meteorological Society, 21(14), 1733-1757.

Nicholson, S. E., and Grist, J. P. (2003). The seasonal evolution of the atmospheric circulation over West Africa and equatorial Africa. Journal of Climate, 16(7), 1013-1030.

Nicholson, S. E., Barcilon, A. I., Challa, M., and Baum, J. (2007). Wave activity on the tropical easterly jet. Journal of the atmospheric sciences, 64(7), 2756-2763.

Nicholson, S. E., Some, B., and Kone, B. (2000). An analysis of recent rainfall conditions in West Africa, including the rainy seasons of the 1997 El Niño and the 1998 La Niña years. Journal of climate, 13(14), 2628-2640.

Nikulin, G., Jones, C., Giorgi, F., Asrar, G., Büchner, M., Cerezo-Mota, R., van Meijgaard, E., Christensen, O.B., Déqué, M., Fernandez, J., Hänsler, A., Samuelsson, P., Sylla, M.B., and Sushama, L. (2012). Precipitation climatology in an ensemble of CORDEX-Africa regional climate simulations. Journal of Climate, 25(18), 6057-6078.

Nikulin, G., Lennard, C., Dosio, A., Kjellström, E., Chen, Y., Hänsler, A., van Meijgaard, E., Kupiainen, M., Laprise, R., Mariotti, L., Maule, C.F., Panitz, H.-J., Scinocca, J.F., and Somot, S. (2018). The effects of 1.5 and 2 degrees of global

warming on Africa in the CORDEX ensemble. Environmental Research Letters, 13(6), 065003.

Nobre, P., Moura, A. D., and Sun, L. (2001). Dynamical downscaling of seasonal climate prediction over Nordeste Brazil with ECHAM3 and NCEP's regional spectral models at IRI. Bulletin of the American Meteorological Society, 82(12), 2787-2796.

Novella, N. S., and Thiaw, W. M. (2013). African rainfall climatology version 2 for famine early warning systems. Journal of Applied Meteorology and Climatology, 52(3), 588-606.

Okonkwo, C., Demoz, B., and Tesfai, S. (2014). Characterization of West African jet streams and their association to ENSO events and rainfall in ERA-Interim 1979–2011. Advances in Meteorology, 2014.

Oladipo, E. O., and Kyari, J. D. (1993). Fluctuations in the onset, termination and length of the growing season in Northern Nigeria. Theoretical and applied climatology, 47(4), 241-250.

Olaniyan, E. A., Adefisan, A., Oni, F., Afiesimama, E., Balogun, A., and Lawal, K. (2018). Evaluation of the ECMWF Sub-seasonal to Seasonal Precipitation Forecasts During the Peak of West Africa Monsoon in Nigeria. Frontiers in Environmental Science, 6, 4. doi: 10.3389/fenvs.2018.00004

Omotosho, J. B. (1990). Onset of thunderstorms and precipitation over northern Nigeria. International Journal of Climatology, 10(8), 849-860.

Omotosho, J. B. (1992). Long-range prediction of the onset and end of the rainy season in the West African Sahel. International Journal of Climatology, 12(4), 369-382.

Omotosho, J. B., and Abiodun, B. J. (2007). A numerical study of moisture build-up and rainfall over West Africa. Meteorological Applications, 14(3), 209-225. DOI: 10.1002/met.11

Omotosho, J. B., Balogun, A. A., and Ogunjobi, K. (2000). Predicting monthly and seasonal rainfall, onset and cessation of the rainy season in West Africa using only surface data. International Journal of Climatology, 20(8), 865-880.

Pohl, B., and Douville, H. (2011). Diagnosing GCM errors over West Africa using relaxation experiments. Part II: intraseasonal variability and African easterly waves. *Climate dynamics*, *37*(7-8), 1313-1334.

Ratna, S. B., Ratnam, J. V., Behera, S. K., Ndarana, T., Takahashi, K., and Yamagata, T. (2014). Performance assessment of three convective parameterization schemes in WRF for downscaling summer rainfall over South Africa. Climate dynamics, 42(11-12), 2931-2953.

Riede, J. O., Posada, R., Fink, A. H., and Kaspar, F. (2016). What's on the 5th IPCC Report for West Africa?. In *Adaptation to Climate Change and Variability in Rural West Africa* (pp. 7-23). Springer International Publishing. DOI 10.1007/978-3-319-31499-0_2

Roca, R., Chambon, P., Jobard, I., Kirstetter, P. E., Gosset, M., and Bergès, J. C. (2010). Comparing satellite and surface rainfall products over West Africa at

meteorologically relevant scales during the AMMA campaign using error estimates. *Journal of Applied Meteorology and Climatology*, *49*(4), 715-731.

Roja Raman, M., Jagannadha Rao, V. V. M., Venkat Ratnam, M., Rajeevan, M., Rao, S. V. B., Narayana Rao, D., and Prabhakara Rao, N. (2009). Characteristics of the Tropical Easterly Jet: Long-term trends and their features during active and break monsoon phases. *Journal of Geophysical Research: Atmospheres*, *114*(D19).

Roncoli, C., Ingram, K., and Kirshen, P. (2001a). The costs and risks of coping: household impacts and farmer responses to drought in Burkina Faso. *Clim Res*, *19*(2), 119-132.

Roncoli, C., Ingram, K., and Kirshen, P. (2002). Reading the rains: local knowledge and rainfall forecasting in Burkina Faso. *Society and Natural Resources*, *15*(5), 409-427.

Rowell, D. P., Booth, B. B., Nicholson, S. E., and Good, P. (2015). Reconciling past and future rainfall trends over East Africa. *Journal of Climate*, *28*(24), 9768-9788.

Sarr, B. (2012). Present and future climate change in the semi-arid region of West Africa: a crucial input for practical adaptation in agriculture. *Atmospheric Science Letters*, *13*(2), 108-112. **DOI:** 10.1002/asl.368.

Saha, S., Moorthi, S., Pan, H. L., Wu, X., Wang, J., Nadiga, S., Liu, H., Tripp, P., Kistler, R., Woollen, J., Behringer, D., Stokes, D., Grumbine, R., Gayno, G., Wang, J., Hou, Y.-T., Chuang, H., Juang, H.-M.H., Sela, J., Iredell, M., Treadon, R., Kleist, D., Delst, P.V., Keyser, D., Derber, J., Ek, M., Meng, J., Wei, H., Yang, R., Lord, S., van den Dool, H., Kumar, A., Wang, W., Long, C., Chelliah, M., Xue, Y., Huang, B., Schemm, J.-K., Ebisuzaki, W., Lin, R., Xie, P., Chen, M.,

Zhou, S., Higgins, W., Zou, C.-Z., Liu, Q., Chen, Y., Han, Y., Cucurull, L., Reynolds, R.W., Rutledge, G., and Goldberg, M. (2010). The NCEP climate forecast system reanalysis. Bulletin of the American Meteorological Society, 91(8), 1015-1058.

Saha, S., Moorthi, S., Wu, X., Wang, J., Nadiga, S., Tripp, P., Behringer, D., Hou, Y.-T., Chuang, H., Iredell, M., Ek, M., Meng, J., Yang, R., Mendez, M.P., van den Dool, H., Zhang, Q., Wang, W., Chen, M., and Becker, E. (2014). The NCEP climate forecast system version 2. Journal of Climate, 27(6), 2185-2208.

Senior, C. A., Andrews, T., Burton, C., Chadwick, R., Copsey, D., Graham, T., Ringer, M., Hyder, P., Jackson, L., McDonald, R., Ridley, J., Tsushima, Y. (2016). Idealized climate change simulations with a high-resolution physical model: HadGEM3-GC2. *Journal of Advances in Modeling Earth Systems*, *8*(2), 813-830.

Seth, A., Rauscher, S. A., Biasutti, M., Giannini, A., Camargo, S. J., and Rojas, M. (2013). CMIP5 projected changes in the annual cycle of precipitation in monsoon regions. *Journal of Climate*, *26*(19), 7328-7351.

Sheen, K. L., Smith, D. M., Dunstone, N. J., Eade, R., Rowell, D. P., and Vellinga, M. (2017). Skilful prediction of Sahel summer rainfall on inter-annual and multi-year timescales. *Nature communications*, *8*, 14966.

Sivakumar, M. V. K. (1988). Predicting rainy season potential from the onset of rains in Southern Sahelian and Sudanian climatic zones of West Africa. *Agricultural and Forest Meteorology*, *42*(4), 295-305.

Smith, J., Smith, P., and Addiscott, T. (1996). Quantitative methods to evaluate and compare soil organic matter (SOM) models. In Evaluation of soil organic matter models (pp. 181-199). Springer, Berlin, Heidelberg.

Stern, R. D., Dennett, M. D., and Garbutt, D. J. (1981). The start of the rains in West Africa. *International Journal of Climatology*, *1*(1), 59-68.

Sultan, B., Baron, C., Dingkuhn, M., Sarr, B., and Janicot, S. (2005). Agricultural impacts of large-scale variability of the West African monsoon. *Agricultural and forest meteorology*, *128*(1-2), 93-110.

Sylla, M. B., Dell'Aquila, A., Ruti, P. M., and Giorgi, F. (2010). Simulation of the intraseasonal and the interannual variability of rainfall over West Africa with RegCM3 during the monsoon period. *International Journal of Climatology*, *30*(12), 1865-1883. DOI: 10.1002/joc.2029

Sylla, M. B., Diallo, I., and Pal, J. S. (2013). West African monsoon in state-of-the-science regional climate models. In *Climate Variability-Regional and Thematic Patterns*. InTech. London, SE19SG. http://dx.doi.org/10.5772/55140

Sylla, M. B., Gaye, A. T., Pal, J. S., Jenkins, G. S., and Bi, X. Q. (2009). High-resolution simulations of West African climate using regional climate model (RegCM3) with different lateral boundary conditions. *Theoretical and Applied Climatology*, *98*(3-4), 293-314.

Sylla, M. B., Giorgi, F., Pal, J. S., Gibba, P., Kebe, I., and Nikiema, M. (2015). Projected changes in the annual cycle of high-intensity precipitation events over West Africa for the late twenty-first century. *Journal of Climate*, *28*(16), 6475-6488. http://dx.doi.org/10.1175/JCLI-D-14-00854.s1.

Sylla, M. B., Nikiema, P. M., Gibba, P., Kebe, I., and Klutse, N. A. B. (2016). Climate Change over West Africa: Recent Trends and Future Projections. In *Adaptation to Climate Change and Variability in Rural West Africa* (pp. 25-40). Springer International Publishing. DOI 10.1007/978-3-319-31499-0_3

Tall, M., Sylla, M. B., Diallo, I., Pal, J. S., Faye, A., Mbaye, M. L., and Gaye, A. T. (2017). Projected impact of climate change in the hydroclimatology of Senegal with a focus over the Lake of Guiers for the twenty-first century. *Theoretical and Applied Climatology*, *129*(1-2), 655-665. DOI 10.1007/s00704-016-1805-y

Tarhule, A., and Lamb, P. J. (2003). Climate Research and Seasonal Forecasting for West Africans: Perceptions, Dissemination, and Use? Perceptions, Dissemination, and Use?. *Bulletin of the American Meteorological Society*, *84*(12), 1741-1760.

Tchotchou, L. D., and Kamga, F. M. (2010). Sensitivity of the simulated African monsoon of summers 1993 and 1999 to convective parameterization schemes in RegCM3. *Theoretical and applied climatology*, *100*(1-2), 207-220.

Tetzlaff, G., and Peters, M. (1986). The atmospheric transport potential for water vapour and dust in the Sahel region. *GeoJournal*, *12*(4), 387-398.

Tompkins, A. M., and Adebiyi, A. A. (2012). Using CloudSat cloud retrievals to differentiate satellite-derived rainfall products over West Africa. *Journal of Hydrometeorology*, *13*(6), 1810-1816.

Tompkins, A. M., and Di Giuseppe, F. (2015). Potential predictability of malaria in Africa using ECMWF monthly and seasonal climate forecasts. *Journal of applied meteorology and climatology*, *54*(3), 521-540. DOI: 10.1175/JAMC-D-14-0156.1

Tompkins, A. M., and Feudale, L. (2010). Seasonal ensemble predictions of West African monsoon precipitation in the ECMWF System 3 with a focus on the AMMA special observing period in 2006. *Weather and Forecasting*, *25*(2), 768-788. DOI: 10.1175/2009WAF2222236.1

Troccoli, A. (2010). Seasonal climate forecasting. *Meteorological Applications*, *17*(3), 251-268.

UNFCCC, C. (2015). Adoption of the Paris Agreement. *I: Proposal by the President (Draft Decision), United Nations Office, Geneva (Switzerland)*, (s 32).

Vautard, R., Gobiet, A., Sobolowski, S., Kjellström, E., Stegehuis, A., Watkiss, P., Mendlik, T., Landgren, O., Nikulin, G., Teichmann, C., and Jacob, D. (2014). The European climate under a 2 C global warming. *Environmental Research Letters*, *9*(3), 034006. doi:10.1088/1748-9326/9/3/034006

Vellinga, M., Arribas, A., and Graham, R. (2013). Seasonal forecasts for regional onset of the West African monsoon. *Climate dynamics*, *40*(11-12), 3047-3070. DOI 10.1007/s00382-012-1520-z

Watterson, I. G., Bathols, J., and Heady, C. (2014). What influences the skill of climate models over the continents?. *Bulletin of the American Meteorological Society*, *95*(5), 689-700.

White, C. J., Franks, S. W., and McEvoy, D. (2015). Using subseasonal-to-seasonal (S2S) extreme rainfall forecasts for extended-range flood prediction in Australia. *Proceedings of the International Association of Hydrological Sciences*, *370*, 229-234. doi:10.5194/piahs-370-229-2015

Williams, K. D., Copsey, D., Blockley, E. W., Bodas-Salcedo, A., Calvert, D., Comer, R., Hyder, P., Davis, P., Graham, T., Hewitt, H.T., Hill, R., Ineson, S., Johns, T.C., Keen, A.B., Lee, R.W., Megann, A., Milton, S.F., Rae, J.G.L., Roberts, M.J., Scaife, A.A., Schiemann, R., Storkey, D., Thorpe, L., Watterson, I.G., Walters, D.N., West, A., Wood, R.A., Woollings, T., and Xavier, P.K. (2018). The Met Office global coupled model 3.0 and 3.1 (GC3. 0 and GC3. 1) configurations. *Journal of Advances in Modeling Earth Systems*, *10*(2), 357-380.

Williams, K. D., Harris, C. M., Bodas-Salcedo, A., Camp, J., Comer, R. E., Copsey, D., Fereday, D., Graham, T., Hill, R., Hinton, T., Hyder, P., Ineson, S., Masato, G., Milton, S.F., Roberts, M.J., Rowell, D.P., Sanchez, C., Shelly, A., Sinha, B., Walters, D.N., West, A., Woollings, T., and Xavier, P.K. (2015). The met office global coupled model 2.0 (GC2) configuration. *Geoscientific Model Development*, *8*(5), 1509-1524.

Willmott, C. J., and Matsuura, K. (2005). Advantages of the mean absolute error (MAE) over the root mean square error (RMSE) in assessing average model performance. Climate research, 30(1), 79-82.

Xie, P., Janowiak, J. E., Arkin, P. A., Adler, R., Gruber, A., Ferraro, R., Huffman, G.J., and Curtis, S. (2003). GPCP pentad precipitation analyses: An experimental dataset based on gauge observations and satellite estimates. *Journal of Climate*, *16*(13), 2197-2214.